Doctoral theses at NTNU, 2020:289

Inge Madshaven

Simulating electron-avalanche-driven positive streamers in dielectric liquids

Doctoral thesis

Inge Madshaven

ISBN 978-82-326-4926-6 (printed ver.)
ISBN 978-82-326-4927-3 (electronic ver.)
ISSN 1503-8181

NTNU
Norwegian University of
Science and Technology

NTNU
Norwegian University of Science and Technology
Thesis for the Degree of
Philosophiae Doctor
Faculty of Natural Sciences
Department of Chemistry

Doctoral theses at NTNU, 2020:289

NTNU
Norwegian University of
Science and Technology

Inge Madshaven

Simulating electron-avalanche-driven positive streamers in dielectric liquids

Thesis for the Degree of Philosophiae Doctor

Trondheim, October 2020

Norwegian University of Science and Technology
Faculty of Natural Sciences
Department of Chemistry

NTNU
Norwegian University of
Science and Technology

NTNU
Norwegian University of Science and Technology

Thesis for the Degree of Philosophiae Doctor

Faculty of Natural Sciences
Department of Chemistry

ISBN 978-82-326-4926-6 (printed ver.)
ISBN 978-82-326-4927-3 (electronic ver.)
ISSN 1503-8181

Doctoral theses at NTNU, 2020:289

Printed by NTNU Grafisk senter

Abstract

This thesis presents a novel predictive model for simulating positive streamers in dielectric liquids. Such liquids are commonly used for electrical insulation of high-power equipment, for example power transformers, which are essential parts of the electrical distribution network. A "streamer" is the phenomenon leading to electrical breakdown in dielectric liquids. Modeling and simulating streamers to better understand the phenomenon is crucial to improve the performance of electrical insulation and electrical equipment alike.

In this work, streamer propagation is modeled in a needle–plane electrode gap, with cyclohexane as a model for the insulating liquid. The needle and the extremities of the streamer (streamer heads) are modeled by hyperboloids. In the strong electric field, close to the needle or the streamer, electrons detach from anions and form electron avalanches. The streamer grows when the size of an avalanche exceeds the Townsend–Meek criterion. Each streamer head is modeled as an RC-circuit to calculate its potential. Resistance in the channel and capacitance in the gap towards the planar electrode are taken into consideration. A high electric field within a channel can give a breakdown, a reillumination of the channel, equalizing the potential of the needle and the streamer head. The streamer transitions into a fast mode of propagation when radiation from the streamer head causes photoionization. This occurs when the field-dependent ionization potential is reduced below the energy of this radiation.

The streamer conductivity regulates the propagation speed, and reilluminations increase the average conductivity. Simulated streamers can change from fast to slow mode if the conductivity of the channel is low. Conversely, the streamer can change to a fast mode during propagation if the conductivity is high. This change can be triggered by a reillumination.

This work demonstrates that an avalanche-driven streamer breakdown is possible. However, the propagation voltage is high compared to experiments. The limitations of the model are discussed and several possible improvements are suggested. The software developed to simulate the model is published as open-source software.

Sammendrag

Denne avhandlingen presenterer en ny modell for simulering av positive i dielektriske væsker. Slike væsker blir mye brukt til elektrisk isolasjon av høyspenningsutstyr, for eksempel transformatorer, som er en essensiell del av det elektriske distribusjonsnettet. En "streamer" er fenomenet som fører til elektrisk gjennomslag i dielektriske væsker. Modellering og simulering av streamere er viktig for å forstå fenomenet bedre for å forbedre ytelsen til elektrisk isolasjon og elektrisk utstyr.

I dette arbeidet er streamere modellert i et nål–plan elektrodegap, med sykloheksan som modell for den isolerende væsken. Nålen og streamerhodene (ytterpunktene på streameren) er modellert som hyperboloider. I det sterke elektriske feltet, nær nålen eller streameren, frigjøres elektroner fra anioner og kan danne elektronskred. Streameren vokser når størrelsen på et elektronskred overskrider Townsend–Meek-kriteriet. Hvert streamerhode er modellert som en RC-krets, og denne brukes for å regne ut potensialet til streamerhodet. Motstanden er gitt av kanalen mellom nålen og hodet, og kapasitansen av gapet mellom hodet og planelektroden. Et høyt elektrisk felt i kanalen kan gi et gjennomslag i kanalen, en reilluminasjon, som utjevner potensialet mellom nålen og streamerhodet. Streameren øker drastisk i hastighet når stråling fra streamerhodet kan forårsake fotoionisering. Dette skjer når det feltavhengige ioniseringspotensialet blir lavere enn energien til denne strålingen.

Konduktiviteten i kanalene regulerer hastigheten til streameren, og reilluminasjoner øker gjennomsnittlige konduktiviteten. De simulerte streamerene kan bytte fra rask til sakte propageringsmode om konduktiviteten til streameren er lav. Og omvendt, ved høy konduktivitet kan streamere bytte fra sakte til rask propagering. Denne endringen kan skje som følge av en reilluminasjon.

Dette arbeidet viser at elektronskred er en mekanisme som kan brukes for å simulere streameroverslag. Propageringsspenningen er imidlertid høy sammenlignet med eksperimenter. Begrensningene til modellen blir diskutert og flere forbedringsmuligheter blir foreslått. Programvaren som er utviklet for å simulere modellen er publisert med open kildekode.

Acknowledgments

When I started vocational studies to become an electrician at age fifteen, I was presented with a "staircase", detailing the steps from where I was standing at the time, up to a doctorate. It was a long staircase indeed, and I was convinced that I would never climb it to the end. Perhaps I would reach a bachelor, at the most. However, one thing led to another, and this thesis is the result of me climbing the final step of that staircase.

I would like to thank my supervisors Per-Olof Åstrand and Øystein Hestad, as well as the project leader Lars Lundgaard, for granting me the position and guiding me along the way. The doctoral work has been part of the project "Performance of dielectric liquids for land based and subsea environmental friendly transformers". The project is a collaboration between SINTEF Energy, ABB, Statnett, and NTNU, and is supported by the Research Council of Norway under the contract 228850. Our project meetings have been insightful and motivating.

Working on the doctorate has been extremely interesting, challenging, and at times difficult. I would never have managed it without the good support of family, friends, and colleagues. I am afraid of naming names, because it is difficult to know where to draw the line, and there really are too many to thank. Nevertheless, I would like to mention a few of those who helped me through this. I have had countless hours of making dinner, watching movies, and brewing beer with Christian. Erik has been a good friend for most of my life, and he is probably the reason I managed to complete this work, since he convinced me to continue those times I really wanted to quit. My vacations with Ali have included: eating frogs and insects; drinking fermented mare's milk; riding motorbikes, horses, and ostriches; and sightseeing in everything from medieval cities, to swamps and mountains.

Special thanks to Paola for supporting me through the final months of the writing, to Ali for creating the excellent LaTeX template used for this thesis, and again to Paola, Ali, and Erik for suggesting improvements to the text. I am also very grateful for all my good friends in the office. All the coffee breaks, discussions, and distractions have been important for keeping me sane. The same is true for every other friend I have, in Trondheim in particular. I am grateful for all of you.

List of publications

I am the first author of publications I, II, III, and IV, which are included as part of this thesis. I have written the software, conducted all calculations, and written the first draft of all the papers. A summary of each publication is given in chapter 5. These publications are referenced below and included in the appendix.

I. **Inge Madshaven, Per-Olof Åstrand, Øystein Leif Hestad, Stian Ingebrigtsen, Mikael Unge, Olof Hjortstam**
Simulation model for the propagation of second mode streamers in dielectric liquids using the Townsend–Meek criterion
Journal of Physics Communications **2**:105007 (2018)
DOI: 10/CXJF | ARXIV: 1804.10473

II. **Inge Madshaven, Øystein Leif Hestad, Mikael Unge, Olof Hjortstam, Per-Olof Åstrand**
Conductivity and capacitance of streamers in avalanche model for streamer propagation in dielectric liquids
Plasma Research Express **1**:035014 (2019)
DOI: 10/C933 | ARXIV: 1902.03945

III. **Inge Madshaven, Øystein Leif Hestad, Mikael Unge, Olof Hjortstam, Per-Olof Åstrand**
Photoionization model for streamer propagation mode change in simulation model for streamers in dielectric liquids
Plasma Research Express **2**:015002 (2020)
DOI: 10/DG8M | ARXIV: 1909.12694

IV. **Inge Madshaven, Øystein Leif Hestad, Per-Olof Åstrand**
Cerman: Software for simulating streamer propagation in dielectric liquids based on the Townsend–Meek criterion
Submitted | ARXIV: 2007.02999

I developed the software *Cerman* to carry out the simulations for my publications. This software is published in a repository for which I am responsible, see reference S1 below. The conference publications C1, C2, and C3 referenced below are not a part of this thesis. Publication C1 is based on my master thesis. I have also contributed to a chapter in a forthcoming CIGRE brochure, see B1, in particular to a chapter on models for breakdown in liquids.

S1. **Inge Madshaven**
Cerman: Simulating streamer propagation in dielectric liquids
Open-source software. MIT License. (2020)
GitHub: `github.com/madshaven/cerman`

C1. **Inge Madshaven**, **Hans Sverre Smalø**, **Mikael Unge**, **Øystein Leif Hestad**
Photoionization model for the transition to fast mode streamers in dielectric liquids
2016 IEEE Conference on Electrical Insulation and Dielectric Phenomena (CEIDP), 400–403
DOI: 10/cx9v

C2. **Øystein Leif Hestad**, **Au-Dung Vuong**, **Inge Madshaven**, **Per-Olof Åstrand**
Thermal decomposition of cyclohexane by kinetic Monte Carlo simulations and its relevance to streamer formation
2016 IEEE Conference on Electrical Insulation and Dielectric Phenomena (CEIDP), 404–407
DOI: 10/cxmm

C3. **Inge Madshaven**, **Per-Olof Åstrand**, **Øystein Leif Hestad**, **Mikael Unge**, **Olof Hjortstam**
Modeling the transition to fast mode streamers in dielectric liquids
2017 IEEE 19th International Conference on Dielectric Liquids (ICDL), 1–4
DOI: 10/cx9w

B1. **Lars Esben Lundgaard et al.**
Dielectric performance of insulating liquids for transformers
Brochure by CIGRE Study Committee D1, Working Group WG D1.70, Task Force TF3
(under preparation)

Contents

1 Introduction 1

2 Background 3
- 2.1 Conduction, insulation, and breakdown 3
- 2.2 Observations 6
- 2.3 Mechanisms 8
- 2.4 Ionization and electronic states 11

3 Simulation models 13
- 3.1 Lattice 13
- 3.2 Connected points 14
- 3.3 Cells 15

4 Avalanche model 17
- 4.1 Electric field 17
- 4.2 Avalanches 17
- 4.3 Streamer structure 20
- 4.4 Algorithm 21
- 4.5 Optimizations 22

5 Results and discussion 25
- 5.1 Avalanche model 25
- 5.2 Conductivity and capacitance 28
- 5.3 Photoionization 30
- 5.4 The software 32
- 5.5 Discussion 34

6 Conclusion 37

Bibliography 39

Publication I 51

Publication II 81

Publication III 95

Publication IV 109

1 Introduction

Dielectric liquids, transformer oils in particular, are commonly used for electrical insulation in high-voltage equipment such as power transformers. Liquids provide high electrical withstand strength and good thermal conductivity compared to gases. Moreover, operational damage to solid insulating materials causes permanent defects, whereas liquids can reorient and are self-healing over short time scales [1]. Electrical discharges occur in the liquid if the electrical withstand strength of the liquid is exceeded, for instance, due to an operational error. Sophisticated imaging techniques reveal a gaseous channel, called a "streamer", which grows into the liquid in a bushy or branched fashion [2, 3]. The streamer acts as an extension of the electrode, carrying the electric potential and electric field deeper into the liquid. If a streamer grows to bridge the gap between two electrodes, it can act as a conductor, leading to an electrical breakdown.

Streamers have been investigated for decades [4–8]. A better understanding of the streamer phenomenon can prevent electrical breakdowns and subsequent equipment damage. Benchmark testing is performed to evaluate the performance of a given liquid and electrode geometry. Furthermore, in sophisticated experiments, model systems are designed to isolate and examine given properties or mechanisms of the streamer phenomenon to make predictive models [9, 10]. Simulations are an important tool to verify that models correspond to experiments. However, simulation is challenging as mechanisms acting on a range of time and length scales are involved in the streamer phenomenon. Good simulation models, predicting the performance of new systems or configurations, can provide safer systems and reduce the need for costly testing.

This thesis encompasses the development of a model and a software package to simulate streamer propagation. The four publications included in the appendix detail the progression of the modeling and simulation work. Publication I provides details on our model, which has been built on the basis of the Townsend–Meek streamer-to-avalanche criterion. The propagation and breakdown properties of the model are

examined in the same paper. Publication II includes streamer conductivity and capacitance in the model, as well as breakdown within the streamer channel. Radiation and photoionization are investigated in Publication III, where we also model changes between slow and fast mode of streamer propagation. The software implementation of our model, called *Cerman*, is published as open-source software. Publication IV describes the functionality and implementation of Cerman. As such, each publication included in this thesis focuses on different aspects of the complete simulation model.

The simulation software allows the user to design a series of experiments where one or more parameters are varied. These parameters can relate to the modeled experiment (e.g. voltage, gap size, and needle size), the nature of the liquid (e.g. streamer conductivity, electron mobility, and avalanche parameters), or the algorithm itself (e.g. time step). The finer details of a simulation (e.g. individual avalanche growth, streamer head potential, and electric breakdown within the channel) can be examined as a function of time and position. The results of individual simulations include the propagation length, the propagation speed, and the streamer shape. The simulation software facilitates plotting the results of several simulations together. Several plots, for instance of the streamer shape, can be superimposed. Furthermore, a given result of a simulation, such as the propagation speed, can be plotted as a function of a given parameter, e.g. voltage.

The next chapter provides some background on the streamer phenomenon, from general considerations regarding conduction and breakdown, to experimental observations and mechanisms that can explain such observations. The various attempts (by others) to model streamer breakdown are outlined in chapter 3, and our model is given in chapter 4. The results and discussion of the work, given as summaries of publications I, II, III, and IV, are included in chapter 5. Finally, chapter 6 offers the conclusions and some prospects for future development.

2 Background

After briefly introducing streamers in the previous chapter, a more in-depth background to the streamer phenomenon is given in this chapter. The first section provides an introduction to conduction and breakdown in different materials, with a focus on comparing solids and gases to liquids. Observations of streamer propagation characteristics and the mechanisms proposed to influence the streamer phenomenon are discussed in the two sections thereafter, respectively. Finally, special attention is given to the molecular properties of the liquid. Specifically, how the ionization potential and the electronically excited states of molecules influence the streamer propagation.

2.1 Conduction, insulation, and breakdown

Solid materials can be divided into conductors, semiconductors, and insulators. Applying an electric field to a conductor, which contains a large number of free electrons, results in an electric current proportional to the field strength. The current is limited by collisions between electrons and atoms. As the name implies, a semiconductor material has (typically) a limited number of charge carriers (electrons or holes) at room temperature. A low electric field results in an electric current proportional to the field strength and to the number of charge carriers. High electric fields can inject charge carriers into the material. The amount of injected charge carriers is proportional to the field, which makes the current a cubic function of the external field (space charge limited current). Semiconductors can be doped with impurities and combined in many ways, giving interesting and useful behaviors.

An ideal insulator does not conduct electric current when exposed to electric fields below a given threshold. If the electric withstand strength is exceeded, however, the material undergoes an electric breakdown and begins to conduct electricity. A dielectric breakdown in one part of a bulk material can lead to electrical discharges into the affected region, i.e. a partial discharge. Whereas, a complete electrical breakdown is when an electrical discharge occurs from one electrode to another,

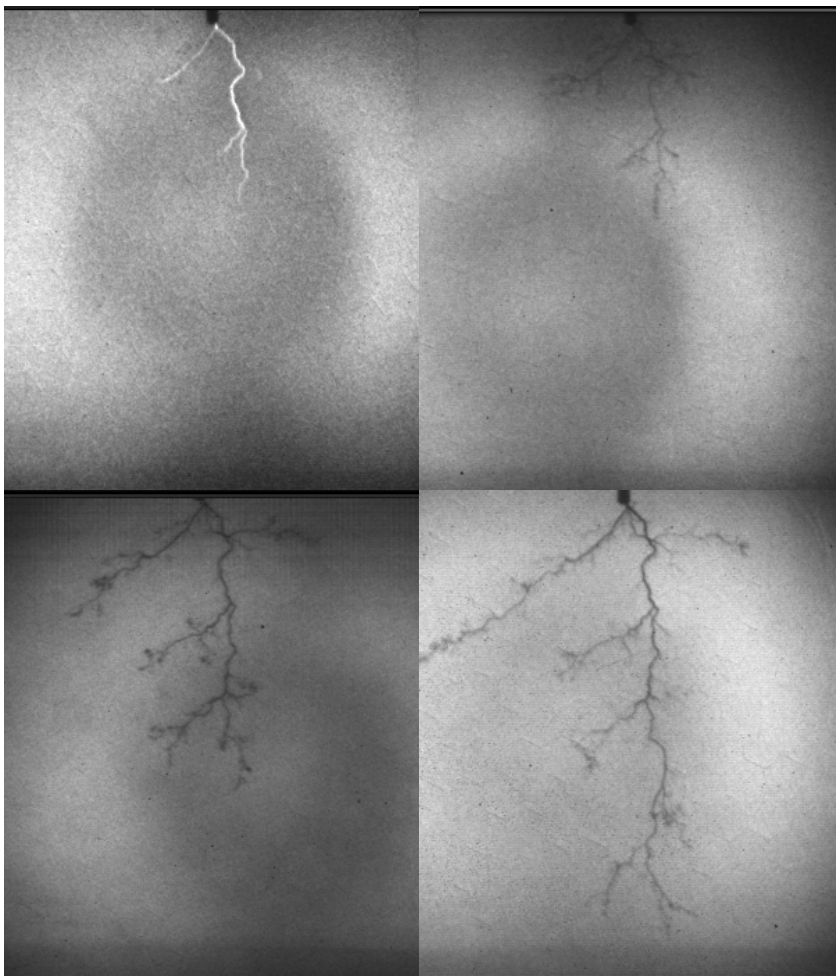

Figure 1: Sequential image frames of streamer propagation in a 77 mm needle–plane gap insulated by cyclohexane. The needle tip is visible in the center at the top of each frame. The planar electrode is located slightly below each frame. Light from the streamer channel illuminates the streamer in the first frame, whereas the streamer channel is dark in the other frames. The image frames, arranged from left-to-right and top-to-bottom, were taken at 1 µs, 3 µs, 11 µs, and 23 µs, respectively, after a step voltage of 122 kV was applied. Breakdown occurred after 27 µs. The propagation speed exceeded 60 km/s until the first frame, and slowed down to a few km/s thereafter. The images were kindly provided by Dag Linhjell, SINTEF Energy Research.

through the insulating material. Such a discharge is typically preceded by several partial discharges. Initially, a dielectric breakdown occurs in the region of the material exposed to the highest electric stress, and is followed by a partial discharge. Sequential partial breakdowns and discharges can propagate the high electric stress further and further into the material, until a complete breakdown occurs.

In contrast to solids, the atoms and molecules in gases can move and reorient. Cations and anions can contribute greatly to conduction in gases. Free electrons can travel farther between collisions in gases than in solids since the distance between the molecules is greater. Electrons gain energy as they move in the electric field, and lose energy through collisions with molecules. Such a collision can result in an ionization, i.e. the molecule emits an electron and becomes an ion, if the energy of the collision exceeds the molecule's ionization potential (IP). In a sufficiently strong electric field, this process can repeat, in such a way that one electron can become two, then four, and so forth. The resulting exponential growth of electrons is called an "electron avalanche" and is an important mechanism for electrical breakdown in gases [11].

The "seed" electron to start an avalanche can be produced by a number of processes, for instance by injection from an electrode, detachment from an anion, or photoionization. Radiation from electron avalanches is important for creating new seed electrons. The light electrons move much faster than the heavy ions, and the electron avalanche leaves a cloud of cations behind. This separation of charge changes the electric field, which can facilitate new avalanches. Successive avalanches can lead to an electric breakdown when forming an ionized path between two electrodes. Reducing the number of free electrons, for instance by electronegative additives, can increase the electrical withstand strength of a gas [12]. Increasing the pressure reduces the mean free path for electrons and thus the energy of the collisions, which consequently inhibits electron avalanches.

Solid and liquid insulating materials have a higher electric withstand strength than gases. However, whereas defects and damages from production or partial discharges will remain in solids, fluids can reorient over a short time scale to maintain a uniform insulating medium. Solid insulation provides mechanical protection and structural integrity, and is often combined with liquid insulation, which also provides good

thermal conductivity that is often needed for electrical power equipment. Liquids have properties of both solids and gases, with a short distance between molecules that can move and reorient. A liquid can be approximated as a dense gas [13], but also as a solid over short time scales [14]. As such, mechanisms leading to breakdown in either solid and gas insulation can also play an important role in liquid insulation. However, electrical breakdown in liquids is more complex, because it also involves the creation of a gaseous channel: a streamer. Experiments, where liquids are exposed to high electrical stress, reveal how a gaseous streamer initiates and grows in a branched fashion, see figure 1. While the streamer propagates, a weak continuous current is measured along with irregular spikes, which are associated with brief reilluminations of the streamer filaments [15]. The streamer itself is considered a prebreakdown phenomenon, whereas a streamer growing to bridge the gap between two electrodes can lead to a complete electrical breakdown. Experimental observations and proposed mechanisms for electrical breakdown in liquids are discussed in the following sections.

2.2 Observations

There are many methods to study electrical breakdown in liquids. Standardized setups are used to compare the performance of different insulating liquids. Given geometries and liquids are benchmark tested to validate equipment design; such tests are important for the industry. However, to gain further knowledge on the mechanisms involved in a breakdown, it is better to design model experiments where the effect of given parameters can be isolated. The course of an electrical breakdown is dependent on several factors: the geometry of the electrodes, the nature of the insulating liquid, as well as the magnitude, polarity, and shape of the applied voltage, are all of high importance. Applying a constant voltage to a needle–plane gap is an experimental setup that allows good control of the course of the breakdown [4]. A uniform field is desired in practical applications, however, the highly divergent field in a needle–plane gap gives better control of streamer initiation and propagation [16]. When a streamer initiates in a uniform field, it enhances the local field and can propagate to the opposing electrode. Conversely, in a divergent field, the streamer propagation length is de-

pendent on the applied voltage. The propagation speed of the streamer is dependent on the applied voltage, but it can also change drastically during propagation [17].

Streamers are classified according to their polarity, that is the polarity of their initiation site, i.e. positive for needle anode and negative for needle cathode. Negative streamers initiate at lower voltages than positive streamers, however, positive streamers grow farther than negative streamers. Thus, to prevent electrical breakdown, the focus is often on positive streamers [18, 19].

A common method of exploring the properties of a system consists in exposing it to a range of voltages, from low to high. The same voltage is applied multiple times to capture the stochastic nature of the streamer phenomenon. The initiation voltage V_i is the voltage with a more than 50 % probability of streamer inception. The propagation voltage V_p, the breakdown voltage V_b, the acceleration voltage V_a, are defined in a similar way by measuring the share of propagating filamentary streamers, streamers leading to breakdown, and streamers propagating very fast, respectively.

Streamers are commonly divided into four modes, primarily distinguished by their propagation speed [17]. The 1st mode expands slowly at about 100 m/s in a bubbly or bushy fashion. This mode is typical for sharp needles when the applied voltage V is below the propagation voltage, $V_i < V < V_p$. By increasing V above V_p, the 2nd mode is initiated directly. These streamers propagate at speeds on the order of km/s in a branched fashion, creating a tree-like structure, and can lead to breakdown when $V > V_b$. The propagation length ℓ_2 of the 2nd-mode streamers is dependent on the applied voltage and the external pressure, but the propagation velocity is not significantly influenced by these factors [20]. 2nd-mode streamers emit a continuous glow from the extremities during propagation and irregular reilluminations light up one or more of the filaments [15, 18]. Reilluminations are more frequent in 3rd-mode streamers than 2nd-mode streamers, which also propagate faster, at some tens of km/s. The 3rd mode initiates at voltages higher than the 2nd mode, and propagates a distance ℓ_3 before the streamer changes to the 2nd mode, if the voltage is below the acceleration voltage V_a. This is well illustrated in figure 1, where the streamer begins in a fast, luminous 3rd mode, and then propa-

gates in a 2nd mode for the remainder of the gap. For voltages above V_a, the streamer changes to the very fast, luminous 4th mode, which propagates at speeds exceeding 100 km/s for the final portion of the gap [15]. Increasing the voltage increases the proportion propagated in the 4th mode, while the time from initiation to breakdown decreases consequently.

2.3 Mechanisms

The streamer channel consists of weakly ionized gas, i.e. plasma [21]. As such, it can be considered a conducting object, acting as an extension of the electrode where the streamer initiated. Mechanisms that are important for the streamer phenomenon can take place within the channel, at the interface between the gas and the liquid, or in the liquid itself [22]. The focus here is on how mechanisms in the liquid can expand the streamer, and how mechanisms within the streamer channel can influence the mechanisms for expansion. The mechanisms involved in streamer propagation range over several orders of magnitude in both time and length scale [7].

Dielectric liquids like transformer oils are very good insulators, but there are several mechanisms that deteriorate the insulating properties when the liquids are exposed to sufficiently high electric stress. Onsager theory describes how molecules split into anions and cations, which increases conductivity at field strengths on the order of tens of kV/mm [23, 24]. Conduction models such as Schottky-injection, Fowler–Nordheim, Poole–Frenkel, "hopping conduction", and field ionization become relevant at much higher fields [25–27]. The increased number of charge carriers by injection or charge separation increases the conduction, but also shields the external field, making the current in this regime space-charge limited [25, 26, 28]. This can also be viewed as having a space-charge-limited electric field [29, 30]. These mechanisms are more relevant for slow than fast streamers, since it takes some time to build up the space charge to limit the field. Space charge can also be an important aspect when considering the influence of voltage rise time in experiments [31].

How the streamer is created and propagates are important questions, and several mechanisms can contribute to such processes. Charges moving in strong electric fields can heat the liquid through collisions

(Joule heating), which can cause the liquid to boil, i.e. resulting in bubble nucleation [16]. By considering the energy required to form the channel and the speed of the streamer, a streamer head can be compared to a moving heat source of 10 W [16]. Moving charged particles can set up a flow in the liquid, in a phenomenon called "electrohydrodynamics" (EHD) [28, 32]. It is possible that EHD can cause bubble nucleation, since an increase in flow gives a decrease in pressure according to the Bernoulli principle [6, 33].

Strong electrostatic forces within the medium can create cracks in solid insulation materials, and this mechanism has also been proposed to act in liquids [34]. The electric field creates an underpressure that tears apart the liquid and forms a gaseous channel. The length of the channel is dependent on the amount of energy stored in the electric field. The resulting streamer propagates in a stepwise process, where energy is supplied through the streamer channel, and this energy builds up until the streamer channel can expand.

The electron avalanche mechanism is important for breakdown in gases, but its contribution to breakdown in liquids is somewhat disputed. For instance, strong electron scattering suggests that electron avalanches are not possible in liquid water [35]. Experiments in non-polar liquids, however, point to electron avalanches in the liquid phase, which in turn cause bubbles nucleation [36, 37]. The growth of an avalanche can be modeled [38, 39] and the model parameters can be estimated from experiments [13, 40]. The Townsend–Meek avalanche-to-streamer criterion states that avalanches must obtain a critical size for a streamer breakdown to occur, and this criterion has been used to model streamer initiation, propagation, and breakdown [12, 38, 41].

Rayleigh theory, which describes the growth and collapse of bubbles, provides also a good model for the radial expansion and collapse of streamer channels [16, 37]. The predicted growth, on the order of 100 m/s, is also well matched by the growth of slow streamers, but far slower than the axial growth of filamentary streamers. The time it takes for a channel to expand and collapse is dependent on the external pressure. The streamer propagation stops when the channel collapses, so increasing the external pressure reduces the propagation length of streamers and can even inhibit streamer initiation [16]. However, the propagation speed of filamentary streamers is not significantly influ-

enced by the external pressure, which indicates that the mechanism for propagation occurs in the liquid phase [4, 7].

A streamer structure often consists of several branches. The degree of branching in cyclohexane, cf. figure 1, is low compared to mineral oils [42]. The mechanism behind branching is not clear. However, both microscopic and macroscopic inhomogeneities, such as varying charge density, molecular orientation, impurities, and micro-bubbles, have been suggested to contribute to the process [43, 44]. Microscopic inhomogeneities can give large fluctuations in the microscopic electric field [45], which can be relevant for branching. Conversely, since the speed is not significantly affected by the external pressure, it is unlikely that micro-bubbles are important for propagation [4, 7, 34]. Furthermore, a breakdown within a micro-bubble would register at a spike in the measured current, however, the spikes in the current are correlated with reilluminations of the streamer channel [7, 15].

The electric current measured while a streamer grows can be seen as a displacement current. There is conduction within the gaseous streamer, but not within the liquid, since the dielectric time constant of a non-polar liquid is greater than the time for a streamer breakdown [7]. The average electric field within the streamer channel is on the order of kV/mm [46–48]. The streamer channel can be non-conductive or weakly conductive, except during reilluminations, which are electric breakdowns within the streamer channel [7, 17]. The electric field at the tip of the streamer can be calculated when the electric field in the channel is known [48, 49]. In large needle–plane gaps, the field in front of the streamer decreases in the first part of the propagation, and increases as the streamer gets closer to the opposing electrode.

Field ionization [4, 9, 25] and photoionization [6, 7, 50] have been proposed as mechanisms involved in streamer propagation that can be particularly relevant for the propagation of fast streamers. The creation of a gaseous channel requires some time and this can be important for slow streamers. However, there is no evidence that fast streamers need a channel to propagate [51].

2.4 Ionization and electronic states

It has long been known that additives with low ionization potential (IP) can lower the breakdown voltage of a liquid [4]. This effect makes sense intuitively since many of the mechanisms involved in streamer propagation are concerned with charge generation. However, while low-IP additives do facilitate positive streamers, their effect on negative streamers is not significant [18]. Not only do low-IP additives facilitate positive 2nd-mode streamers, while reducing the breakdown voltage; they also increase the degree of branching and the acceleration voltage [15, 18, 42]. Natural esters can be a safer and more environmental-friendly alternative to mineral oils, and their low acceleration voltage can be improved with additives [19, 52].

The transformer oils commonly used for insulation consist of numerous molecules with different properties. For this reason, it is challenging to identify the properties that facilitate or hinder streamer propagation. Correlations between liquid properties and the streamer phenomenon can be established by testing a large number of liquids [53], however, a change of liquid entails a change of several parameters. The influence of specific properties can be examined by starting from a simple, well-defined liquid, such as cyclohexane, and blending in additives with given properties [54]. The methodology with a base liquid and an additive is also applied in our model, see chapter 4.

The IP is the energy required to excite an electron from the ground state of a molecule to an unbound state. The electronically excited states between the ground state and the IP are bound states and correspond to energies in the range of several eV. Molecules are excited or relaxed from one state to another by absorbing or releasing the energy difference between the states, respectively. Having more available states gives more options for such transitions. The probabilities for transitions between states are important to consider, because these give both the likelihood for excitation and the states' lifetimes. The energy of the excited states are not significantly dependent on the electric field [55]. However, increasing the electric field lowers the IP, and states with an energy above the IP are unbound [27, 55]. Lowering the IP obviously promotes any ionization mechanism, but the removal of bound states can influence other mechanisms as well.

Additives with energetically low excited states can reduce the propagation speed of 2nd-mode streamers, while increasing both the breakdown and the acceleration voltage [15, 19, 56]. The reason why these additives cause such effects remains unknown, however, one or more of the following concepts can be involved:

1. States with lower energies sustain to higher fields [27, 55]. A mode change can be the result of excited states becoming unbound.
2. The energy emitted from additives has low probability of being absorbed when it is lower than the excitation energy of the other molecules. This ability to transport energy away from the streamer can be essential [III].
3. Absorption can hinder radiative transport of energy away from the streamer. For instance, UV absorption close to the streamer can increase the ionization rate in the high-field region, which in turn increases the electric field [56].
4. The states of low energy can reduce the energy of free electrons through collisions, which hinders electron avalanche growth [19].
5. A molecule in a high-energy state generally relaxes through several states, emitting visible light, before emitting UV when relaxing to the ground state [III]. The states' lifetimes and the energy emitted can be important and depend on the available states.
6. Photons or electrons need less energy to ionize an excited molecule, and having more available states can thus increase the chance of a two-step ionization [19]. Additives can have long-lived excited states, which makes two-step mechanisms probable [III]. Two-step mechanisms can promote, for instance:
   a. creation of seed electrons for avalanches,
   b. overall avalanche growth, or
   c. overall ionization close to the streamer.

Furthermore, it is important to consider the energy difference between available states in the base liquid and in the additive. For instance, radiation from the lowest excited state of cyclohexane is sufficient to ionize pyrene, whereas this radiation is not significantly absorbed by cyclohexane [III]. Such radiation can even cause ionization in the base liquid if the IP is reduced by a sufficiently strong field [III]. Finally, it should be emphasized that the states do not contribute equally. The excitation cross-sections, the probabilities for transitions between states, and the states' lifetimes are all important aspects to consider.

3 Simulation models

As discussed in chapter 2, there are several candidate mechanisms to explain various aspects of streamer initiation, propagation, and breakdown. Below follows some notable attempts to model one or more mechanisms together in order to simulate the streamer phenomenon. Our model to simulate streamers is detailed in chapter 4.

3.1 Lattice

The first models to simulate streamers explored the streamers' fractal nature [57–59]. These models used a 2D-lattice, where each lattice point was either an electrode or part of the liquid. The potential of each lattice point in the liquid is calculated from the potential of the electrodes. The streamer acts as an extension of the anode, and grows by "breaking" the link from a point in the streamer to a point in the liquid. The probability P_i for growth to a point through a link i is a function of the electric field E_i raised to an exponent η

$$P_i \sim E_i^\eta, \quad \text{or} \quad k_i = cE_i^\eta. \tag{1}$$

The link to break is selected at random, but according to the probabilities P_i. The probabilities P_i can be stated as rate constants k_i given some scaling constant c. Breaking a link, adding a new point to the streamer, changes the electric field, and then the process of choosing a new link to break is repeated. The fractal structure of the streamer is a function of η, where higher values yield higher field dependence resulting in lower degrees of branching. If the rates are known, the stochastic time τ between events can be calculated [60]

$$\tau = \frac{-\ln r}{\sum_i k_i}. \tag{2}$$

where r is a random number between 0 and 1. When the time is known, the propagation speed can be calculated [61]. Another approach is to scale the rate constants in such a way that the propagation speed matches experimental values [62].

The bushy streamers resulting from low η propagate slowly, whereas a high η yields faster propagation speed. Transitions between slow and fast modes can be induced by letting η be some function of the propagation length [63]. However, this approach lacks physical motivation. The mode change is a result of a change in a physical property, and not a function of position in the gap.

The probability of streamer propagation does not need to be directly related to the electric field strength as in equation (1). In [64], the rates are calculated as a function of time t by considering the production of free electrons R within a critical volume Γ

$$P(t) \sim 1 - e^{-\Gamma R t}. \tag{3}$$

It is implicit that increasing the electric field strength increases the critical volume. The study indicated that electron production by cosmic radiation was too low to explain streamer propagation. Although most models employ the macroscopic electric field, it should be noted that the microscopic fluctuations in the field can be substantial [45]. This aspect can be important when the production of free electrons depends on the electric field strength. Rather than randomly selecting and breaking one link, given the probabilities in equation (1), the fluctuations in the field can be taken into account [65], and every link below a given threshold may be broken at once.

Streamer propagation is mainly dependent on the processes at the extremities of the streamer, which in turn can be dependent on processes within the streamer channel, such as conductivity [66] or pressure [67]. The hydroelectric flow in a system with both a liquid and a gaseous phase can be simulated by Lattice Boltzmann methods [68].

3.2 Connected points

In the electric network model [69], as well as in our model based on avalanches [I], the streamer points are created as the streamer develops, based on the propagation criteria. Conversely, lattice models divide the simulated space into discrete points at predetermined positions, and assign certain properties to each point.

Conductivity within the streamer is an integral part of the simulation when modeling the streamer as an electrical network of resistors and capacitors [69–71]. In this approach, there is a resistance within the streamer and a capacitance between the extremities of the streamer and the planar electrode. The streamer propagates when there is

enough energy available to evaporate the liquid and create a new branch. The direction of the branch is chosen according to a probability distribution, and the calculated current pulses as new branches are added. A limitation of this model is that it does not differentiate between positive and negative streamers.

3.3 Cells

Computational fluid dynamics (CFD) is group of methods for calculation of flow. The space is divided into cells with given properties, such as the density of electrically charged particles. Flow between the cells changes these properties. CFD models can encompass e.g. ionization, recombination, electron attachment, and diffusion of particles.

Electric breakdown in a water-filled parallel electrode gap is investigated in [72, 73]. A breakdown within an air-filled micro-bubble in the gap enhances the electric field and initiates a streamer. The streamer propagates by field-ionization in the strong electric field and results in a complete breakdown. Micro-bubbles are not the cause of breakdown in oil [7]. However, water has a much higher permittivity and conductivity than oil, which can make other mechanisms important.

Field-ionization is a relevant mechanism in oil [25], and one model [9] assumes that the 2nd- and 4th-mode streamers propagate when the electric field at the tip of the streamer is strong enough to ionize low-IP molecules and the main molecules in the liquid, respectively. The work by [74] investigates field-ionization for different combinations of base liquid and additives. This model has some weaknesses as it predicted branching while modeling on rotational symmetry, which is unphysical. Further development of that model introduced branching in 3D employing microscopic impurities [44]. The model also demonstrated a propagation speed of streamers similar to experimental values by regulating the electron saturation velocity [75].

CFD models are powerful but very computationally demanding, and the extra complication of phase change from liquid to gas is often ignored. However, simplified 1.5D models for single-channel streamers can also consider the phase change [41]. In this case, the streamer propagates when the energy density is high enough to evaporate the liquid. The channel expands to a diameter given by the external pressure, which enables simulation of the effects of external pressure. The processes within the channel itself, and how these affect streamer stopping, are by similar means explored in [76].

4 Avalanche model

The foundation of the model is the electron avalanche mechanism. Electrons detach from anions in regions where the electric field is strong, and can form avalanches as they move towards the streamer. If an avalanche grows sufficiently large, the streamer propagates to the position of that avalanche. Electrical breakdowns are rare under operating conditions. Hence, we simulate in a needle–plane gap, which is often used in experiments to ensure streamer initiation. The needle–plane geometry is useful for controlling the initiation and propagation of a streamer. A conceptual illustration of the geometry and details of the simulation are included in figure 2.

4.1 Electric field

When the simulation begins, the electric field is set up between the needle and the planar electrode. Using a hyperbolic needle, the electric potential V and electric field $\boldsymbol{E}$ can be calculated analytically [I]. The streamer, when initiated, is composed of "virtual" hyperbolic electrodes, "streamer heads", see figure 2. For a given position $\boldsymbol{r}$, V and $\boldsymbol{E}$ are calculated by the superposition principle, i.e. a summation over each electrical hyperboloid h

$$V(\boldsymbol{r}) = \sum_h k_h \, V_h(\boldsymbol{r}) \quad \text{and} \quad E(\boldsymbol{r}) = \sum_h k_h \, \boldsymbol{E}_h(\boldsymbol{r}) \,. \tag{4}$$

The coefficients k_h compensate for electrostatic shielding [I].

4.2 Avalanches

Free electrons have a short lifetime in dielectric liquids because they attach rapidly to neutral particles, forming anions. In a strong electric field, the electrons can detach from anions, and this "seed" electron can then grow into an electron avalanche. We simulate a number of particles, which we call "seeds", in a region surrounding the needle and

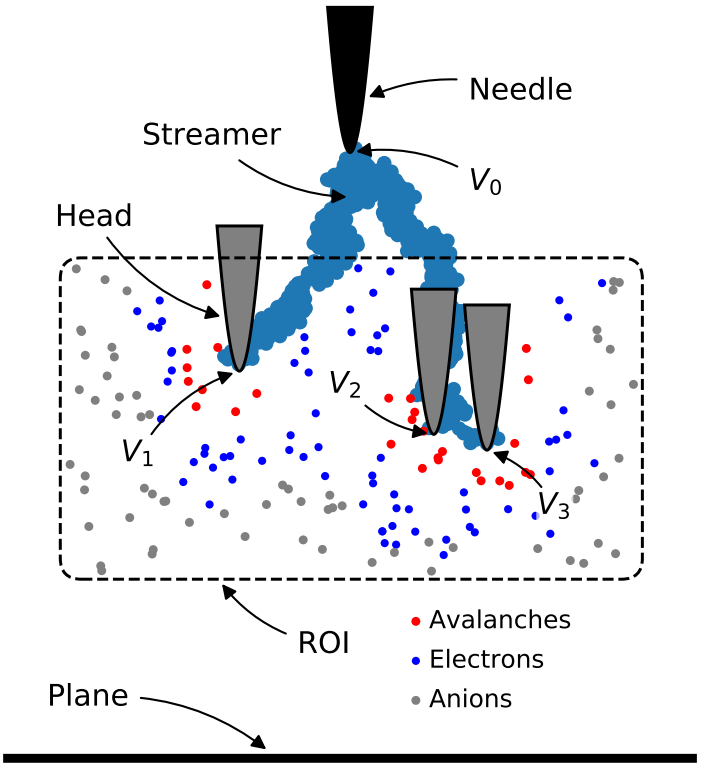

Figure 2: Conceptual illustration of the elements of the simulation model. A needle–plane electrode gap is insulated by a liquid. The needle and the extremities of the streamer (streamer heads) are modeled as hyperboloids. The hyperboloids have a tip potential V and give rise to an electric field $\boldsymbol{E}$. Anions, electrons, and electron avalanches are controlled by a region of interest (ROI). Figure adapted from figure 1 in Publication IV.

the streamer, see figure 2. Each seed is classified as an anion, electron, or electron avalanche, depending on the electric field strength at its position

$$E_{\text{anion}} < E_{\text{d}} \leq E_{\text{electron}} < E_{\text{c}} \leq E_{\text{avalanche}}\,, \tag{5}$$

where E_{d} and E_{c} are the thresholds for detachment and electron multiplication, respectively. For a simulation time step Δt, each seed moves a distance $\Delta \boldsymbol{s}$ proportional to the electric field $\boldsymbol{E}$ and its mobility μ

$$\Delta s = \mu E \Delta t\,. \tag{6}$$

Anions have much lower mobility than electrons, whereas the mobility of electron avalanches is set equal to the electron mobility.

Calculating the speed of the electrons from the mobility implies that an average speed is calculated. The electrons gain energy in the electric field, and lose energy when colliding with other particles. An electron avalanche grows when some fraction of such collisions causes ionization, i.e. creating new free electrons. The probability per length for an electron to multiply is denoted by α, which is a function of the electric field and the properties of the liquid. The number of electrons N_{e} in an avalanche is given by integration over the avalanche path

$$\mathrm{d}N_{\text{e}} = \alpha N_{\text{e}}\, \mathrm{d}s \quad \Longrightarrow \quad N_{\text{e}} = \exp \int \alpha \, \mathrm{d}s\ . \tag{7}$$

The above expression assumes that an avalanche starts from a single electron. The size of the avalanche can then be defined by the exponent alone,

$$Q_{\text{e}} = \ln N_{\text{e}} = \sum_i \Delta s\, \alpha\,, \tag{8}$$

by summation over simulation iterations i. The Townsend–Meek streamer-to-avalanche criterion then states that a streamer breakdown can occur when avalanches grow above a critical size Q_{c} [38]

$$Q_{\text{e}} > Q_{\text{c}}\,. \tag{9}$$

When an avalanche meets this criterion, the streamer expands to the position of the avalanche, i.e. a new streamer head is placed there.

4.3 Streamer structure

The streamer is modeled by a collection of streamer heads. The focus is on representing the electric field in the region surrounding the extremities of the streamer. The streamer grows by the addition of a new streamer head when an avalanche meets equation (9). The potential of a new streamer head is calculated considering the potential of the needle [I] or by charge transfer from nearby streamer heads [II].

Conduction within the streamer channel can increase the potential of a streamer head whose potential is lower than that of the needle. Each streamer head is associated with a resistance in the channel towards the needle and a capacitance in the gap between itself and the planar electrode, used to calculate a time constant τ [II]. For every simulation iteration i, conduction in the streamer channel reduces the potential difference ΔV_h between the needle n and each streamer head h. First the current difference is calculated,

$$\Delta V_h = V_n - V_h \,, \tag{10}$$

then the potential of the head is updated,

$$V_h \longleftarrow V_n - \Delta V_h \, e^{-\Delta t / \tau_h} \,. \tag{11}$$

A potential difference ΔV_h implies an average electric field E_s within the streamer channel

$$E_s = \Delta V_h / \ell_s \,, \tag{12}$$

where ℓ_s is the length of the channel. Reilluminations are interpreted as a consequence of an electric breakdown within the streamer channel, which occurs when the average field exceeds a threshold E_{bd} [II]. This equalizes the potential between the needle and a streamer head, as follows

$$E_s > E_{\mathrm{bd}} \quad \Longrightarrow \quad \tau = 0 \quad \Longrightarrow \quad V_h = V_n \,. \tag{13}$$

Slow 2nd-mode streamers have few reilluminations, 3rd-mode streamers have several, and the fast 4th mode is very luminous, however, in addition, there is a weak glow from the streamer heads [15]. We explored how radiation is emitted and absorbed in Publication III,

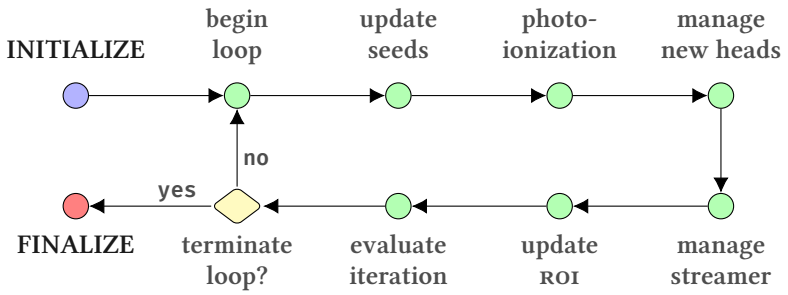

Figure 3: The principal steps of the simulation algorithm. A description is given in section 4.4. A detailed flowchart of the algorithm is included in Publication IV.

and created a model in which photoionization is responsible for the propagation of fast streamers. The model assumes energetic radiation from the streamer head, namely fluorescent radiation from excited molecules. The strong electric field surrounding a streamer head lowers the ionization potential (IP). Reducing the IP below the energy of the fluorescent radiation, increases the photoionization cross-section, and increases the propagation speed. This is implemented as follows

$$E_h > E_w \quad \Longrightarrow \quad \Delta \boldsymbol{s}_h = -v_w \Delta t \, \hat{\boldsymbol{z}} \,. \tag{14}$$

That is, if the electric field E_h at the tip of a streamer head exceeds a threshold E_w, then the streamer head is given a "photoionization speed" v_w. This implies that the streamer head is moved a distance Δs_h towards the planar electrode in the given iteration.

4.4 Algorithm

The main components of a simulation are the *seeds* and the *streamer*, which are each updated iteratively in a simulation loop outlined in figure 3. The seeds are classified as anions, electrons, or avalanches, and then they move and multiply as described in section 4.2. Next, each streamer head exceeding the threshold field for photoionization is moved a distance given by equation (14). Moving a streamer head implies replacing it with a new head at the new position. Any other new heads are then classified and added to the streamer. Thereafter, the streamer's potential is updated (see section 4.3), before the streamer

structure is optimized (see section 4.5). When the streamer is updated, the ROI can be updated as well, essentially removing seeds that are no longer needed and creating new seeds as needed. Finally, the iteration results are evaluated to decide whether to start a new iteration or to finalize the simulation. Typically, a simulation is ended because the streamer propagation is very slow (stopping) or the streamer has reached the planar electrode (breakdown).

4.5 Optimizations

Optimizing the computational cost is important for any simulation. A key feature of our model is that simulations are computationally efficient and can be performed on a personal computer. Calculating the electric field is by far the most expensive part of the algorithm. Consequently, the computational cost of a simulation scales linearly with the number of streamer heads N_h, and the number of seeds N_s, summed over all iterations i. A reduction in either of these is beneficial to the cost, but the efforts to reduce the cost should not affect the simulations to a large degree.

The number of streamer heads N_h is kept low by several means. Firstly, any head with a tip point "inside" the hyperboloid of another head is removed. For instance, when a new head is created in the high-field area in front of an existing head, the existing one is removed if the point of its tip is within the new streamer head. Secondly, if a new head is created too close to an existing head, then the head furthest from the planar electrode is removed. (It is assumed that a certain minimum distance is needed for branching to occur.) Finally, if the electrostatic shielding is high, i.e. the k_h of a head is low, then the head has low influence and is removed. The "streamer" in figure 2 consists of each point where a streamer head has been added, however, most of them have been removed and just three remains.

The number of seeds N_s is controlled by limiting the seeds to a cylinder, a region of interest (ROI), surrounding the streamer, see figure 2. When a seed moves past this region or ends up within a streamer head, it is replaced by a new seed.

All avalanches are simulated in an inner loop, since these are in the high-field area, they require greater precision than the other seeds. Each avalanche is moved and multiplied N_n times, up to a maximum

of N_{MSN} times. The cost K of an iteration becomes

$$K = N_h(N_s - N_a) + N_h N_a N_n \,. \tag{15}$$

where N_a is the number of avalanches. Note that $K = N_h N_s$ for $N_n = 1$, and increasing N_n increases the cost of an iteration. However, the time simulated in one iteration, $N_n \Delta t$, also increases, resulting in a decreased cost for the overall simulation. The cost per simulated time for a given iteration is

$$\frac{K}{N_n \Delta t} = \frac{N_h(N_s - N_a)}{N_n \Delta t} + \frac{N_h N_a}{\Delta t} \,. \tag{16}$$

The computational cost of the avalanches is the same, but for all the other seeds, the number of times the electric field is calculated is reduced. Since the number of seeds is far greater than the number of avalanches, $N_s \gg N_a$, the computational cost of a simulation is reduced by a factor close to the average of N_n.

5 Results and discussion

The work has consisted of developing a model for the propagation of streamers, as described in chapter 4. The result is a simulation model where the electron avalanche mechanism is responsible for streamer propagation, the potentials of the streamer extremities are given by an RC-model, and photoionization can cause a change to fast streamer propagation. The simulation model has been implemented in Python and published as open-source software. A summary of each publication, with a focus on its motivation and main research results, is given below, followed by a summarizing discussion.

5.1 Avalanche model

We explore the governing principles of the model in Publication I, mainly streamer propagation given by the Townsend–Meek criterion. The framework is a needle–plane electrode gap and a streamer composed of "virtual" electrodes, c.f. figure 2. We argue that even though the amount of free electrons is low in a non-polar liquid, there can be a substantial amount of anions in the liquid, these anions can act as "seeds" for electron avalanches. The algorithm and implementation details are presented, including how the streamer structure is optimized and how the ROI limits the seeds to a given region in space.

The motivation of Publication I was to demonstrate how electron avalanches could lead to streamer propagation, and to then explore how the various parameters affected the simulation results. The simulated streamers can be visualized by plotting the positions of all the simulated streamer heads, which gives a "shadow", as shown in figure 4(a). This type of plot is used to inspect if the shape and branching qualitatively resemble that of actual streamers, c.f. figure 1. Another common method of capturing a streamer in experiments is through "streak" imaging. In this imaging method, a series of narrow photographs are taken and placed sequentially, resulting in a picture with one spatial axis and one temporal axis. We achieve a similar result by plotting time on the x-axis and the distance to the plane of the streamer head

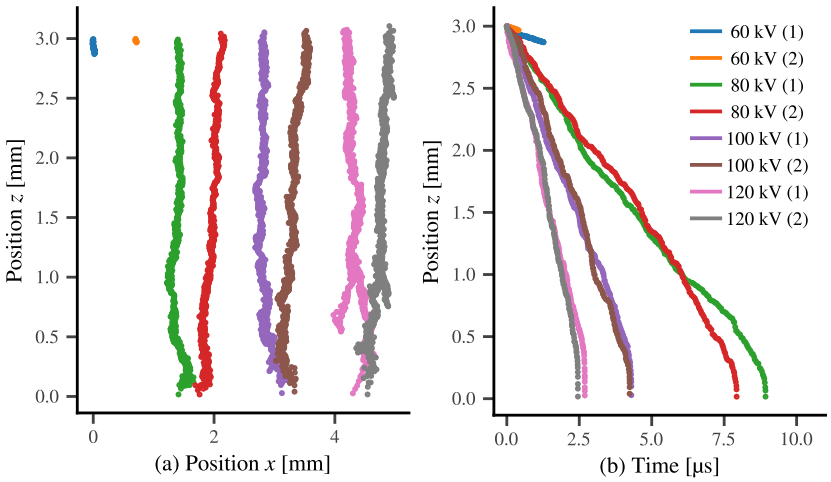

Figure 4: A shadow plot (a) and a streak plot (b) for four different voltages and two different initial seed configurations. Reproductions of figure 9 and figure 7 in Publication I.

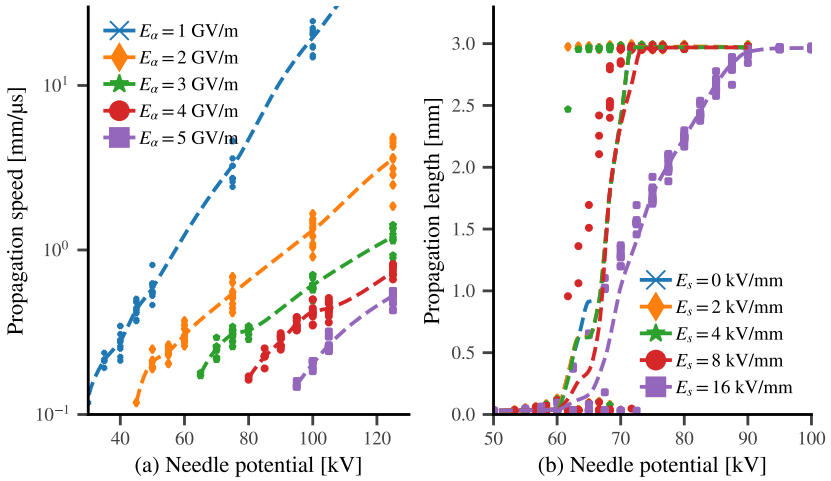

Figure 5: (a) Streamer propagation speed as a function of voltage for various values of the avalanche growth parameter E_α. (b) Streamer propagation length as a function of voltage for various values of the electric field within the streamer E_s. Each marker is a simulation and the dashed lines are interpolated to the average. Reproductions of figure 15 and figure 17 in Publication I.

closest to the plane on the z-axis, as shown in figure 4(b). The gradient in streak images gives the propagation speed of the streamer, and mode propagation change would give an abrupt change in the gradient. The simulations in figure 4 demonstrate two different aspects of the model, namely: how the speed increases with increasing voltage, and how the stochasticity influences the development of a streamer. The initial configuration of seeds, as well as their subsequent placement, is based on the initialization of the random number generator. In simulations where just the initial seed configuration differs, the streamers often have similar speed and branching tendencies. However, even streamers starting from the same seed configuration but different voltage diverge quickly after initiation. When the voltage is changed, the branching tendency and the speed differ as well.

Plotting the course of individual streamers, like in figure 4, is useful for qualitative analysis. However, streamer breakdown is stochastic and several simulations must be performed to capture this. A large number of simulations are presented in figure 5, with interpolations made to the average value at each voltage. Figure 5(a) shows that the average propagation speed is highly affected by the avalanche parameter E_α. Lowering E_α increases the propagation speed and lowers the propagation voltage. As long as the average electric field within the streamer channel E_s is low, propagating streamers lead to breakdown, as is the case in figure 4. In general, E_s has a low influence over a short gap, however, at high values for E_s, streamer stopping does occur mid-gap, even in a short gap, see figure 5(b). Plots such as those in figure 5 provide good insight on how sensitive the model is to variation in parameters when the outcome is stochastic.

We demonstrate in Publication I that streamer breakdown can be simulated with a model based on the electron avalanche mechanism. The simulated streamer propagation speed was lower than expected, however, this is a consequence of the high voltage required for propagation. The parameters related to calculating the avalanche growth, E_α in particular, have a huge impact on both propagation voltage and propagation speed. Furthermore, both the number of available anions and the mobility of electrons are important for the speed of the streamer. The degree of branching was found to be low, as seen in figure 4(a). However we demonstrated how the parameters controlling the streamer can be changed to facilitate or hinder streamer branching.

5.2 Conductivity and capacitance

The potential of each streamer head in Publication I is calculated given a fixed electric field within the streamer channel. Publication II makes the overall model more dynamic by considering the conductivity of the streamer channel and the capacitance between the streamer and the planar electrode. The potential of new heads is calculated by considering a transfer of charge between the new head and the closest existing head. If the average field within the streamer channel exceeds a threshold field E_{bd}, there is a breakdown within the channel, equalizing the potential between the given streamer head and the needle electrode. New heads are generally given a lower potential than that of the needle, however, conductivity in the streamer channel gradually increases the potential of the streamer heads. The resistance of the streamer channels scales with the time constant τ_0, i.e. a low τ_0 implies high conductivity and vice versa.

The effect of the updated model is well illustrated in figure 6, showing several simulations for various values of τ_0 and E_{bd}. A low τ_0 or E_{bd} gives a low average field within the streamer channel E_s and results similar to those in Publication I. Even though the streamers in figure 6 start with identical anion placement, they quickly diverge. Figure 6(a) indicates a greater degree of branching than figure 4(a), but the figures are not directly comparable since some of the parameters used in Publication I and Publication II are not equal. Figure 6(a) demonstrates that the updated model facilitates the propagation of several branches at the same time, whereas in Publication I, the main streamer branch would suppress other branches to a large degree. This effect is obtained by regulating the potential of the branches: fast-moving branches lose potential faster than slow-moving branches.

Regulating the potential of the streamer implies regulation of the propagation speed as well, which is seen as increased time-to-breakdown in figure 6(b). Figure 6(c) and (d) illustrate how the potential of the streamers change as a function of their position in the gap. Low conductivity (high τ_0) reduces the potential of the streamer during propagation in figure 6(c), while figure 6(d) demonstrates how lowering E_{bd} increases the average streamer potential through numerous breakdowns within the channel (reilluminations).

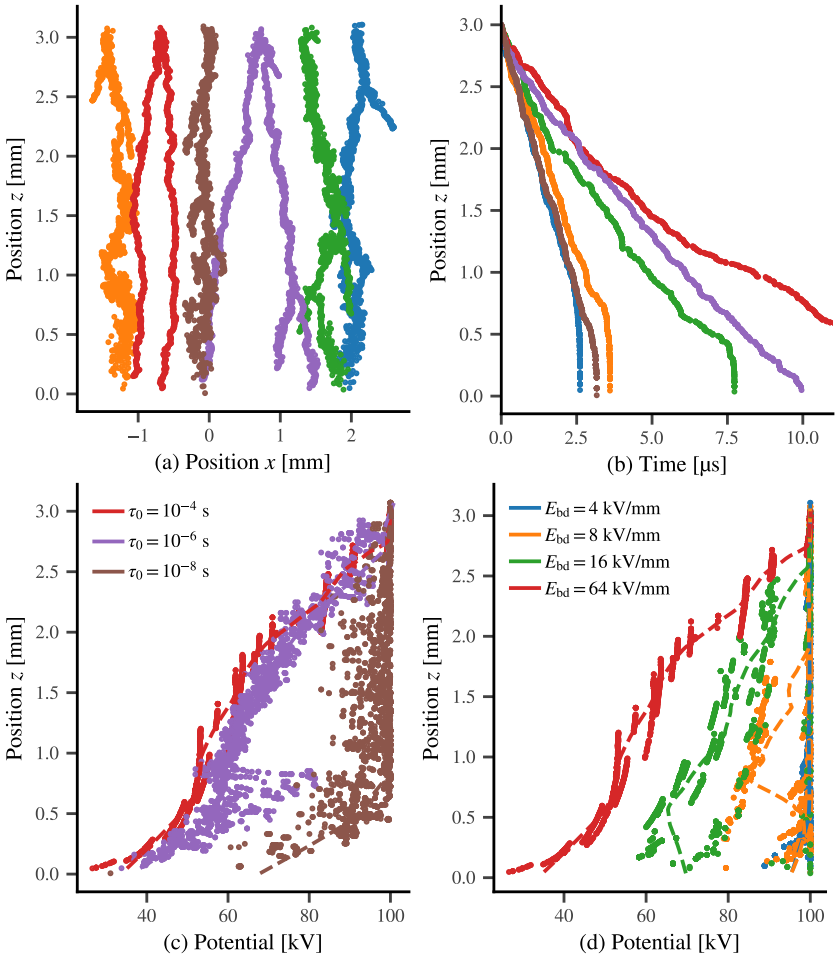

Figure 6: (a) Shadow plot of the positions of all the streamer heads. (b) Streak plot where only the position of the streamer head with the lowest z-value is shown. (c & d) The potential of each active streamer head, sampled 1000 times during propagation. All simulations in (c) have $E_{bd} = 64$ kV/mm and all simulations in (d) have $\tau_0 = 10^{-4}$ s. The legends for (c) and (d) are also valid for (a) and (b). The plots illustrate the influences of the streamer conductivity and the threshold for breakdown within the streamer channel. Reproductions of figure 5 in Publication II.

The improved model facilitates branching streamers, but the effect is not significant. A low propagation speed was already a weakness of the model, and this addition does not improve on that point, however, the dynamics of the streamer channel are now better represented. The model demonstrates how streamers with low conductivity stop when the streamer potential drops below the propagation voltage, and the model also captures how channel breakdowns can lead to increased streamer potential. Furthermore, an interesting aspect is that streamer branching, adding an extra streamer head without removing an existing head, causes a distinct reduction in streamer potential that can trigger a channel breakdown (reillumination).

5.3 Photoionization

A model for fast-mode streamer propagation through photoionization is developed in Publication III. Radiation is potentially an important part of streamer breakdown, however, its actual effect is not well-known. The motivation behind the work was to explore how radiation might affect streamer propagation. In particular, how photoionization can be involved in transitions between slow and fast modes.

Streamer breakdown is an energetic event where both emission and absorption of radiation can be important processes. We focus on photons from fluorescent radiation, because these are likely the most abundant photons of high energy. Under normal circumstances, when such radiation is absorbed by a molecule, it can excite an electron to a bound state. However, strong electric fields reduce the ionization potential (IP) of the molecules, and bound states can become unbound, ionizing a molecule excited to that state. In the model we developed for the photoionization cross-section, the likelihood of absorption causing photoionization is dependent on the electric field through the field-dependent IP. It is found that ionizing radiation is rapidly absorbed in a liquid, at a sub-μm scale. We argue that when the electric field exceeds a threshold E_w, fluorescent radiation from the streamer head becomes ionizing, and can lead to an increase in the propagation speed of the streamer. However, the energy of this radiation and the increase in propagation speed are not known.

The photoionization mechanism is included in the overall model by adding a speed v_w to any streamer head with an electric field ex-

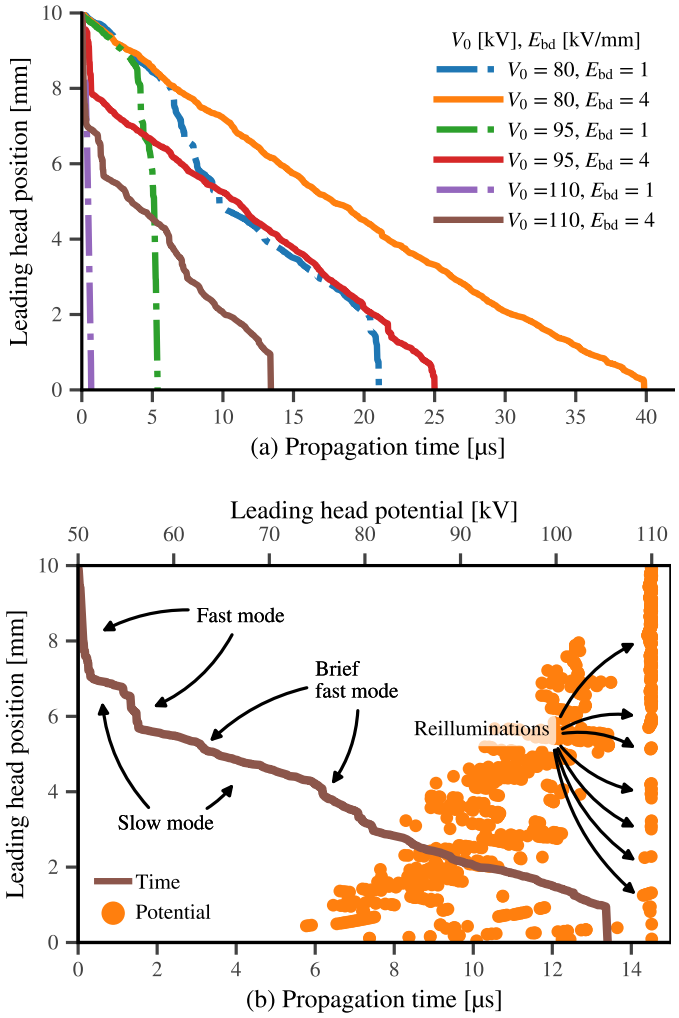

Figure 7: (a) Streak plot of streamer propagation, i.e. the position of the part of the streamer closest to the planar electrode, as a function of time. This illustrates how a streamer may switch between modes in different parts of the electrode gap. (b) Further details of one of the streamers in (a). Segments of slow and fast mode are indicated on the streak plot. A fast mode often corresponds to a reillumination, as indicated by an abrupt change to high potential. The potential of each active streamer head is plotted for every 10 µm of streamer propagation. Reproduction of figure 6 in Publication III.

ceeding E_w at the tip. Streamers with an electric field above E_w at the tip of a streamer head start in a fast mode, but will change to a slower mode if the field falls below the threshold during propagation. Conversely, if the field increases and exceeds the threshold during propagation, the streamer changes to a fast propagation mode. The change between different modes is well illustrated in figure 7(a) where streamers with a low E_{bd} can change to a fast mode, while streamers with a higher E_{bd} change to a slower mode. Having a higher E_{bd} gives a higher average (in time) field within the streamer channel, resulting in a lower (on average) field at the streamer head. The streamer detailed in figure 7(b) begins in a fast mode, but changes to a slow mode after propagating a few mm since the potential at the streamer head is reduced. As the streamer propagates farther, a series of channel breakdowns (reilluminations) occurs, resulting in brief durations of fast streamer propagation.

Radiation from the streamer head can be a method of transporting energy away from the critical part of the streamer. However, an electric field decreases the IP of the molecules and ionizing radiation is rapidly absorbed, facilitating the propagation of a streamer. Both the creation and the absorption of radiation are dependent on the composition of the liquid. Consequently, the effect of increased ionization, as well as the electric field strength required, are liquid dependent and hard to assess. Photoionization is often a topic mentioned in streamer literature, but the short range of ionizing radiation is seldom appreciated.

5.4 The software

The streamer model has been implemented in Python [77] and this software for simulating streamers has been released as open-source software (MIT license) under the name "Cerman" [S1]. Publication IV describes how to use Cerman, as well as its implementation.

Simulations series can be defined by a master input file, an example is shown in listing 1. The command "`cerman`" is used to control all aspects of the software through a command-line interface. Listing 2 demonstrates all the steps required for a simulation, from expanding the master input file, through simulation, to evaluating the results. The software works on a file specified by a "`filename`" or files matching a given "`pattern`". Several simulations can be performed in parallel

by specifying "no" number of threads. Plots of streamer "streak" and "speed" are created in the same way as the "shadow" plot demonstrated in listing 2. Many commands take extra "options" to further detail their function, and these options are printed by adding "-o help" to the command. The saved files can be parsed to find certain results, such as propagation length and average speed, which are saved in an archive. These results are plotted in an automated way by specifying which "parameter" to use for the x-axis. The legend for each other varied parameter is generated automatically.

Listing 1: Example of JSON-master file. A number of simulations are specified, varying the needle radius, the needle voltage, and the initial seed placement. The default values are used for non-specified parameters. Default values are found in Publication IV or by typing "cerman dump_defaults".

```
{
  "gap_size": 0.010,
  "needle_radius": [3e-6, 6e-6, 12e-6]
  "needle_voltage": "linspace(60e3, 150e3, 10)",
  "simulation_runs": 10
}
```

Listing 2: Example of how to create parameter files, run a simulation, and evaluate the results in a command-line interface. A description of these actions is included in section 5.4, and further information can be found in Publication IV.

```
# create input files
cerman ci -f <filename>
# simulate in sub-processes
cerman sims -g <pattern> -m <no>
# plot simulation - shadow plot
cerman ps shadow -g <pattern> -o <options>
# parse and combine archive of simulation results
cerman ca -g <pattern>
# plot the combined results
cerman pr <parameter> -f <file> -o <options>
```

A simulation is initiated by reading a parameter file to initialize various data structures used by the simulation. The simulation is essentially a loop, illustrated by figure 3, where the seeds and the streamer are updated iteratively. At the end of each iteration, relevant data is saved and information is printed, as specified by the user. When the simulation loop is terminated, any unsaved data is dumped to disk and a final entry in the log file is written.

The software facilitates creation and evaluation of simulations. Both the simulation and the plotting of results are done in a semi-automatic manner via the scripting interface. There exist a few different models for simulating streamers in liquid, as mentioned in chapter 3, but the code is rarely available. Furthermore, our model is built on different principles than other existing models for streamer breakdown in liquids. The purpose of Publication IV is to make the program available, and explain how the software is used. Different features of streamer propagation can already be captured by modifying the simulation parameters, however, the open-source code enables others to make modifications and contribute to the code.

5.5 Discussion

The model can be used to investigate several aspects of electrical breakdown: from streamer inception, propagation, and branching, to the breakdown itself. These aspects are dependent on the physical parameters given as input to the simulation model. The results demonstrate that electron avalanches can be responsible for streamer propagation.

Some properties can be improved to better align the modeled results with results from experiments: for instance, propagation voltage, propagation speed, and degree of branching. These three properties are also entwined in many ways. Reducing the propagation voltage will often increase the propagation speed and/or the branching tendency. However, increased branching also moderates the propagation speed in the model, as in experiments [42].

The high propagation voltage of the avalanche model is discussed in Publication I. The avalanche growth parameters give streamer inception in the correct range for propagating streamers. However, the simulated streamers do not propagate far at inception voltage, and the actual propagation voltage is high compared with experiments [I]. Just

above the inception voltage, the avalanches become critical in close proximity to the streamer, and do not add much to streamer expansion. The closer the streamer heads are, the more they also shield each other, which increases the chance of streamer stopping. An improvement is needed to make the streamer propagate at the correct propagation voltage, possibly by introducing a model for avalanche growth that reduces the inception voltage [I].

The speed of the simulated streamers depends on how often an avalanche becomes critical and how far from the streamer this occurs. This distance depends on the potential of the streamer through the model for avalanche growth, which in turn depends strongly on the electric field. The time between avalanches depends not only on the electric field, but also on the electron mobility and the number of seeds. Better representation of these properties, as well as of the model for avalanche growth, can improve the quality of the overall model.

The streamer structure gives rise to the electric field. Each streamer head is "connected" directly to the needle and all heads are included in the calculation to set shielding coefficients. How the potential of the streamer heads is set and how the streamer heads shield each other are important aspects of the model. The dynamics of the channel were improved in Publication II. Further development towards an electric network model can give a better representation of how charges move within the streamer structure. The computational cost of representing the streamer structure in such a way would be small compared to the cost of moving the seeds. Nevertheless, the current implementation is a good approximation for the electric field close to the streamer heads.

Photoionization was introduced to the model in Publication III as a mechanism for change to a fast mode. This model has some limitations, in particular that the energy of the radiation is unknown. Improvements to this mechanism, or the introduction of a different mechanism, are needed for a proper representation of a fast streamer. However, the simplified implementation still demonstrates the importance of streamer channel conductivity in changing from fast to slow modes. Consequently, reilluminations can trigger the change to a fast mode by increasing the conductivity.

6 Conclusion

Electrical breakdown in liquids, streamers in particular, is an interesting and challenging topic to research. Numerous mechanisms can influence the streamer, at various length and time scales, and it is difficult to differentiate the contribution of each mechanism. The motivation behind the modeling work has been to create an efficient model where the contributions of individual mechanisms can be investigated in conjunction with the model as a whole.

The model is realized in the framework of a needle–plane gap, where the needle electrode is modeled by an electrically charged hyperboloid, and the streamer is modeled by a set of virtual needles. The needle and the streamer give rise to an electric field in the liquid. The foundation of the model is the electron avalanche mechanism. Anions in the liquid can release electrons, which can become electron avalanches. Streamer growth is governed by avalanches obtaining a critical size. The model has an elevated propagation voltage, which results in a propagation speed that is low compared to experimental values. However, we have demonstrated that the avalanche mechanism is sufficient to capture several aspects of electrical breakdown in liquids.

The streamer conductivity, streamer capacitance, and streamer channel breakdown (reilluminations), improve the physical representation of the streamer structure. The model of the streamer structure needs further improvements, but even this simplified model of conductivity and breakdown within the streamer channel furthered our understanding of the dynamics of a streamer breakdown. The interaction between reilluminations and streamer mode change is particularly interesting.

Radiation is important for streamer breakdown, but the effect is difficult to differentiate from other contributions. The work on photoionization highlighted several interesting aspects, such as the long lifetimes of fluorescent states in cyclohexane, the electric field dependence of the photoionization cross-section, and the extremely short reach of ionizing radiation in liquids. We modeled an increase in propagation speed when the fluorescent radiation from the streamer head can cause ionization. This is possible when the IP of the liquid is reduced by

a strong electric field. Several parameters of this model are unknown, however, the simulations with this simplified model demonstrate the importance of channel conductivity for streamer mode change.

The complete simulation model is implemented in Python and published as open-source software. This enables others to replicate published results, design and perform simulations, as well as make modifications and contributions to the software. The software facilitates the creation of large simulation series and evaluation of the results in a semi-automatic manner through a command-line interface. It is easy to inspect details like the development of the potential of individual streamer heads, as well as the propagation length, shape, and speed of the streamers. The simulation results from whole series are easily extracted and combined to evaluate the influence of given parameters.

Future development of the simulation model should keep the main focus on the mechanisms leading to propagation. Some propagation mechanisms, like electron avalanches, are stepwise processes consisting of sequential expansions. The speed is then given by the frequency and the length of the expansions. Similarly, for electrohydrodynamics, some time is needed to create the motion, before the channel can expand. Other mechanisms, like field ionization, can be seen as a continuous process in some contexts. Different mechanisms require different field strengths to propagate a streamer at different speeds in different liquids. An effort is needed to systematize and quantify the contributions from the various mechanisms. The electric field is the foundation for the propagation and as such is of key importance for the model's accuracy and performance. Hence, future development should also aim to improve the representation of the streamer structure, particularly to enhance the calculation of the electric field accordingly. In this respect, the calculation of charge and energy balance are two aspects that can prove important alike. Furthermore, development towards simulating streamers in other geometries or streamers with negative polarity can offer additional insights.

Bibliography

1. **P. Wedin**.
Electrical breakdown in dielectric liquids - a short overview.
IEEE Electr. Insul. Mag. 30, 20–25 (2014).
DOI: 10/CXMK

2. **B. Farazmand**.
Study of electric breakdown of liquid dielectrics using schlieren optical techniques.
Br. J. Appl. Phys. 12, 251–254 (1961).
DOI: 10/BHCRHP

3. **S. Sakamoto, H. Yamada**.
Optical study of conduction and breakdown in dielectric liquids.
IEEE Trans. Electr. Insul. EI-15, 171–181 (1980).
DOI: 10/DWK579

4. **J.C. Devins, S.J. Rzad, R.J. Schwabe**.
Breakdown and prebreakdown phenomena in liquids.
J. Appl. Phys. 52, 4531–4545 (1981).
DOI: 10/FNC58F

5. **A. Beroual, R. Tobazeon**.
Prebreakdown Phenomena in Liquid Dielectrics.
IEEE Trans. Electr. Insul. EI-21, 613–627 (1986).
DOI: 10/BQBFJ4

6. **R. Tobazéon**.
Prebreakdown phenomena in dielectric liquids.
IEEE Trans. Dielectr. Electr. Insul. 1, 1132–1147 (1994).
DOI: 10/BHXNF8

7. **O. Lesaint**.
Prebreakdown phenomena in liquids: propagation 'modes' and basic physical properties.
J. Phys. D: Appl. Phys. 49, 144001 (2016).
DOI: 10/CXMF

8. **A. Sun, C. Huo, J. Zhuang.**
Formation mechanism of streamer discharges in liquids: a review.
High Volt. 1, 74–80 (2016).
DOI: 10/DBT2

9. **P. Biller.**
A simple qualitative model for the different types of streamers in dielectric liquids.
ICDL'96. 12th Int. Conf. Conduct. Break. Dielectr. Liq. 189–192 (1996).
DOI: 10/DHJCVX

10. **A. Beroual.**
Pre-breakdown mechanisms in dielectric liquids and predicting models.
2016 IEEE Electr. Insul. Conf. 117–128 (2016).
DOI: 10/CXMR

11. **A.E.D. Heylen.**
The relationship between electron-molecule collision cross-sections, experimental Townsend primary and secondary ionization coefficients and constants, electric strength and molecular structure of gaseous hydrocarbons.
Proc. R. Soc. A Math. Phys. Eng. Sci. 456, 3005–3040 (2000).
DOI: 10/DW9BFW

12. **A. Pedersen.**
On the electrical breakdown of gaseous dielectrics - an engineering approach.
IEEE Trans. Electr. Insul. 24, 721–739 (1989).
DOI: 10/D2KTHJ

13. **M. Haidara, A. Denat.**
Electron multiplication in liquid cyclohexane and propane.
IEEE Trans. Electr. Insul. 26, 592–597 (1991).
DOI: 10/DK77WH

14. **O.L. Hestad, P.O. Åstrand, L.E. Lundgaard.**
N-tridecane as a model system for polyethylene: Comparison of pre-breakdown phenomena in liquid and solid phase stressed by a fast transient.
IEEE Trans. Dielectr. Electr. Insul. 18, 1929–1946 (2011).
DOI: 10/FX2XS4

15. **D. Linhjell, L. Lundgaard, M. Unge, O. Hjortstam.**
Prebreakdown phenomena in hydrocarbon liquids in a point-plane gap under step voltage. Part 1: Behaviour at positive polarity.
J. Phys. Commun. (2020).
DOI: 10/DRSC

16. **P. Gournay, O. Lesaint.**
On the gaseous nature of positive filamentary streamers in hydrocarbon liquids. II: propagation, growth and collapse of gaseous filaments in pentane.
J. Phys. D: Appl. Phys. 27, 2117–2127 (1994).
DOI: 10/DW59F5

17. **O. Lesaint, G. Massala.**
Positive streamer propagation in large oil gaps: experimental characterization of propagation modes.
IEEE Trans. Dielectr. Electr. Insul. 5, 360–370 (1998).
DOI: 10/DCVZH7

18. **N.V. Dung, H.K. Høidalen, D. Linhjell, L.E. Lundgaard, M. Unge.**
Effects of reduced pressure and additives on streamers in white oil in long point-plane gap.
J. Phys. D: Appl. Phys. 46, 255501 (2013).
DOI: 10/CZM2

19. **M. Unge, S. Singha, N.V. Dung, D. Linhjell, S. Ingebrigtsen, L.E. Lundgaard.**
Enhancements in the lightning impulse breakdown characteristics of natural ester dielectric liquids.
Appl. Phys. Lett. 102, 172905 (2013).
DOI: 10/C9RD

20. **D. Linhjell, L.E. Lundgaard, M. Unge.**
Pressure Dependent Propagation of Positive Streamers in a long Point-Plane Gap in Transformer Oil.
2019 IEEE 20th Int. Conf. Dielectr. Liq. 1–3 (2019).
DOI: 10/DVBZ

21. **N.J. Felici.**
Blazing a fiery trail with the hounds.
IEEE Trans. Electr. Insul. 23, 497–503 (1988).
DOI: 10/BFVR8F

22. **P.J. Bruggeman, M.J. Kushner, B.R. Locke, et al.**
Plasma–liquid interactions: a review and roadmap.
Plasma Sources Sci. Technol. 25, 053002 (2016).
DOI: 10/CXMN

23. **L. Onsager.**
Deviations from Ohm's Law in Weak Electrolytes.
J. Chem. Phys. 2, 599–615 (1934).
DOI: 10/D9NZK5

24. **U. Gafvert, A. Jaksts, C. Tornkvist, L. Walfridsson.**
Electrical field distribution in transformer oil.
IEEE Trans. Electr. Insul. 27, 647–660 (1992).
DOI: 10/DBQ69G

25. **B. Halpern, R. Gomer.**
Field ionization in liquids.
J. Chem. Phys. 51, 1048–1056 (1969).
DOI: 10/C465G6

26. **A. Denat.**
Conduction and breakdown initiation in dielectric liquids.
2011 IEEE Int. Conf. Dielectr. Liq. (2011).
DOI: 10/BBM27M

27. **H.S. Smalø, O.L. Hestad, S. Ingebrigtsen, P.-O. Åstrand.**
Field dependence on the molecular ionization potential and excitation energies compared to conductivity models for insulation materials at high electric fields.
J. Appl. Phys. 109, 073306 (2011).
DOI: 10/DMKSZM

28. **L. Dumitrescu, O. Lesaint, N. Bonifaci, A. Denat, P. Notingher.**
Study of streamer inception in cyclohexane with a sensitive charge measurement technique under impulse voltage.
J. Electrostat. 53, 135–146 (2001).
DOI: 10/B26HNG

29. **T. Hibma, H.R. Zeller.**
Direct measurement of space-charge injection from a needle electrode into dielectrics.
J. Appl. Phys. 59, 1614–1620 (1986).
DOI: 10/DW6F29

30. **S. Boggs.**
Very high field phenomena in dielectrics.
IEEE Trans. Dielectr. Electr. Insul. 12, 929–938 (2005).
DOI: 10/DMRB95

31. **P. Gournay, O. Lesaint.**
A study of the inception of positive streamers in cyclohexane and pentane.
J. Phys. D: Appl. Phys. 26, 1966–1974 (1993).
DOI: 10/CK4HXG

32. **A. Denat, J.P. Gosse, B. Gosse.**
Electrical conduction of purified cyclohexane in a divergent electric field.
IEEE Trans. Electr. Insul. 23, 545–554 (1988).
DOI: 10/FF86GV

33. **O. Lesaint, L. Costeanu.**
Positive streamer inception in cyclohexane: Evidence of formative time and cavitation process.
2017 IEEE 19th Int. Conf. Dielectr. Liq. 1–4 (2017).
DOI: 10/CZMZ

34. **T.J. Lewis.**
A new model for the primary process of electrical breakdown in liquids.
IEEE Trans. Dielectr. Electr. Insul. 5, 306–315 (1998).
DOI: 10/CWT2G2

35. **R.P. Joshi, J. Qian, G. Zhao, J. Kolb, K.H. Schoenbach, E. Schamiloglu, J. Gaudet**.
Are microbubbles necessary for the breakdown of liquid water subjected to a submicrosecond pulse?
J. Appl. Phys. 96, 5129–5139 (2004).
DOI: 10/CT3SK3

36. **S.E. Derenzo, T.S. Mast, H. Zaklad, R.A. Muller**.
Electron avalanche in liquid xenon.
Phys. Rev. A 9, 2582–2591 (1974).
DOI: 10/BKRDCV

37. **R. Kattan, A. Denat, O. Lesaint**.
Generation, growth, and collapse of vapor bubbles in hydrocarbon liquids under a high divergent electric field.
J. Appl. Phys. 66, 4062–4066 (1989).
DOI: 10/C9Z5K2

38. **W. Knorr, D. Breitfelder**.
Breakdown in transformer oil with AC and impulse voltage stress.
1984 IEEE Int. Conf. Electr. Insul. 291–296 (1984).
DOI: 10/DPFQ

39. **V.M. Atrazhev, E.G. Dmitriev, I.T. Iakubov**.
The impact ionization and electrical breakdown strength for atomic and molecular liquids.
IEEE Trans. Electr. Insul. 26, 586–591 (1991).
DOI: 10/D2MG8N

40. **G.V. Naidis**.
On streamer inception in hydrocarbon liquids in point-plane gaps.
IEEE Trans. Dielectr. Electr. Insul. 22, 2428–2432 (2015).
DOI: 10/GBF7X2

41. **G.V. Naidis**.
Modelling of streamer propagation in hydrocarbon liquids in point-plane gaps.
J. Phys. D: Appl. Phys. 48, 195203 (2015).
DOI: 10/CXMJ

42. **O. Lesaint, M. Jung.**
On the relationship between streamer branching and propagation in liquids: influence of pyrene in cyclohexane.
J. Phys. D: Appl. Phys. 33, 1360–1368 (2000).
DOI: 10/c4xf84

43. **A. Luque, U. Ebert.**
Electron density fluctuations accelerate the branching of positive streamer discharges in air.
Phys. Rev. E 84, 046411 (2011).
DOI: 10/dfc4s2

44. **J. Jadidian, M. Zahn, N. Lavesson, O. Widlund, K. Borg.**
Stochastic and deterministic causes of streamer branching in liquid dielectrics.
J. Appl. Phys. 114, 063301 (2013).
DOI: 10/cxmq

45. **N. Davari, S. Haghdani, P.-O. Åstrand, G.C. Schatz.**
Local electric field factors by a combined charge-transfer and point–dipole interaction model.
RSC Adv. 5, 31594–31605 (2015).
DOI: 10/drbj

46. **P. Atten, A. Saker.**
Streamer propagation over a liquid-solid interface.
10th Int. Conf. Conduct. Break. Dielectr. Liq. 441–445 (1993).
DOI: 10/dzgjfd

47. **A. Saker, P. Atten.**
Properties of streamers in transformer oil.
IEEE Trans. Dielectr. Electr. Insul. 3, 784–791 (1996).
DOI: 10/dgms5p

48. **G. Massala, O. Lesaint.**
Positive streamer propagation in large oil gaps: electrical properties of streamers.
IEEE Trans. Dielectr. Electr. Insul. 5, 371–380 (1998).
DOI: 10/cfk7km

49. **T. Top, G. Massala, O. Lesaint.**
Streamer propagation in mineral oil in semi-uniform geometry.
IEEE Trans. Dielectr. Electr. Insul. 9, 76–83 (2002).
DOI: 10/DK4VTG

50. **L. Lundgaard, D. Linhjell, G. Berg, S. Sigmond.**
Propagation of positive and negative streamers in oil with and without pressboard interfaces.
IEEE Trans. Dielectr. Electr. Insul. 5, 388–395 (1998).
DOI: 10/CN8K5W

51. **O. Lesaint.**
"Streamers" in liquids: Relation with practical high voltage insulation and testing of liquids.
2008 IEEE Int. Conf. Dielectr. Liq. 1–6 (2008).
DOI: 10/BWM3JR

52. **S. Singha, J. Viertel, M. Unge, J. Karlsson, K. Johansson, H. Faleke.**
Development of a natural ester liquid with significantly enhanced dielectric characteristics.
2014 IEEE 18th Int. Conf. Dielectr. Liq. 1–4 (2014).
DOI: 10/C9RF

53. **T.G. Aakre, L.E. Lundgaard, M. Unge.**
Time to breakdown studies for liquids of different physico-chemical nature.
2017 IEEE 19th Int. Conf. Dielectr. Liq. 1–4 (2017).
DOI: 10/DZC7

54. **S. Ingebrigtsen, H.S. Smalø, P.-O. Åstrand, L.E. Lundgaard.**
Effects of electron-attaching and electron-releasing additives on streamers in liquid cyclohexane.
IEEE Trans. Dielectr. Electr. Insul. 16, 1524–1535 (2009).
DOI: 10/FPTPT5

55. **N. Davari, P.-O. Åstrand, S. Ingebrigtsen, M. Unge.**
Excitation energies and ionization potentials at high electric fields for molecules relevant for electrically insulating liquids.
J. Appl. Phys. 113, 143707 (2013).
DOI: 10/CX9X

56. **S. Liang, F. Wang, Z. Huang, W. Chen, Y. Wang, J. Li.**
Significantly improved electrical breakdown strength of natural ester liquid dielectrics by doping ultraviolet absorbing molecules.
IEEE Access 7, 73448–73454 (2019).
DOI: 10/C6V7

57. **L. Niemeyer, L. Pietronero, H.J. Wiesmann.**
Fractal dimension of dielectric breakdown.
Phys. Rev. Lett. 52, 1033–1036 (1984).
DOI: 10/D35QR4

58. **H.J. Wiesmann, H.R. Zeller.**
A fractal model of dielectric breakdown and prebreakdown in solid dielectrics.
J. Appl. Phys. 60, 1770–1773 (1986).
DOI: 10/BFTK47

59. **S. Satpathy.**
Dielectric breakdown in three dimensions: results of numerical simulation.
Phys. Rev. B 33, 5093–5095 (1986).
DOI: 10/FP7PBK

60. **D.T. Gillesple.**
Exact Stochastic Simulation of couple chemical reactions.
J. Phys. Chem. 81, 2340–2361 (1977).
DOI: 10/DRNSJM

61. **P. Biller.**
Fractal streamer models with physical time.
Proc. 1993 IEEE 11th Int. Conf. Conduct. Break. Dielectr. Liq. (ICDL '93) 199–203 (1993).
DOI: 10/DCTXZ7

62. **A. Kupershtokh, D. Karpov.**
Stochastic features of initiation of liquid dielectric breakdown at small area of positive electrode.
Proc. 1999 IEEE 13th Int. Conf. Dielectr. Liq. (Cat. No.99CH36213) 203–206 (1999).
DOI: 10/BX42SN

63. **B.T. Murphy, R.E. Hebner, E.F. Kelley**.
Simulating mode transitions during breakdown in liquids.
IEEE Trans. Dielectr. Electr. Insul. 18, 682–691 (2011).
DOI: 10/CFKBV5

64. **M. Kim, R. Hebner, G. Hallock**.
Modeling the growth of streamers during liquid breakdown.
IEEE Trans. Dielectr. Electr. Insul. 15, 547–553 (2008).
DOI: 10/BNTB22

65. **A. Ershov, A. Kupershtokh**.
Fluctuation model of liquid dielectrics breakdown with incomplete charge relaxation.
Proc. 1993 IEEE 11th Int. Conf. Conduct. Break. Dielectr. Liq. (ICDL '93) 194–198 (1993).
DOI: 10/DRCNX3

66. **D.I. Karpov, A.L. Kupershtokh**.
Models of streamers growth with "physical" time and fractal characteristics of streamer structures.
Conf. Rec. 1998 IEEE Int. Symp. Electr. Insul. (Cat. No.98CH36239) 607–610 (1998).
DOI: 10/BXR8CT

67. **A. Kupershtokh, D. Karpov**.
Models of pulse conductivity of streamers propagating in dielectric liquid.
IEEE Int. Conf. Dielectr. Liq. 2005. ICDL 2005. 85–88 (2005).
DOI: 10/CFP9ZB

68. **A.L. Kupershtokh, D.A. Medvedev**.
Lattice Boltzmann equation method in electrohydrodynamic problems.
J. Electrostat. 64, 581–585 (2006).
DOI: 10/BRNX49

69. **I. Fofana, A. Beroual**.
Predischarge models in dielectric liquids.
Jpn. J. Appl. Phys. 37, 2540–2547 (1998).
DOI: 10/BM4SD5

70. **T. Aka-Ngnui, A. Beroual.**
Modelling of multi-channel streamers propagation in liquid dielectrics using the computation electrical network.
J. Phys. D: Appl. Phys. 34, 794–805 (2001).
DOI: 10/BNHS3K

71. **T. Aka-Ngnui, A. Beroual.**
Determination of the streamers characteristics propagating in liquids using the electrical network computation.
IEEE Trans. Dielectr. Electr. Insul. 13, 572–579 (2006).
DOI: 10/B8DR5T

72. **J. Qian, R.P. Joshi, J. Kolb, et al.**
Microbubble-based model analysis of liquid breakdown initiation by a submicrosecond pulse.
J. Appl. Phys. 97, 113304 (2005).
DOI: 10/DMHK4F

73. **J. Qian, R.P. Joshi, E. Schamiloglu, J. Gaudet, J.R. Woodworth, J. Lehr.**
Analysis of polarity effects in the electrical breakdown of liquids.
J. Phys. D: Appl. Phys. 39, 359–369 (2006).
DOI: 10/C75HFF

74. **J.G. Hwang, M. Zahn, L.A.A. Pettersson.**
Mechanisms behind positive streamers and their distinct propagation modes in transformer oil.
IEEE Trans. Dielectr. Electr. Insul. 19, 162–174 (2012).
DOI: 10/CXMP

75. **J. Jadidian, M. Zahn, N. Lavesson, O. Widlund, K. Borg.**
Abrupt changes in streamer propagation velocity driven by electron velocity saturation and microscopic inhomogeneities.
IEEE Trans. Plasma Sci. 42, 1216–1223 (2014).
DOI: 10/F55GJ5

76. **G.V. Naidis.**
Modelling the dynamics of plasma in gaseous channels during streamer propagation in hydrocarbon liquids.
J. Phys. D: Appl. Phys. 49, 235208 (2016).
DOI: 10/CXMG

77. **Python Software Foundation**.
Python Language Reference.
https://www.python.org.

I

Inge Madshaven, Per-Olof Åstrand, Øystein Leif Hestad, Stian Ingebrigtsen, Mikael Unge, Olof Hjortstam
Simulation model for the propagation of second mode streamers in dielectric liquids using the Townsend–Meek criterion
Journal of Physics Communications **2**:105007 (2018)
DOI: 10/CXJF | ARXIV: 1804.10473

IOP Publishing J. Phys. Commun. 2 (2018) 105007 https://doi.org/10.1088/2399-6528/aae0e6

Journal of Physics Communications

OPEN ACCESS

RECEIVED
30 May 2018

REVISED
26 July 2018

ACCEPTED FOR PUBLICATION
12 September 2018

PUBLISHED
10 October 2018

PAPER

Simulation model for the propagation of second mode streamers in dielectric liquids using the Townsend-Meek criterion

I Madshaven[1], P-O Åstrand[1], O L Hestad[2], S Ingebrigtsen[2,4], M Unge[3] and O Hjortstam[3]

[1] Department of Chemistry, NTNU - Norwegian University of Science and Technology, 7491 Trondheim, Norway
[2] SINTEF Energy Research, 7465 Trondheim, Norway
[3] ABB Corporate Research, 72178 Västerås, Sweden
[4] Present address: ABB AS, 5257 Kokstad, Norway.

E-mail: per-olof.aastrand@ntnu.no

Keywords: simulation model, streamer, electron avalanche, Townsend-Meek criterion, dielectric liquid, electrical breakdown

Abstract

A simulation model for second mode positive streamers in dielectric liquids is presented. Initiation and propagation is modeled by an electron-avalanche mechanism and the Townsend–Meek criterion. The electric breakdown is simulated in a point-plane gap, using cyclohexane as a model liquid. Electrons move in a Laplacian electric field arising from the electrodes and streamer structure, and turn into electron avalanches in high-field regions. The Townsend–Meek criterion determines when an avalanche is regarded as a part of the streamer structure. The results show that an avalanche-driven breakdown is possible, however, the inception voltage is relatively high. Parameter variations are included to investigate how the parameter values affect the model.

1. Introduction to streamers

Dielectric liquids are widely used for insulation of high power equipment, such as transformers, since liquid insulation has good cooling properties, high electrical withstand strength, and recovers from an electrical discharge within short time [1]. Electric breakdown in liquids is preceded by the formation of a prebreakdown channel called a streamer [2]. A partial discharge, a local electric breakdown, changes the electric field distribution, which could cause another local breakdown, and in this way, a streamer may propagate through a liquid. A streamer bridging the gap between two electrodes, for instance an energized part and a grounded part, lowers the electrical withstand strength and may cause a complete electric breakdown, possibly destroying the equipment [1].

A streamer consists of a gaseous and partly ionized structure, originating in one location and branching out in filaments as it propagates through the liquid. This structure may be observed through shadowgraphic or schlieren photography since its refractive index differs from the surrounding liquid [3]. Streamers are classified as positive or negative, depending on the polarity of the initiation site. Streamer experiments are often carried out in needle-plane gaps since a strongly divergent field allows control of where the streamer initiates, the polarity of the streamer, and also enables the study of streamers that initiate, propagate, and then stops without causing an electric breakdown [2, 3]. Conversely, in a gap with a uniform field, inception governs the breakdown probability, since an initiated streamer is always able to propagate the gap due to the high background field.

The nature of streamers has been investigated for decades [1–14], but is still not well understood. For positive streamers in non-polar liquids, it is common to define four distinct modes of propagation, mainly characterized by their speed [2, 15]. The streamer mode depends on the applied voltage, and may change during propagation. The 1st mode propagates in a bubbly or bushy fashion with a speed of the order of 100 m s^{-1}, the 2nd mode is faster, of the order of 1 km s^{-1}, and has a branched or tree-like structure. The even faster 3rd and 4th modes propagates at speeds of the order of 10 km s^{-1} and 100 km s^{-1}, respectively. The 1st mode is only observed for very sharp needles and will usually not lead to a breakdown by itself, but the streamer may change to the 2nd mode. The 2nd mode may initiate for voltages below the voltage required for breakdown, and increases in propagation length and number of branches at higher voltages. Often, a 2nd mode streamer sporadically emits

visible light [3], re-illuminations, from one or more of its branches. Above the breakdown voltage, streamers may change between the 2nd, the 3rd, and the 4th mode during propagation. There are usually more re-illuminations in the 3rd mode than the 2nd mode. The inception of the 4th mode is associated with a drastic increase in speed and fewer, more luminous, branches [2].

There are numerous mechanisms that can be involved in the streamer phenomena, the challenge is identifying their importance during initiation and propagation. Applying a potential to a needle can cause charge injection, giving a space-charge limited current [16] causing Joule heating [16], which in turn can cause bubble nucleation [17]. A breakdown in the gas bubble can then propagate the needle potential, and the process may repeat. This is one way to explain 1st mode propagation. Electric fields can also cause electrohydrodynamic flow, which could cause streamer formation through cavitation [18]. Electrostatic cracking has also been proposed as a cavitation mechanism [19]. A main topic of discussion is whether a lowering of the liquid density is needed before charge generation can occur. Electron avalanches are important in gas discharge, but their importance in liquid breakdown is still disputed. In water, strong scattering could prevent electrons from forming avalanches in the liquid phase [20]. Therefore, discharges in micro-bubbles can be important for charge generation [10, 14, 20]. The same mechanism was also proposed for non-polar liquids [19], however, the relative permittivity is about 80 in water and about 2 in a typical oil, and this difference can prove important since the field enhancement within a bubble in oil is much lower than in water. Contrary to water, there are indications of electron avalanches in non-polar liquids [16, 21, 22], furthermore, while the initiation and the propagation length of 2nd mode streamers are dependent on the pressure, their propagation velocity is not pressure dependent [16, 23]. This implies that the mechanism responsible for propagation occurs in the liquid phase and that the gaseous channel follows as a consequence. In very high electric fields, field-ionization can occur [24, 25], and this mechanism has been proposed for the fast 3rd and 4th propagation modes [7]. As the streamer gains length, the properties of the channel could also prove important. The streamer channel is a partly ionized, low-temperature plasma, having a varying conductance [8, 26]. The mechanisms involved when a plasma is in contact with a liquid is often overlooked and is in itself a very complex problem [27].

The development of models is important for improving electrical equipment as well as the prevention of equipment failure. An early simulation model for liquid breakdown uses a lattice to investigate the fractal nature of the streamer structure as a function of the electric field E [28], and has been expanded to incorporate needle-plane geometry [29], a 3D-lattice [30], statistical time [31], availability of seed electrons [32], and varying conductance of the streamer channels [33]. Charge generation and transport in an electric field have also been solved by a finite element method (FEM) approach, to simulate streamer propagation in 2D and 3D, adding impurities to generate streamer branching [34–37]. A major difference between breakdown in gases and liquids is that a phase change is involved when making the streamer channel in liquids. The phase change is difficult to model, but it is possible to make approximations [38], or to focus on the plasma within the channel [39].

Both lattice and FEM simulations require considerable computational power, and therefore, the simulations are often done for either very short timescales or very simplified models. The work presented here is based on [40], which chooses a different approach. It is a computational model for 2nd mode positive streamers in non-polar liquids, driven by electron avalanches in the liquid phase. A point-plane geometry is modeled, with the point being a positively charged hyperbolic needle. Cyclohexane is used as a model liquid, since it is a well defined system used extensively in experiments [5, 11, 22, 25, 41].

The model and the theoretical background is presented in section 2, as well as the parameters and the algorithm used for the simulations. In section 3, the results are given and discussed. First a baseline is established, then parameter variations and alternative parameter values are investigated. A general discussion, outlining the weaknesses and strengths of the model, is given in section 4. Finally, the main conclusions are summarized in section 5. The Appendix contains additional details on the coordinate system used in the model.

2. Simulation model and theory

The model is built on the assumption that electron avalanches occur in the liquid phase, and that these govern the propagation of 2nd mode, positive streamers [40].

Applying a potential to the needle in a needle-plane geometry gives rise to an electric field. A number of anions and electrons, assumed to be already present in the liquid, are accelerated by the electric field. Subsequently, electron multiplication occurs in areas where the electric field is sufficiently strong, turning electrons into electron avalanches. An avalanche is assumed to be 'critical' if it reaches a magnitude given by the Townsend–Meek criterion [42], and the position of such an avalanche is regarded as a part of the streamer. Then the electric field is reevaluated, accounting for the potential of both the needle and the streamer. This work investigates liquid cyclohexane as the insulating liquid, with the option to add dimethylaniline (DMA) as an

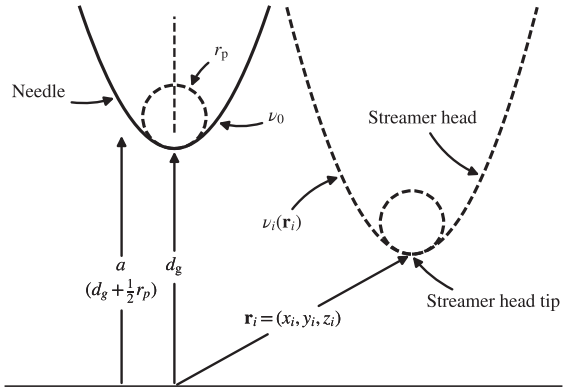

Figure 1. The hyperbolic needle and a streamer head, with relevant variables shown. The distance to the plane is usually far greater than illustrated here.

additive, but the model can be used for other base liquids and additives as well, if the parameter values are available.

2.1. Geometrical and electrical properties

A hyperbolic needle electrode with a tip radius r_p is placed at a distance d_g from a planar electrode, as illustrated in figure 1 where all important geometric variables are shown. In prolate spheroid coordinates $(\mu, \nu, \phi; a)$, a hyperboloid is represented by a single coordinate ν, and the 3D Laplace equation becomes separable, see appendix for details and definitions. The potential is (cf. (A.15))

$$V_i = C_i \ln \tan \frac{\nu_i}{2}, \tag{1}$$

and the electric field is (cf. (A.17))

$$\boldsymbol{E}_i = \frac{C_i\, \hat{\boldsymbol{\nu}}_i}{h_{\nu_i} \sin \nu_i}, \tag{2}$$

where C_i is a constant. The subscript i refers to a given hyperboloid (the needle or a streamer head), hence, the subscript in ν_i implies a transformation to a coordinate system centered at hyperboloid i,

$$\nu_i(\boldsymbol{r}) = \nu(x - x_i,\, y - y_i,\, z;\, a_i). \tag{3}$$

The constant C_i (cf. (A.16)) is given by the boundary condition, the potential at the surface $\nu_i(\boldsymbol{r}_i)$,

$$C_i \approx \frac{2V_i(\boldsymbol{r}_i)}{\ln(4z_i/r_{p,i})}, \tag{4}$$

which is valid for a sharp needle, $r_p \ll z_i$. The other boundary condition, that the potential is zero at the plane $V_i(\boldsymbol{r}\hat{\boldsymbol{z}} = 0) = 0$, is already accounted for. For the needle, $V_i(\boldsymbol{r}_i) = V_0$, which is the applied potential. Calculating the electric field in (2) is the most expensive part of the computer simulation, although explicit calculation of the trigonometric functions can be avoided (cf. appendix). Using the Laplace equation instead of the Poisson equation is a simplification that will be discussed further in section 4.

2.2. Electrons and ions in dielectric liquids

Naturally occurring radiation is of the order of $D_r = 1$ mSv per year [43] and may produce electron-cation pairs by ionizing neutral molecules. The production rate is [44]

$$R_e = D_r\, \rho\, G, \tag{5}$$

where the density ρ is 0.78 kg/l for cyclohexane. The yield G is usually given in events per 100 eV. Hydrocarbons typically have an ion yield G_{ion} of about 4 [45], and for cyclohexane it is 4.3 [46]. However, the free electron yield G_{free} is much lower, about 0.15 [46, 47], which implies that most electrons recombines geminately. This gives a production of $R_e = 2.3 \times 10^8$ m^{-3} s^{-1}. The recombination process is rapid, and the electron lifetime is [44]

$$\tau_r = \frac{4\pi\epsilon_0\epsilon_r r_0^3}{3\mu_{el} e}, \tag{6}$$

where ϵ_0 is the vacuum permittivity, $\epsilon_r = 2.0$ is the typical relative permittivity for hydrocarbons, r_0 is the recombination distance, μ_e is the electron mobility, and e is the elementary charge. Inserting the thermalization distance (the most likely distance) $r_0 = 5.9$ nm[46] and a mobility $\mu_e = 45$ mm^2 V^{-1} s^{-1} [47, 48], yields $\tau_r = 1.7$ ps.

The average drift velocity v_d of an electron or ion is given by its mobility μ and the local electric field $\boldsymbol{E}$,

$$\boldsymbol{v}_d = \mu \boldsymbol{E}. \tag{7}$$

In liquids where the electron mobility is low ($\mu_e < 10^2$ mm^2 V^{-1} s^{-1}), the electron is regarded as localized, and electron transport is explained either through a hopping or a trapping mechanism [49, 50]. The drift velocity is proportional to the electric field when the electric strength is low, however, for low-mobility liquids, it becomes superlinear in high fields [44, 49]. The lifetimes of free electrons and ions can be related to the reaction rates. The reaction rate constants k_r are found by the Debye relation [44, 51],

$$k_r = \frac{e}{\epsilon_0 \epsilon_r}(\mu_- + \mu_+), \tag{8}$$

where $\mu_\pm$ is the mobility of the respective reacting species. This relation assumes that recombination is limited by diffusion, which is related to the mobilities, and the relation holds as long as the mobilities are low ($<10^4$ mm^2 V^{-1} s^{-1}) [44]. In cyclohexane, the ion mobility is of the order of 10^{-2} to 10^{-1} mm^2 V^{-1} s^{-1} [16, 25, 46, 52–54] and the electron mobility is of the order of 10 mm^{2}V^{-1}s^{-1} [46, 47, 55, 56]. Using $\mu_e = 45$ mm^{2}V^{-1}s^{-1} and $\mu_{ion} = 0.1$ mm^2 V^{-1} s^{-1}, yields $k_r = 4.1 \times 10^{-13}$ m^3/s for electron-ion recombination and $k_r = 1.8 \times 10^{-15}$ m^3/s for ion-ion recombination according to (8). This implies that there is a far greater number of anions than electrons. However, small impurities, such as O_2, have higher mobilities [44].

The low-field conductivity for the liquid σ is given by the number density of charge carriers n_i for species i and their mobilities,

$$\sigma = e \sum_i n_i \mu_i. \tag{9}$$

By assuming that the measured conductivity is due to ions only and that the ions are similar in number and mobility, the number density of the anions is

$$n_{ion} = \frac{\sigma}{2e\mu_{ion}}, \tag{10}$$

which yields $n_{ion} = 6.2 \times 10^{12}$ m^{-3} for $\sigma = 0.2$ pS/m [54, 57]. A similar result is obtained by considering a steady-state condition,

$$\frac{dn_e}{dt} = R_e - k_r n_e n_p - \frac{n_e}{\tau_a} = 0, \tag{11}$$

where n_e is the electron density, n_p is the cation density, and t is the time. If the electron attachment time τ_a is large [58],

$$n_e \approx n_p \approx \sqrt{\frac{R_e}{k_r}}, \tag{12}$$

which yields $n_e = 2.4 \times 10^{10}$ m^{-3}. However, τ_a is assumed small, about 200 ns [37], which implies that $n_{ion} \approx n_p$. Using (12) with the ion-ion recombination rate yields $n_{ion} = 3.6 \times 10^{11}$ m^{-3}, about an order of magnitude lower than what obtained from (10). With rapid attachment, (11) is

$$n_e \approx R_e \, \tau_a. \tag{13}$$

and yields $n_e = 46$ m^{-3}, which shows that the assumption $n_{ion} \approx n_p$ holds.

2.3. Electron avalanches

The main concept the model is that electrical breakdown is driven by electron avalanches occurring in the liquid phase [11, 22, 40]. A number of anions, calculated by (10), is considered as the source of electrons by an electron-detachment mechanism. These electrons initiates the avalanches. As shown in section 2.2, the number of anions is far greater than the number of electrons, and it is also far greater than the number of electrons produced within a simulation (a volume less than $1cm^3$ and a time less than 1 s).

The needle electrode and the streamer creates an electric field $\boldsymbol{E}$. Transformer oils experience increased conductivity due to ion dissociation when the electric field exceeds some MV/m [59]. The model assumes that also electrons detach from anions for field strengths exceeding $E_d = 1$ MV/m. This is a low threshold, in the sense that most electrons detach, therefore, the effect of increasing it is explored as well. The movement Δs of each electron or anion i is calculated by

$$\Delta \boldsymbol{s}_i = \boldsymbol{E}_i \, \mu_i \, \Delta t. \tag{14}$$

The simulation time step Δt is chosen low enough, typically 1 ps to 10 ps, to ensure that Δs is less than 0.1 μm. For a positive streamer, the negative charged species move towards higher field strengths. Increasing the electric field strength, increases the kinetic energy an electron gains between colliding with molecules as well as lowering the ionization potential (IP) of the molecules [13], which increases the probability of impact ionization. As electron attachment processes dominate at low field strengths, an electric field exceeding $E_a = 0.2$ GV/m is required for electron multiplication to be observed in cyclohexane [22]. The electric field at a streamer head must not only exceed E_a, but also be strong enough to cause electron multiplication over a sufficient distance, for the streamer to propagate.

An electron avalanche occurs when electron multiplication is dominant and the number of electrons N_e grows rapidly. The growth of such an avalanche is modeled as [42]

$$\mathrm{d}N_e = N_e \, \alpha \, \mathrm{d}s, \tag{15}$$

where α is the average number of electrons generated per unit length. For discharges in gases, α is assumed to be dependent on the type of molecules, the density, and the electric field strength [60]. Assuming that the same holds for a liquid, considering a constant liquid density [22, 61], yields

$$\alpha = \alpha_m \exp\left(-\frac{E_\alpha}{E}\right). \tag{16}$$

The maximum avalanche growth α_m and the inelastic scattering constant E_α are dependent on the liquid and are found from experimental data [22, 62]. Equation (15) leads to an exponential growth of electrons in an avalanche,

$$N_e = N_0 \exp\left(\int \alpha \, \mathrm{d}s\right) = N_0 \exp Q_e, \tag{17}$$

where N_0 is the initial number of electrons, and Q_e is introduced as a measure of the avalanche size. At each simulation step, Q_e for each avalanche is increased by

$$\Delta Q = \alpha \, \Delta s = \alpha \, E \, \mu \, \Delta t. \tag{18}$$

For discharges in gases it is assumed that an electron avalanche becomes unstable when the electron number N_e exceeds some threshold N_c, which is known as the Townsend–Meek avalanche-to-streamer criterion [42]. In the model, an avalanche obtaining this criterion is removed and its position is considered as a part of the streamer channel. Assuming that an avalanche starts from a single electron, the criterion $N_e > N_c$ is rewritten as

$$Q_e = \ln N_e > Q_c. \tag{19}$$

The Meek constant Q_c is typically 18 in gases [42, 63], but the value is expected to be higher in liquids since the denser media has a higher breakdown strength, and creation of higher electric fields requires more electrons. However, a recent study on liquids found values in the range 5 to 20 when evaluating a number of experiments [62]. Another study found $Q_c = 23$, or an avalanche size of about 10^{10} electrons, by considering the field required for propagation [11], in contrast to the field required for initiation, which is more common.

2.4. Additives

Additives with low IP have proven to facilitate the propagation of 2nd mode streamers, since such additives lower the voltage required for propagation and for breakdown, whereas they increase the voltage required for 4th mode streamers [2]. This is likely a consequence of an increased number of branches, which may increase the electrostatic shielding and thereby reducing the electric field at the streamer heads [9, 41]. To account for the effect of low-IP additives on electron avalanche growth, the mole fraction c_n of the additive and the IP difference between the base liquid I_b and the additive I_a, is used to modify the expression for α in (16) as [11]

$$\alpha' = \alpha(1 - c_n + c_n \, e^{k_\alpha (I_b - I_a)}), \tag{20}$$

where the parameter $k_\alpha = 2.8$ eV^{-1} is estimated from experiments [11]. For example, an additive with an IP difference of 3.1 eV from the base liquid, in a concentration c_n of 0.1%, yields $\alpha' = 6.9\alpha$. Equation (20) is derived assuming that ionization is caused by electrons in the exponentially decaying, high-energy tail of a Maxwellian distribution, and that the introduction of an additive does not significantly change the energy distribution [11].

2.5. Streamer representation

The model focuses on the processes occurring in front of the streamer. The streamer is represented by a collection of hyperboloids, approximating the electric field in front of the streamer. The streamer channel, and in particular its dynamics, is not included in the model. The streamer hyperboloids are referred to as 'streamer heads', and the initial streamer consists of only one streamer head: the needle. The needle, one other streamer head, and relevant variables, are shown in figure 1.

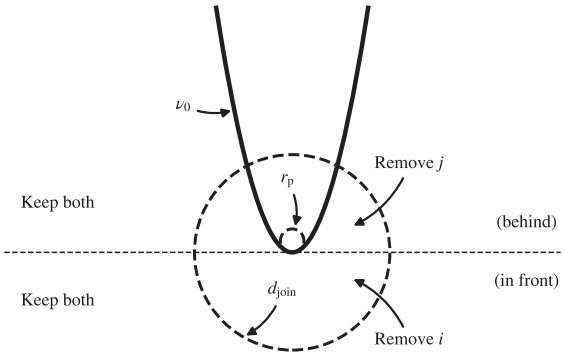

Figure 2. For given a streamer head i (shown), other positions are considered to be within, behind, in front, and/or within join distance.

The potential V at position $\boldsymbol{r}$ is given by a superposition of the potential V_i in (1) of each streamer head,

$$V(\boldsymbol{r}) = \sum_i k_i \, V_i(\boldsymbol{r}), \tag{21}$$

where the coefficients k_i are introduced to account for electrostatic shielding between the heads. The electric field is found in a similar manner,

$$\boldsymbol{E}(\boldsymbol{r}) = \sum_i k_i \, \boldsymbol{E}_i(\boldsymbol{r}), \tag{22}$$

where $\boldsymbol{E}_i$ in (2) is the electric field arising from streamer head i. The electric field arising from a streamer head is strongly dependent on its tip radius r_p. Experiments have shown that there exists a critical tip radius for the inception of 2nd mode streamers, which is $r_p = 6$ μm for cyclohexane [5, 64].

When an electron avalanche meets the Townsend–Meek criterion in (19), a new streamer head is added at the position of the avalanche. The potential at the tip of streamer head i is given by

$$V_i(\boldsymbol{r}_i) = V_0 - E_s \, \ell_i, \tag{23}$$

where V_0 is the potential at the needle, E_s is the electric field within the streamer channel, and ℓ_i is the distance from the tip of the needle to the tip of streamer head i,

$$\ell_i = |\boldsymbol{r}_i - d_g \, \hat{\boldsymbol{z}}|, \tag{24}$$

again see figure 1 for definitions. Equation (23) is used to find C_i through (4).

The shielding coefficients k_i ensure that the combined potential of all the streamer heads equals the potential at the tip of each streamer head,

$$V(\boldsymbol{r}_i) = \sum_j k_j \, V_j(\boldsymbol{r}_i) \approx V_i(\boldsymbol{r}_i), \tag{25}$$

and are obtained by a non-negative least squares (NNLS) routine [65]. The problem actually solved numerically is stated in a slightly different form. Defining

$$M_{ij} = \frac{V_j(\boldsymbol{r}_i)}{V_j(\boldsymbol{r}_j)} = \frac{\ln \tan\left(\frac{1}{2}\nu_j(\boldsymbol{r}_i)\right)}{\ln \tan\left(\frac{1}{2}\nu_j(\boldsymbol{r}_j)\right)}, \tag{26}$$

which only depend on the geometry and not on the potentials, (25) is rewritten as

$$V_i(\boldsymbol{r}_i) \approx \sum_j M_{ij} \, k_j \, V_j(\boldsymbol{r}_j), \tag{27}$$

which is computationally more convenient to solve.

It is desirable to keep the number of streamer heads to a minimum since it is expensive to calculate the electric field from a head. Also optimization of the potential becomes more difficult and unstable as it tend to become a more overdetermined problem with more heads present, especially when the heads are close or 'within' each other. Streamer heads located within another streamer head are removed, that is, if

$$\nu_i(\boldsymbol{r}_j) < \nu_i(\boldsymbol{r}_i), \tag{28}$$

then streamer head j is removed, which is the same as being above the ν_0-line in figure 2. In addition, if the tip of one streamer head is within a certain distance d_m of the tip of another streamer head,

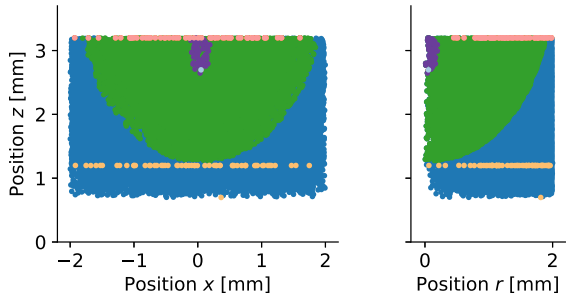

Figure 3. Region of Interest, *xz*- and *rz*-projection. Each seed is represented by a dot; anion (blue), electrons (green), avalanches (purple), behind ROI (pink), newly placed (tan), and a single critical (light blue).

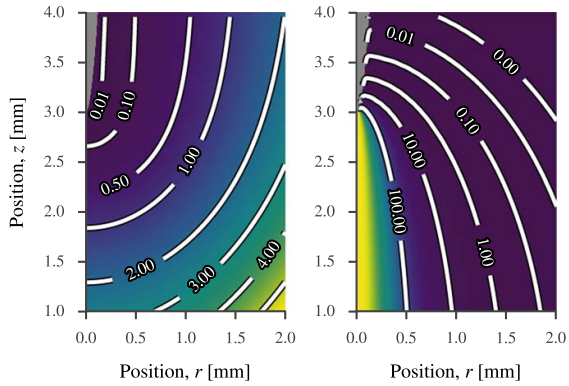

Figure 4. Time to collision t_i (left, in milliseconds) and maximum avalanche size Q_i (right), for an electron originating at a given position. The needle hyperbola is shown in gray. For a gap distance of 3 mm, a tip radius of 6 μm, and at a potential of 100 kV.

$$|\boldsymbol{r}_i - \boldsymbol{r}_j| < d_{\mathrm{m}}, \tag{29}$$

the heads are merged and only the streamer head closest to the plane is kept (see figure 2). Physically, this is motivated as charge transferred from one streamer head to another located closer to the grounded plane. Finally, since fewer heads implies less calculation and faster simulations, streamer heads with a shielding coefficient below a given threshold,

$$k_i < k_{\mathrm{c}}, \tag{30}$$

are also removed. When k_{c} is chosen sufficiently low, only streamer heads that are to a large degree shielded by other heads are removed, and removing them have thus little effect on the simulation results.

The streamer consist of one or more heads as it propagates. When a new head is added, the conditions (28), (29) are used to evaluate whether the new heads should be kept and whether any of the existing heads should be removed. A new head added at a sufficient distance from the existing head(s) can initiate streamer branching. However, for the actual branching to occur, the streamer must be able to propagate (add new heads) both from the new head and from the existing head(s). The result is then that the streamer at some point grows in two directions at the same time. This occurs rarely, since the leading streamer head shields the potential of the other heads and reduces the probability of propagation from those heads.

2.6. Region of interest

Anions, electrons, and avalanches are here referred to as 'seeds'. The seeds are placed as anions, but can become electrons or avalanches, depending on the local electric field strength, which is illustrated in figure 3. To save computational cost, especially for simulations in large gaps, seeds are limited to a region of interest (ROI) surrounding the leading tip, see figure 3. The ROI is a cylinder defined by a radius from the centerline ($x^2 + y^2 = r^2$), a distance in front of the leading streamer head, and a distance behind the leading head. Seed avalanches that obtain a critical size, seeds that collide with a streamer head, and seeds that fall behind the ROI, are removed and replaced by new seeds. A new seed is placed one ROI length from the old seed in the z-direction,

Table 1. Model parameters, physical.

Gap distance	d_g	3.0 mm
Applied voltage (varies)	V_n	—
Needle tip curvature	r_n	6.0 μm
Streamer tip curvature [5]	r_s	6.0 μm
Field in streamer [8, 66]	E_s	2.0 KV mm^{-1}
Electron detachment threshold	E_d	1.0 MV m^{-1}
Avalanche threshold [22]	E_a	0.2 GV m^{-1}
Scattering constant [22]	E_α	3.0 GV m^{-1}
Max avalanche growth [22]	α_m	200 μm^{-1}
Meek constant [11]	Q_c	23
Electron mobility [55, 56]	μ_e	45 mm^2/Vs
Anion mobility [16]	μ_{ion}	0.30 mm^2/Vs
Ion conductivity [54]	σ_{ion}	0.20 pS m^{-1}
Base liquid IP [67]	I_b	10.2 eV
Additive IP [68]	I_a	7.1 eV
Additive IP diff. factor [11]	k_α	2.8 eV^{-1}
Additive number density	$c_{a,n}$	0.0

Table 2. Model parameters, algorithm.

Streamer head merge distance	d_m	50 μm
Potential shielding threshold	k_c	0.10
Time step	Δt	1.0 ps
Micro step number	N_{msn}	100
ROI—behind leading head	z^+_{roi}	0.5 mm
ROI—in front of leading head	z^-_{roi}	1.5 mm
ROI—radius from center	r_{roi}	2.0 mm
Stop—low streamer speed	v_{min}	100 m/s^{-1}
Stop—streamer close to plane	z_{min}	50 μm
Stop—avalanche time	t^{ava}_{max}	100 ns

with random placement within the ROI radius for the x- and y-coordinates. The seed density is thus kept constant as the ROI moves together with the leading streamer head.

Removing or rearranging the seeds does not change the electric field, since the charge from the seeds is not included in the Laplacian field. Charge from single cations, anions, or electrons should not have a big influence, but the charge from electrons and cations created by electrons avalanches is also ignored, and this is a major simplification. An avalanche colliding with the streamer is shielded by the streamer and does not contribute to the streamer propagation. A critical avalanche, however, propagates the streamer potential to its position. In any case, when an avalanche is removed, its charge is considered as absorbed by the streamer.

For a given configuration, it is possible to calculate the time t_i for an electron to travel from a given point to the needle. This is achieved by numeric integration of $\nu_d^{-1}\,\mathrm{d}l$ along an electric field line (constant μ), using $h_\nu = \mathrm{d}l/\mathrm{d}\nu$ (cf. (A.12)),

$$t_i = \int_{\text{position}}^{\text{needle}} \frac{h_\nu}{\nu_d}\,\mathrm{d}\nu. \tag{31}$$

Similarly, the maximum avalanche size Q_i, is computed by

$$Q_i = \int_{\text{position}}^{\text{needle}} \alpha\, h_\nu\,\mathrm{d}\nu. \tag{32}$$

An illustration of (31), (32) is found in figure 4. Both ν_d in (7) and α in (16) are functions of the electric field E in (2), which makes numeric integration straightforward in prolate spheroid coordinates. The time, t_i, provides an indication of how large the ROI should be. Given that a slow streamer may propagate at $1\ \mathrm{km/s}^{-1} = 1\ \mathrm{mm}/\mu\mathrm{s}^{-1}$, the ROI should be chosen so wide that seeds on the sides does not have enough time to collide with the passing streamer. According to figure 4, a width of 1.5 mm gives about 1 μs before collision, both from the sides and from below. As the streamer should propagate about the same length, or more, in this time, is a reasonable value. However, a somewhat wider ROI should be used to account for a streamer propagating off-center, and for branched propagation. Further, figure 4 shows that Q_i is large in the front, but quickly declines for seeds behind the streamer head. This gives an indication on how far behind the streamer head an avalanche may obtain critical size, which is how far behind the streamer head it is interesting to extend the ROI. However,

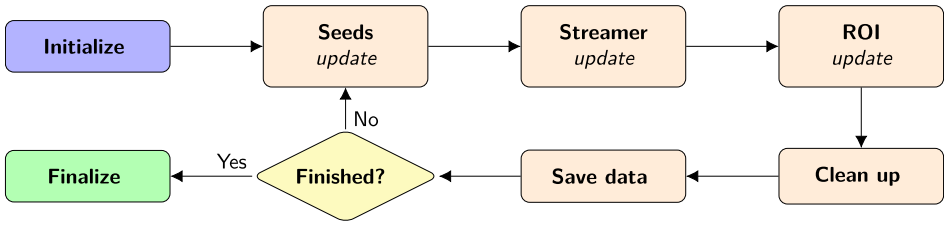

Figure 5. The main steps of the simulation algorithm. The algorithm for the seeds is detailed in figure 6. See section 2.8 for further details on each step.

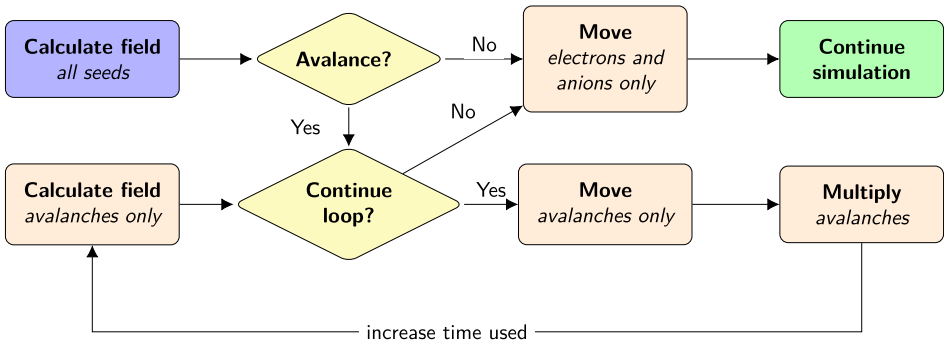

Figure 6. Algorithm for moving and multiplying seeds. This is the block labeled 'Seeds' in figure 5. See section 2.8 for details on each step.

the ROI should also extend far enough behind the leading streamer head to enable the propagation of secondary branches. Even though t_i and Q_i give good indications of how big the ROI should be, it is important to verify the settings after the simulation, or vary the ROI to verify that the results are not affected.

2.7. Parameters

The model parameters may be divided in two groups: physical parameters and parameters for the numerical algorithm. The values of the physical parameters summarized in table 1 are given by the properties of the simulated experiment or based on values available in the literature for the base liquid (cyclohexane) and the additive (dimethylaniline). Since not all the parameter values are available and some are uncertain, a sensitivity analysis is carried out in this work to investigate the influence of individual parameters. Parameter values needed by the simulation algorithm, which are not based on physical properties, are given in table 2 and include the size of the ROI and certain criteria for stopping a simulation.

The initial setup is given by V_n, d_g, and r_n. Then the number fraction of seeds n_{ion} is calculated using μ_{ion} and σ_{ion}, according to (10), and whether a seed is considered as an anion, an electron, or an avalanche is given by E_d and E_a. The electron multiplication probability is given by (16), using E_α and α_m. If an additive is present, then (20) is also applied, where I_b, I_a, $c_{a,n}$, and k_α are used. Equation (18) gives the growth of an avalanche, using Δt and μ_e. Finally, the Townsend–Meek criterion, stated in (19), uses Q_c to evaluate whether the avalanche has obtained a critical size. The streamer branching is regulated by d_m and k_c, by (29), (30), while the streamer head potential, and thus also the electric field at the tip, is dependent on E_s and r_s through (23).

2.8. Algorithm

A simulation begins by reading an input file that is used to initialize the various data classes used by the program, including random placement of seeds within the ROI, thereafter, a loop is executed until the simulation is complete. These main steps are shown in figure 5. The first and most expensive step of the algorithm is the update of the seeds, which is detailed in figure 6. First, the electric field is calculated for all seeds (each anion, electron, and avalanche). All the avalanches are treated separately in a loop, where they are moved, the electrons are multiplied, and the field is calculated for their new positions. This loop, in figure 6, is performed until either N_{msn} steps are done, an avalanche becomes critical (obtaining the Townsend–Meek criterion), or an avalanche

collides with the streamer. Then, all other seeds (anions and electrons) are moved, using a time step equal to the total time used by the avalanches. The next step in figure 5 is to update the streamer structure. Any critical avalanches are added to the streamer, and the streamer structure is optimized by removing heads using (28), (29) and correcting the scaling using (27) to set k_i for each streamer head. Thereafter, if there is a new leading streamer head, the ROI is updated. In the 'clean-up' part, seeds behind the ROI, critical seeds, and seeds that have collided with the streamer, are removed and replaced by new seeds. A number of criteria can be set to determine when the simulation loop in figure 5 should end. For instance, total simulation time, total CPU time, and number of iterations. However, simulations presented in this work ended for one of three reasons: the leading head reached the planar electrode ($z_i < z_{\min}$), low propagation speed ($< v_{\min}$), or long time between critical avalanches ($> t^{\text{ava}}_{\max}$). The final step of the loop is saving data, and finalizing a simulation ensures that all temporary data is properly saved to files.

The implementation has been done in Python [69] using NumPy [70] extensively. During initialization, the seed for random numbers is set in NumPy to ensure reproducible results. The input parameters are given in a JSON-formatted file, which is used for initiation of the simulation. Simulation results are saved with Pickle and illustrated using Matplotlib [71].

3. Simulation results and discussion

The model involves numerous parameters, some of which is given by the experimental setup (e.g. gap distance), others by properties of the liquids (e.g. mobilities), and some are purely for the simulation procedure (e.g. time step). In the first part, the default parameters given by tables 1 and 2 show the basic behavior of the model. Thereafter, a sensitivity analysis is presented, indicating the influence of various parameters. Mainly the propagation speed is used to indicate the differences, but the number of streamer heads, their scaling k_i, the propagation length, and the degree of branching are also investigated. Ten simulations are carried out at each voltage, using the numbers 1 to 10 in the random number generator generating different initial configurations of the seed distribution.

3.1. Simulation baseline

Simulations have been performed for a range of voltages, using the parameters in tables 1 and 2. These simulations are used as a baseline in the sensitivity analysis. As seen from the streak plots in figure 7, a voltage exceeding 60 kV is needed for a breakdown. For lower voltages, the streamer propagates less than 100 μm before the simulation is terminated, either because of waiting too long for an avalanche or because of very slow propagation speed. Above the breakdown voltage, the time to breakdown is reduced as the voltage is increased, and the streamers tend to accelerate towards the end of their propagation. The average propagation speed, shown in figure 8 tells a similar story, but it also indicates that the propagation speed slows down a bit after the first few steps. The speed reduction is possibly due to branching, however, by looking at the streamer in figure 9, it is clear that the degree of branching is very low, but the streamer gets thicker with increasing voltage. This implies that even though branching is not apparent, there are several streamer heads present. The number of streamer heads may increase when the electric field strength increases (at higher voltages or closer to the plane) as seen in figure 10. Values of k_i lower than one implies that the streamer heads shield each other to some degree (cf. (21)), as seen in figure 10, but not enough to stop a propagating streamer. It is of interest to investigate how the leading head is affected by shielding, and the average scaling indicates this. The propagation speed can be described by the time it takes to get a critical avalanche in front of the leading streamer head combined with the distance the leading head is moved, where the latter is presented in figure 11. Increased voltage increases both the maximum and the average propagation 'jumps', especially when the streamer is in the final part of the gap.

The propagation speeds in figure 8 are somewhat low for 2nd mode streamers, which should be 1 km s^{-1} to 10 km s^{-1} [2]. Many, if not most, of the simulation parameters affects the propagation speed. In the case of the electron mobility μ_e, it is easy to see that the propagation speed is directly proportional to μ_e, since it only affects the movement of the electrons (cf. (14)). For most other parameters, it is not that simple.

3.2. Effect of avalanche parameters

The avalanche mechanism is the most important part of the model. For this reason, parameters relevant to the avalanche growth, given in (16), (19), are especially important. To get an avalanche, however, a seed electron is needed. A doubling of the concentration of seeds n_{ion}, gives about a doubling in the propagation speed, as seen in figure 12. The figure shows the average speed for the mid 50% of the gap, that is for a position from 0.75 mm to 2.25 mm. Since streamers terminated in the first quarter of the gap are not shown, the figure also indicates that the breakdown voltage is dependent on n_{ion}, as increasing n_{ion} allows propagation at lower voltages. The streamer is represented by one or more heads, and propagates as new heads are added in front of current heads.

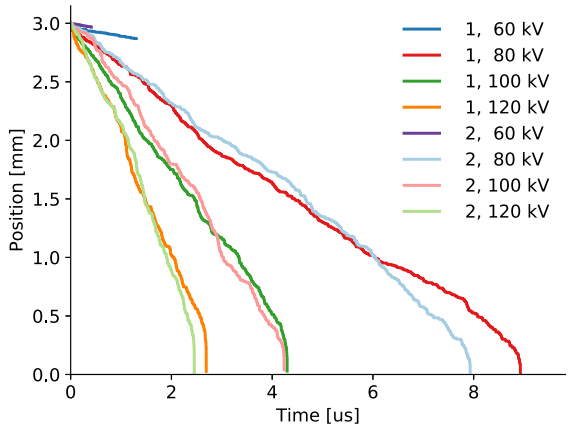

Figure 7. Streak plots, time spent versus leading head position, for two simulations (different initial random numbers) at each voltage. The streamers start a the position of the needle, $z = d_g = 3.0$ mm.

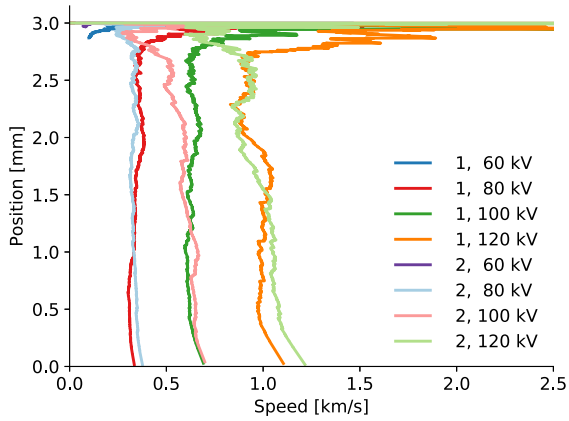

Figure 8. Streamer average speed versus leading head position, that is, the average gradient of the 'streaks' shown in figure 7.

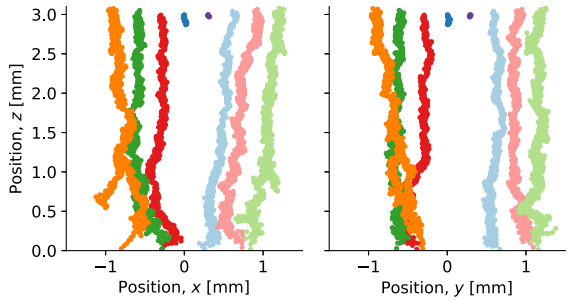

Figure 9. Streamer trails, *xz*- and *yz*-projection for a range of voltages 60 kV to 120 kV, using the same legend as in figure 7. Each dot represents the position of a streamer head at some point of the propagation. The streamers are plotted with an offset to improve the readability.

As such, the leading head moves in a series of discrete 'jumps'. The average streamer head jump length seems independent of n_{ion}, indicating that the linear increase in propagation speed is caused by a reduction in the time required for an electron to become a critical avalanche. At $n_{\text{ion}} = 2 \times 10^{12}$ m^{-3}, the average distance between

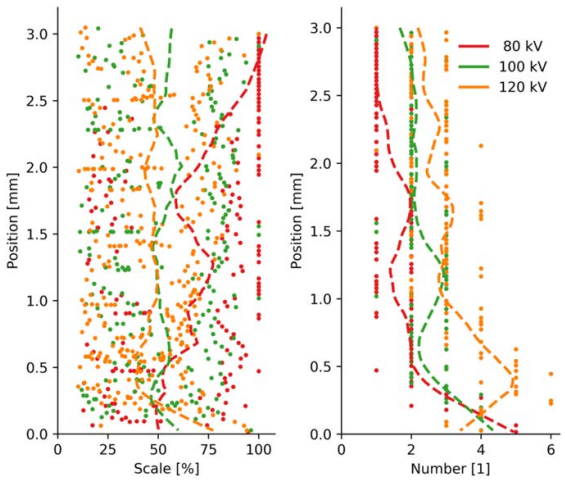

Figure 10. Actual streamer head scale k_i (left) and total number of streamer heads (right). Data are taken every 1% of the gap. The dashed lines are moving averages calculated by loess-regression [72].

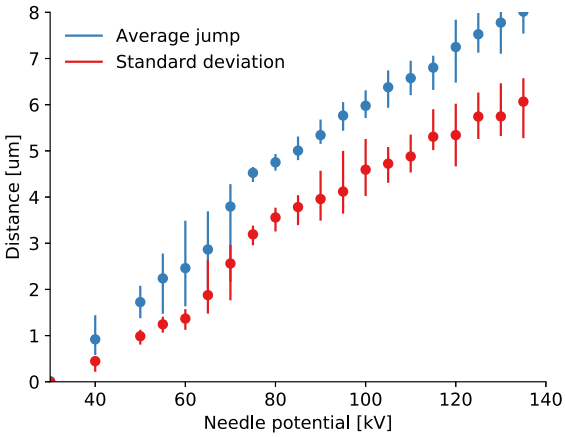

Figure 11. The leading streamer head is moved in a sequence of discrete 'jumps' in the z-direction. The average jump length and the standard deviation of the jumps are found for each individual simulation. The dotted lines are interpolated to the average, and the bars covers the minimum and maximum values for ten simulations at the same voltage.

seeds is 79 μm, while the average jump length is about 6 μm, so n_{ion} would have to be increased by some orders of magnitude to affect the streamer jump distance. Inhomogeneities on the order of 10^{11} m^{-3} was introduced by [37] to explain branching, but this effect is not found here. An upper estimate on the ions available can be calculated from (12) by using G_{ion} instead of G_{free} when calculating R_e in (5) and using a low estimate of $k_r = 10^{-3}$ mm^2 V^{-1} s^{-1} [37, 53], yielding $n_{\text{ion}} = 1.8 \times 10^{13}$ m^{-3} and an average distance of 38 μm between seeds. As such, the simulations in figure 12 cover the most interesting range.

The baseline results in section 3.1 do not show any stopping of streamer propagation mid-gap. The streamers either stop within the first 100 μm or cause a breakdown. This occurs when the supply of electrons is constant and E_s is too low to create a high voltage drop along the streamer. Increasing the electron detachment threshold E_d reduces the number of electrons available, which in turn reduces the density of electrons as electrons are swept out, see figure 13. This results in a negative feedback loop where a lower density of electrons decreases the speed (figure 12) and the decreased speed results in a lower rate of ions turning into electrons. The propagation length is shown as a function of the needle potential and E_d in figure 14. By considering $E_d = 15$ MV m^{-1}, three different regimes is identified. Up to 70 kV, a few avalanches may occur, but then the propagation stops. Above 90 kV, the propagation is fast enough

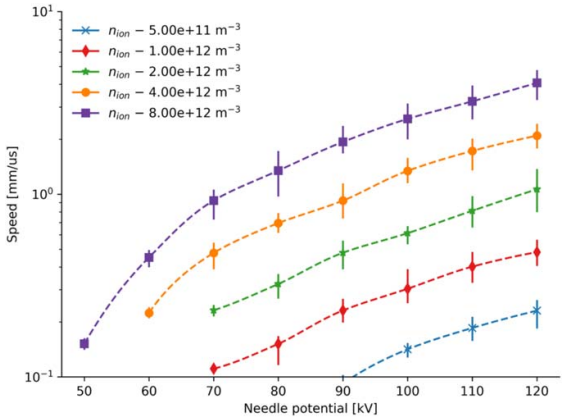

Figure 12. The effect of seed concentration n_{ion} on the average streamer propagation speed for the middle 50% of the gap. Streamers terminated in the first 25% of the gap are excluded. The default concentration is about 2×10^{12} m^{-3}. The dashed lines are interpolated to the average, and the bars covers the minimum and maximum values.

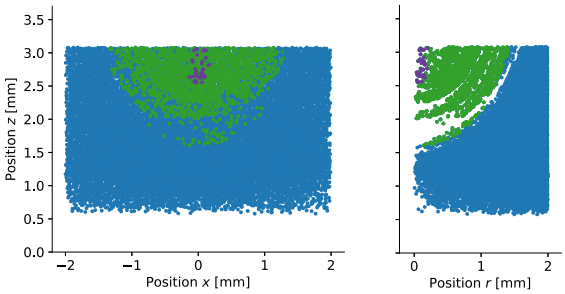

Figure 13. Streamer stop after sweep-out of too many electrons at 90 kV and $E_d = 15$ MV m^{-1}. *xz*- and *rz*-projection where each seed is represented by a dot; anion (blue), electrons (green), and avalanches (purple).

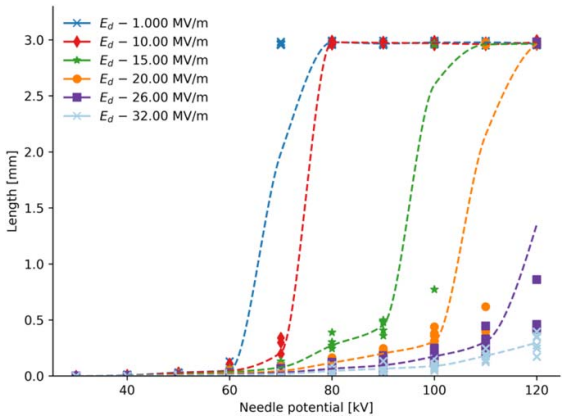

Figure 14. Streamer propagation length as a function of needle potential and electron detachment threshold E_d. Each marker is a simulation and the dotted lines are interpolated to the average.

to provide a stable rate of new electrons, enabling the propagation to continue. In between, the initial electrons allow the streamer to propagate, but the electron density is decreasing and the streamer eventually stops.

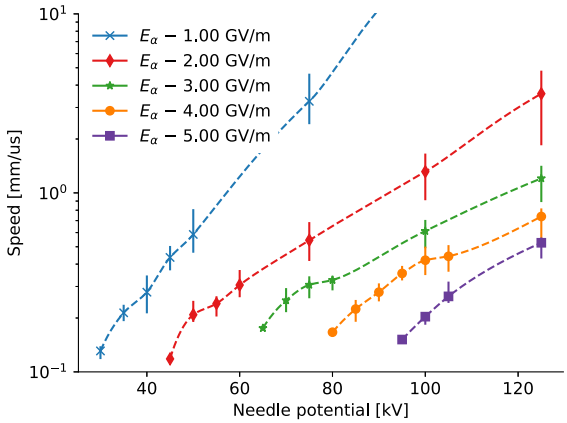

Figure 15. The effect of E_α on the average streamer propagation speed for the middle 50% of the gap. The dashed lines are interpolated to the average, and the bars covers the minimum and maximum values.

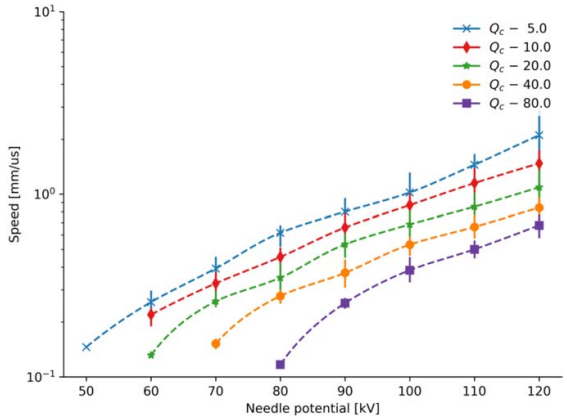

Figure 16. The effect of Q_c on the average streamer propagation speed for the middle 50% of the gap. The dashed lines are interpolated to the average, and the bars covers the minimum and maximum values.

The electric field is important for electron movement and multiplication, and E_α in (16) is therefore an important parameter. The strong influence of E_α is seen in figure 15, where the propagation speed may increase by an order of magnitude when E_α is reduced by 50%. This makes sense as E_α enters exponentially in (16). The propagation speed of 2nd mode streamers is weakly dependent on the applied voltage [2], however, for $E_\alpha = 1$ GV m^{-1} in figure 15, the dependence is much stronger than for the other values. Reducing E_α facilitates streamer propagation and the breakdown voltage is thus strongly influenced. Both E_α and α_m are based on experimental results, and are very important to the model. Instead of varying α_m, however, the Meek-constant Q_c is varied. From (16), (18), (19), it is clear that the avalanche size Q_e is linearly dependent on α_m, which implies that doubling Q_c has the same effect as halving α_m. The speed is not as affected by Q_c as intuitively expected, see figure 16, and changing Q_c by a factor of 4 only changes the speed by a factor of 2. However, Q_c cannot change much before the simulation becomes unphysical. For instance, consider a conducting sphere of $r = 6$ μm with a charge $q = \exp(Q_c)$. The electric field at the surface is

$$E = \frac{eq}{4\pi\epsilon r^2}, \tag{33}$$

where e is the electron charge and ϵ is the permittivity. For Q_c equal 15, 20, and 25, the electric field becomes 6.5×10^7 V m^{-1}, 9.7×10^9 V m^{-1}, and 1.4×10^{12} V m^{-1}, respectively. Increasing Q_c by a little gives too high fields, and a decrease results in low fields. This can, however, be 'fixed' by changing the radius. For instance, $Q_c = 15$ and $r = 1$ μm, results in 2.4×10^9 V m^{-1}, which is more reasonable. To consider the electron avalanche as a charged sphere is of course a simplification, but the majority of the charge does build up over a

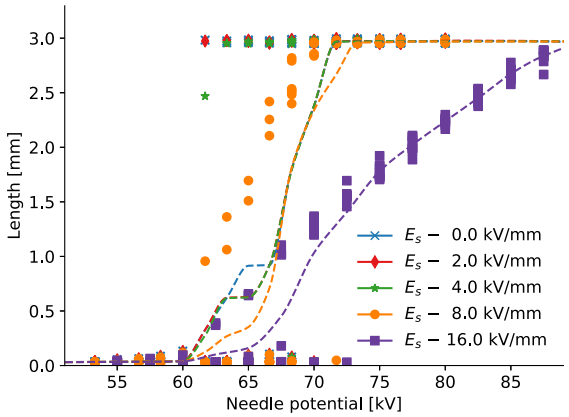

Figure 17. Streamer propagation length as a function of needle potential and electric field in streamer channel E_s. Each marker is a simulation and the dotted lines are interpolated to the average. Note that up to 8 kV m^{-1}, the results overlap to a high degree.

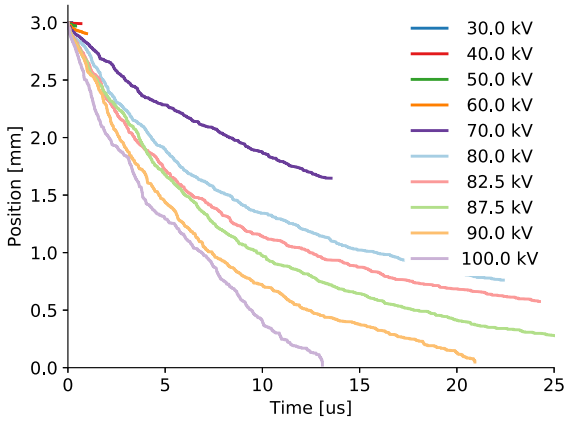

Figure 18. Streak plots of streamer leading head position, using $E_s = 16$ kV mm^{-1}, causing the streamers to slow down and sometimes stop.

length of some μm, and this is also the size used for the streamer heads, which makes the analogy reasonable. While it would seem like increasing Q_c does not make sense, one should remember that it actually has the same effect on the model as decreasing α_m, and the value of that parameter is not certain. For instance, according to [22], $\alpha_m = 200$ μm^{-1}, but [62] finds $\alpha_m = 130$ μm^{-1}, however, the latter study also finds $E_\alpha = 1.9$ GV m^{-1}, and changing this parameter has a big impact on the model, as discussed above.

3.3. Effect of streamer parameters

The streamer structure is responsible for propagating the electric field from the needle into the gap. The electric field in the streamer channel E_s gives a voltage drop from the needle to the streamer head. The electric field in front of a streamer head is also dependent on the tip radius of curvature r_s and the potential scaling of the streamer head k_i. The scaling depends on the potential and position of all the streamer heads, that is, the entire 'streamer'. Both the streamer head merge distance d_m and the potential shielding threshold k_c may be important for the streamer configuration.

Figure 14 demonstrates streamers stopping as a result of a reduction in the seed electron density, however, it is common to explain stopping as a result of an electric field E_s in the streamer channel resulting in a lower field strength at the streamer head [26]. A high E_s is needed to affect the results (see figure 17), conversely, when E_s is low, the streamer either stops quickly or causes a breakdown. When E_s is high, the propagation speed is reduced throughout the gap and the propagation may stop somewhere in the gap, see figure 18 for $E_s = 16$ kV mm^{-1}, which is in contrast to figure 7 for $E_s = 2.0$ kV mm^{-1} where the streamers do not stop. Both figures 17 and 18

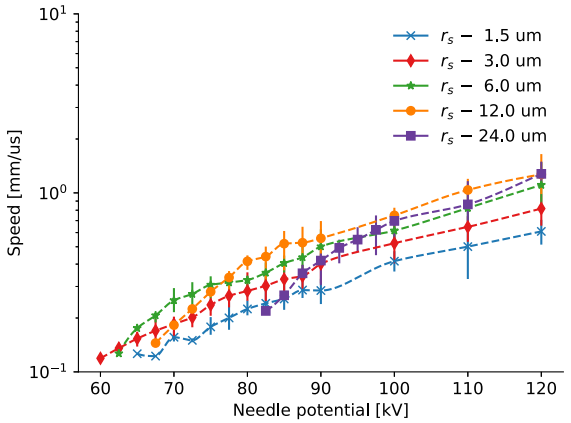

Figure 19. Streamer propagation speed for a series of different streamer head tip curvatures r_s. The dotted lines are interpolated to the average, and the bars covers the minimum and maximum values.

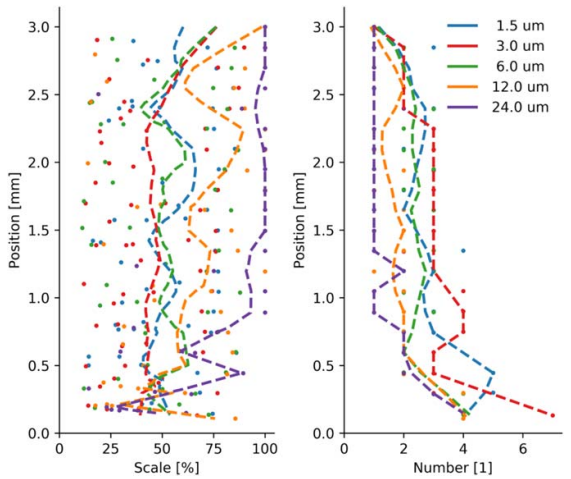

Figure 20. Actual streamer head scale k_i (left) and total number of streamer heads (right) at 100 kV for a series of streamer head tip curvatures r_s. Data are taken every 5% of the gap. The dashed lines are moving averages calculated by loess-regression [72].

indicate that E_s is not important in the beginning of the propagation, but becomes important when a streamer has reached some length. When $E_s = 8$ kV mm^{-1}, the potential is reduced by 24 kV across the gap, but this effect is barely seen (figure 17), since only a few streamers stop mid-gap. However, at 16 kV mm^{-1} the effect is clearly present as many of the streamers stop mid-gap. Notice that at 75 kV to 85 kV, in figure 17 the average propagation length is increased from about 1.7 mm to 2.6 mm, giving an apparent electric field of only 11 kV mm^{-1} and not 16 kV mm^{-1}. This is perhaps an effect of the field increasing as the gap is getting smaller. Also, actual experiments show stopping lengths that are increasing linearly with voltage in the first part of the gap, followed by more scatter and superlinear behavior towards the end of the gap [11, 15, 66]. This behavior is not seen in figure 17, possibly because E_s is kept constant in the simulations, while it has been found to vary with applied voltage [8]. Streamers are subject to re-illuminations, associated with current pulses, which could change the electric field in the streamer channel, however, the propagation of the streamer head seems to be unaffected by these effects [8].

The curvature radius r_s of a streamer head is an interesting parameter since a sharper tip gives a higher field and a larger volume where electron multiplication may occur. Changing r_s from 1.5 μm to 12 μm only changes the speed by a factor of 2, see figure 19. Further increase to 24 μm decreases the speed, and increases the breakdown voltage. Simulations with smaller r_s tend to have more streamer heads, scaled to a lower potential, than the simulations with a larger r_s, indicated in figure 20, although the effect is not visible for the smallest r_s in

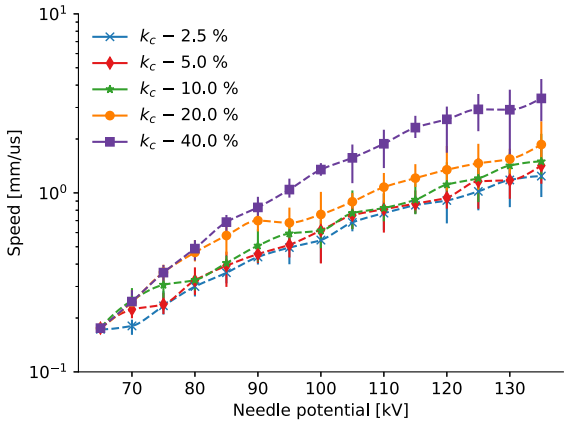

Figure 21. The effect of streamer head scale threshold k_c on the streamer propagation speed, calculated for the mid 50% of the gap. The dotted lines are interpolated to the average, and the bars covers the minimum and maximum values.

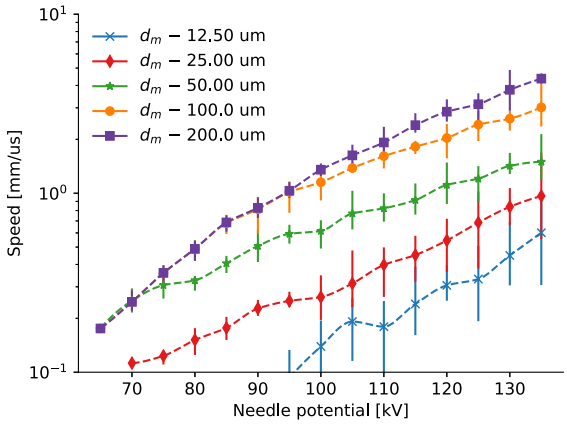

Figure 22. The effect of streamer merge distance d_m on the streamer propagation speed, calculated for the mid 50% of the gap. The dotted lines are interpolated to the average, and the bars covers the minimum and maximum values.

that figure. The increased number of streamer heads seems to act as a regulating mechanism, however, the number of branches is not increased, but there are more streamer heads present simultaneously in the same branch. This is similar to the situation in figures 9 and 10, where an increased voltage does not increase the number of branches, but instead increases the streamer thickness.

An increase in voltage increases the speed (figure 8) as well as the number of streamer heads, while decreasing the scaling of the heads as demonstrated in figure 10. The parameters k_c and d_m are used to remove streamer heads, and therefore they could have a big impact on the model, since the scaling, which the electric field depends on, is strongly dependent on the number of streamer heads as well as their configuration. Also, these parameters are purely a consequence of the model, and do not have an origin in a physical property. Simulation results for varying k_c are found in figure 21 and show that the propagation speed is not that affected, except for $k_c = 40\%$. This figure also indicates that the breakdown voltage is unaffected, since all the values of k_c are present for all the voltages. Setting $k_c = 40\%$ restricts the streamer to one head in most situations, and keeping two heads in rare occasions, which gives an upper bound to the propagation speed for each voltage. From a computational point of view, it is preferable to set k_c high as fewer streamer heads implies less calculation. From a physical point of view, however, it does not make sense to just remove charges from the system, so k_c should be reasonably low. According to figure 21, k_c can be as high as 10% without any particular impact on the results.

The influence of the streamer head merge distance d_m is shown in figure 22. For the lower values, many streamer heads are present at the same time, which in turn lowers the potential scaling of each head, increases the breakdown voltage, and moderates the propagation speed. Increasing d_m increases propagation speeds, up to the

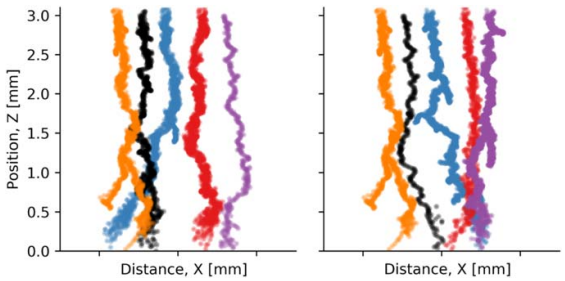

Figure 23. Streamer head positions for simulations at 120 kV. Variation of k_c (left): 10% (yellow), 20% (black), 2.5% (blue), 5.0% (red), and 40% (purple). Variation of d_m (right): 50.0 μm (yellow), 200 μm (black), 25.0 μm (blue), 100 μm (red), and 12.5 μm (purple).

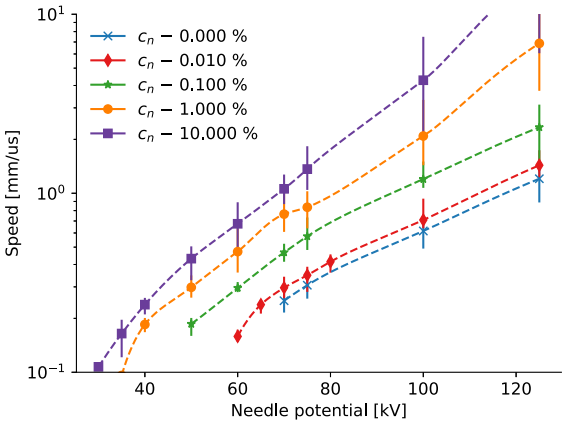

Figure 24. Streamer propagation speed for various fractions of added additive c_n. Average speed for the middle 50% of the gap. Each marker is a simulation and the dotted lines are interpolated to the average.

limit where there is mainly just a single active streamer head. Figure 22 also indicates that at low voltages, the streamers propagate with a single head, but when the voltage is increased and more heads are possible, the propagation speed is moderated. As d_m is increased, the voltage needed to have several heads is also increased, and the propagation speed is thus higher. The set of streamers presented in figure 23 shows that the thickness of the streamers is dependent on k_c and d_m, which is an indication of the number of streamer heads present during propagation. However, the figure does not indicate a change in the number of major branches.

3.4. Effect of additives

Adding small amounts of an additive increases the electron multiplication according to (20). The effect should be similar to an increase of α_m, or a decrease in Q_c, as discussed above and shown in figure 16. This is indeed the case, the propagation speed increases and the breakdown voltage decreases with increasing content of an additive with low ionization potential, see figure 24. When the liquid consists of $c_{a,n} = 10\%$ additive (mole fraction) it cannot be argued to be a 'small amount' of additive. Even as little as 1% could be too much. As mentioned in section 2.4, an addition of just 0.1% increases the avalanche growth by a factor of 6.9, when using (20) and the parameters in table 1. A decrease in breakdown voltage and an increase in propagation speed is also found in experiments with low-IP additives [3, 11, 41], however, increased branching is also seen in the experiments in contrast to the simulation results here.

3.5. Increased speed and branching

The above sections illustrate how the model behaves and how it is affected by the various parameters. In order to reduce the initiation voltage and increase the propagation speed, the avalanche parameters are changed to $E_\alpha = 1.9$ GV m^{-1} and $\alpha_m = 130$ μm^{-1}, and the number of seeds is increased to $c_s = 8 \times 10^{12}$ m^{-3}. In addition, the merge distance is changed to $d_m = 12.5$ μm and the streamer head tip radius to $r_s = 3$ μm in

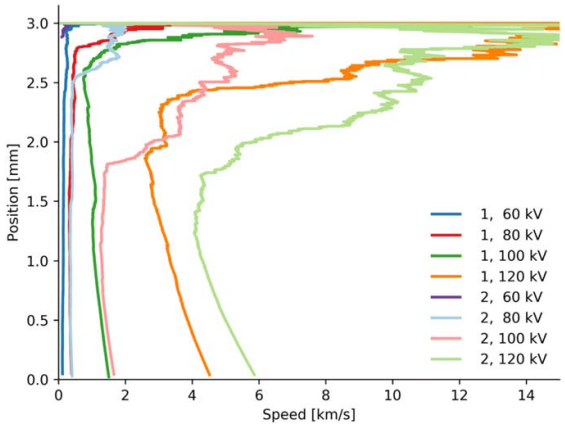

Figure 25. Streamer average speed versus leading head position. The simulations at the same voltage differ only by the initialization of the random number generator.

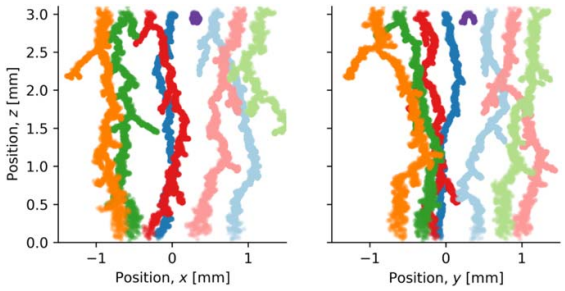

Figure 26. Streamer trails for a range of voltages, using the same colors as in figure 25. Each dot represents the position of a streamer head at some point of the propagation.

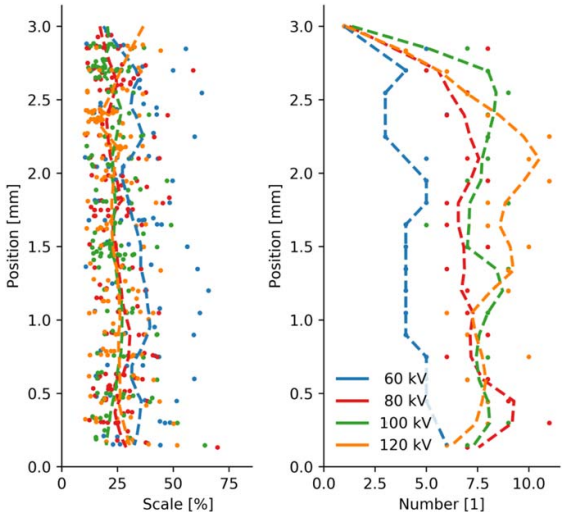

Figure 27. Actual streamer head scale k_i (left) and total number of streamer heads (right). Data are taken every 5% of the gap. The dashed lines are moving averages.

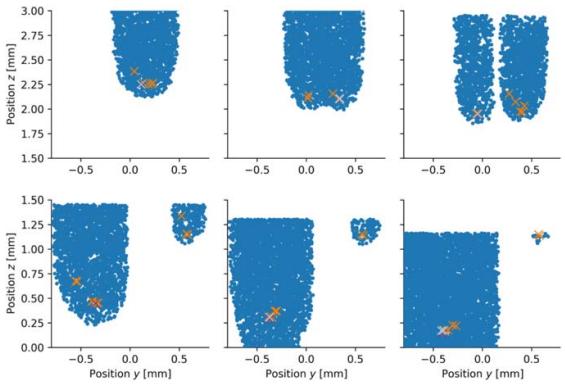

Figure 28. Detailed illustration of streamer branching. The electron avalanches are shown as blue dots, and the streamer head as crosses. The top three plots show streamer bifurcation in the start of the gap, while the bottom three plots show one propagating branch and another stopped branch at the end of the gap.

order to facilitate branching. Also, using $E_s = 8$ kV mm^{-1} should be enough for some of the streamers to stop mid-gap. Most of the predicted results are found: the speed in figure 25 is clearly increased compared to figure 8, the amount of small branches is larger in figure 26 than in figure 9, and the decrease in streamer head scaling and increase in streamer head number is seen by comparing figure 27 to figure 10. The propagation voltage is somewhat lower than the base case, around 60 kV. The streamer propagation begins at high speed, then slows down towards the middle of the gap, before the speed increases towards the end of the gap, see figure 25. This change does not seem to be correlated to the number of streamer heads, which is fairly constant for most of the propagation (figure 27). Branching may have an effect, and streamer branching is illustrated in figure 28, showing 6 snapshots of a single simulation. As the streamer splits into two major branches, the number of electron avalanches surrounding the streamer heads decreases. The branches propagate at different speeds, and the faster one gains a higher potential and thus creates more electron avalanches. As the two branches approaches the end of the gap, one gains speed, while the other one stops.

4. Discussion of the model

Using a Laplace field is of course a simplification compared to a Poisson field. In fact, neither positive nor negative charges are accounted for in the model. The potential is simply calculated by assuming a constant field in the streamer channel, and then superimposing the streamer heads. Including the charge of the avalanches and the ions left behind could improve the model. For the needle and the streamer heads, using a space charge limited field (SCLF) [73, 74] would provide a more physically correct field distribution, but would also increase the computational requirements drastically. Using an SCLF rather than a Laplace field, gives a reduction of the electric field where the field is the strongest, since the maximum field is limited [73], with a corresponding increase everywhere else. The SCLF is time-dependent [74], and the effect increases with time until an steady-state is obtained. The overall effect on the model would be an increase in average jump length, as most jumps would be longer and the shortest ones would not occur. While an SCLF can give more accurate results for slow streamers, a Laplace field could be good enough for fast streamers, since the SCLF-region expands at some finite speed. However, the avalanche parameters in (16) were estimated using a Laplace field, so the current model is internally consistent.

The inception of 2nd mode streamers has been estimated to somewhat less than 15 kV for cyclohexane [5], however, for a propagating 2nd mode streamer, 33kV was found for a 10 mm gap [11]. Since the model uses this as a criterion for inception (getting a critical avalanche, but no movement), a high propagation voltage is actually to be expected. This is well illustrated by the maximum avalanche size in figure 29, obtained by integration of α. Streamer propagation is possible when $Q_f > Q_c$ (cf. (19)). The baseline simulations are performed inserting parameters from [22] in (16) to calculate α. At 33 kV, the maximum possible streamer jump is less than a μm, however, at 60 kV (the breakdown voltage), the value is increased to about 6 μm, possibly indicating that a strong field is needed over some distance. Changing to parameters from [62] decreases the propagation voltage by increasing the possible jump length, however, the decrease is not enough to enable for inception of 2nd mode streamers at 15 kV. As such, figure 29 indicates that streamer inception at 15 kV is not possible with this model when considering a Laplace field, calculating the electron multiplication with (16), and using the

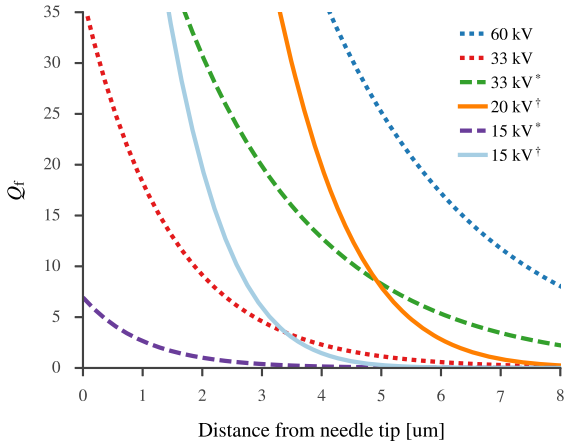

Figure 29. Maximum avalanche size at a distance from the needle tip. The unmarked lines use the same values as the baseline simulations from [22], the * indicates parameter values from [62] as used in section 3.5, and the † indicates formulation and parameter values from [61].

Townsend–Meek criterion for inception of 2nd mode streamers. Using the parameters of either [22] or [62] gives too low avalanche size. According to [61], the correct way of calculating electron multiplication in a dense medium is

$$\alpha = \frac{3IE_\nu^2}{eE}\exp\left(-\frac{E_\nu^2}{E^2}\right) \tag{34}$$

where I is the ionization potential, e is the electron charge, and E_ν is given by properties of the liquid. With this formulation, electron multiplication is more dependent on the electric field, implying that the electron avalanches become shorter, are closer to the streamer heads, and grow faster where the field is strong, which is illustrated in figure 29 using values for n-hexane [61].

The propagation velocity is somewhat low, which is to be expected since the inception voltage is too high. Changing parameters to values that lowers the inception voltage also increases the speed at a given voltage. As mentioned, the speed is proportional to the electron mobility, and it is the low-field mobility that has been used. For low-mobility liquids, such as cyclohexane, the mobility is expected to have a superlinear dependence on the electric field [49, 56]. For this reason, one study multiplies the mobility by 2.5, to make it similar to the gas phase mobility [38], which would increase the streamer propagation speed by the same factor. Conversely, limitations to the maximum speed of electrons have been introduced [75], which would effectively control the maximum speed of a streamer branch. The speed is also proportional to the concentration of seeds (see figure 12), which was calculated from the low-field conductivity of the liquid (see (10)). However, for breakdown in non-polar liquids, the conductivity is not important [2], and hence, it seems unreasonable for this parameter to be as important as demonstrated here. The equilibrium density of ions can also be calculated based on cosmic radiation (17), but obtaining $>10^{11}$ m^{-3} ions, when the production is $\sim 10^8$ m^{-3}s^{-1}, implies that a long time is needed. It is therefore an approximation to simulate a situation where this density is kept constant. By changing the simulation conditions such that all the gap is included in the ROI and such that seeds are not replaced, it can be verified that the seeds present at the beginning of the experiment is not enough. They are swept out very fast if they are electrons and not ions. Increasing E_d so that most seeds remain as anions changes this by allowing the low-mobility anions to live longer before entering the high-field area and ionize into molecules and electrons. Even so, it seems clear that some mechanism for generation of new seeds is warranted. New seeds could be generated in the high-field areas, and near the electrodes. The Zener model [76] (field-ionization) for breakdown in solids has been used also for charge generation in liquids [24, 37]. Photoionization could also have an important role in the generation of new charges [2, 9], and adding field ionization and photoionization could improve the model. In addition, when ionizing neutral molecules, the field-dependent ionization potential [13] should also be taken into account. This kind of additions add complexity to the model, but Monte Carlo (MC) [77] methods can aid in keeping the added computational cost low. There are also some parts of the current model where MC could be reasonable to use. For instance, for electron detachment from an anion and for avalanche growth from a single electron, since a large number of electrons is needed to model an avalanche through the average growth α.

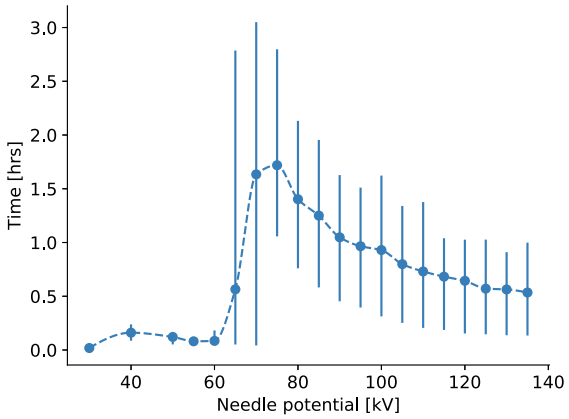

Figure 30. Total computational time for the simulations shown in figure 21. Streamers that terminate in the beginning of the gap require little time, while streamers that slowly bridges the gap requires the most computational time.

The degree of branching is lower than desired, with more or less only one major branch, and thus the simulations resemble more the 3rd mode or the start of the 4th mode than the 2nd mode of a streamer. It is worthwhile noting that streamers branch far less in cyclohexane than in mineral oil, but the addition of low-IP additives increases the branching [41]. The shapes of the simulated streamers do resemble the shape of streamers in longer gaps [41], however, while including additives in the model increases the propagation speed, the degree of branching is not increased. Although branching is thought of as a mechanism for regulating the propagation speed, it could be the other way around. With nothing to hold it back, the foremost head should have the strongest electric field and the fastest propagation. If something is regulating the speed or field of the foremost head, however, then other heads are given a better chance of propagation, increasing the number of branches, which in turn may regulate the electric field of all the branches. In the present model, there is nothing holding the foremost head back, since the only time scale included is that of the electron avalanches. If, for instance, the time required for bubble nucleation or the time for charges to move through the streamer structure (streamer dynamics) is important, it may result in a disadvantage for the foremost head. This is, however, not included, and the potential of each streamer head is instantly updated each simulation step. The shape chosen for the streamer heads could also be a major reason for the low degree of branching. For a hyperboloid, the electric field declines as r^{-1} in front, and the high-field region extends much further in the front than on the sides. Conversely, the field from a monopole declines like r^{-2} in all directions, and could as such facilitate branching. In such a model, however, the high field would be in a region closer to the streamer heads, making an SCLF approach even more relevant.

The simplicity of the presented model comes with several limitations, as discussed above, however, a simple model is also a good place to start. It makes it possible to identify whether a certain mechanism is important or not at a relatively low computational cost. Consider figure 30, which shows that the computational time for breakdown streamers averages to about one hour, using a single core on a regular desktop computer. The simulation time is of course strongly dependent on the number of seeds, streamer heads, and simulation steps, but with such a low base case, it is possible to perform a lot of simulations to gather statistics on a normal desktop computer. Contrary to lattice models, the presented model is based on physical processes, and the results are thus easier to evaluate. FEM models may be better in the end, but for now, such models cannot model a complete breakdown. They are also simplified, for example in the sense that phase changes are not accounted for [75]. Both lattice and FEM models demands much computational power and the mesh size becomes an important parameter, however, this is avoided in the model presented. Instead of dealing with processes at discrete point or in discretized elements, the model deals with discrete points that move. This approach makes sense when considering charge generated by electron avalanches at some distance from the streamer structure, or a streamer moving in discrete steps. For details on processes inside or very close to the streamer, however, a FEM approach seems more reasonable, and could provide valuable input to models on a larger scale.

5. Conclusion

A simple simulation model for streamer propagation has been presented. The streamer is represented by a collection of hyperbolic streamer heads, and is responsible for propagating the electric field from the needle

electrode. In high-field areas, electrons detach from ions present in the liquid, and may turn into avalanches. If an avalanche meets the Townsend–Meek criterion, a new streamer head is added at its position, causing the streamer to propagate. As demonstrated, the model has some limitations, the inception voltage is too high while the degree of branching is low. These issues are discussed and explained, and directions for a systematic way of further developments are described. The main feature missing in the model is a proper representation of the dynamics of the streamer channel, however, the charge generation and the electric field calculation can be improved as well. The approach to streamer propagation applied here is different from that used by other models. The principle behind the model is simple, it is founded on physical mechanisms, and provides interesting information about how an avalanche-driven breakdown may occur. The simple model has its advantages in that it can be used to identify important mechanisms, without demanding excessive computational power.

Acknowledgments

The authors would like to thank Lars Lundgaard and Dag Linhjell for interesting discussions and for sharing their experience about experiments.

This work has been supported by The Research Council of Norway (RCN), ABB and Statnett, under the RCN contract 228850.

Appendix. Prolate spheroid coordinates

Prolate spheroid coordinates involves a set of hyperbolas and ellipsoids revolved around the center axis, forming hyperboloids and prolate spheroids. The two focal points, of the hyperbolas as well as ellipsoids, are located at a distance a from the plane. The hyperbolic coordinate is $\mu \in [0,\ \infty\rangle$, the elliptic coordinate is $\nu \in [0,\ \pi]$, and rotation about the center is given by $\phi \in [0,\ 2\pi]$. The definition used here is

$$x = a\ \sinh\mu\ \sin\nu\ \cos\phi, \tag{A.1}$$

$$y = a\ \sinh\mu\ \sin\nu\ \sin\phi, \tag{A.2}$$

$$z = a\ \cosh\mu\ \cos\nu. \tag{A.3}$$

Figure A1 illustrates the coordinate system, where a constant μ gives a prolate spheroid,

$$\frac{z^2}{a^2\cosh^2\mu} + \frac{x^2+y^2}{a^2\sinh^2\mu} = 1, \tag{A.4}$$

and a constant ν gives a hyperbola,

$$\frac{z^2}{a^2\cos^2\nu} - \frac{x^2+y^2}{a^2\sin^2\nu} = 1. \tag{A.5}$$

Transformation from Cartesian to prolate spheroid coordinates is obtained through

$$2a\cosh\mu = p + m, \tag{A.6}$$

$$2a\cos\nu = p - m, \tag{A.7}$$

$$\tan\phi = y/x, \tag{A.8}$$

where

$$p = \sqrt{x^2+y^2+(z+a)^2}, \tag{A.9}$$

$$m = \sqrt{x^2+y^2+(z-a)^2}, \tag{A.10}$$

and are the distances between a given point and the two focal points. Prolate spheroid coordinates exists in many forms In some cases, it is easier to work with substitutions such as $\xi = \sin\nu$, however, starting with trigonometric functions allows for greater flexibility through relations such as $\sin^2 + \cos^2 = 1$.

Scale factors h are useful to define when transforming between coordinate systems. The scale factor for ν, for instance, is found from

$$h_\nu = \frac{\mathrm{d}l}{\mathrm{d}\nu} = \sqrt{\left(\frac{\mathrm{d}x}{\mathrm{d}\nu}\right)^2 + \left(\frac{\mathrm{d}y}{\mathrm{d}\nu}\right)^2 + \left(\frac{\mathrm{d}z}{\mathrm{d}\nu}\right)^2}. \tag{A.11}$$

Solving this, and the similar expressions for the other coordinates, yields

$$h_\nu = h_\mu = a\ \sqrt{\sinh^2\mu + \sin^2\nu}, \tag{A.12}$$

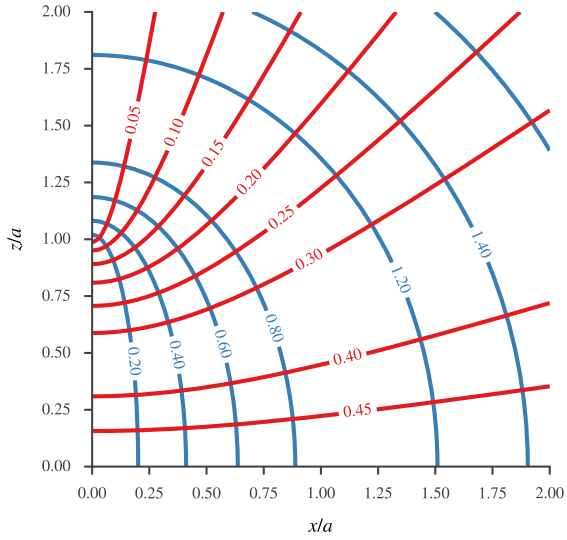

Figure A1. In prolate spheroid coordinates, spheroids (blue) are given by a constant μ, and hyperboloids (red) have a constant ν. Here, ν is given in units of π.

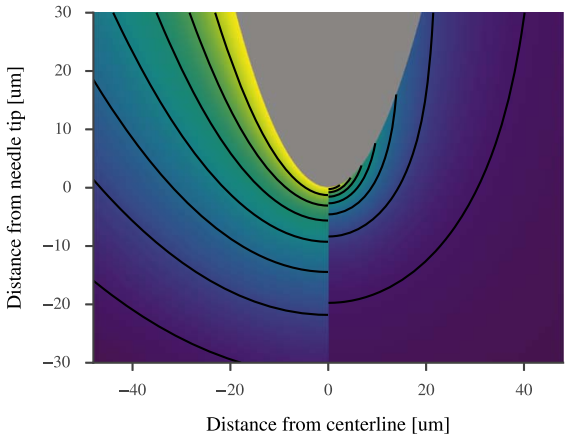

Figure A2. Electric potential (left) and electric field strength (right), for a region close to a needle (center, gray) placed 10 mm from a grounded plane. The contour lines give a qualitative impression of how the respective magnitudes change as a function of position. A linear scale is used for both sides, and the magnitudes are linearly dependent on the potential of the needle.

$$h_\phi = a \sinh\mu \sin\nu. \tag{A.13}$$

These are useful when defining the spatial derivative,

$$\nabla = \frac{\hat{\boldsymbol{\mu}}}{h_\mu}\partial_\mu + \frac{\hat{\boldsymbol{\nu}}}{h_\nu}\partial_\nu + \frac{\hat{\boldsymbol{\phi}}}{h_\phi}\partial_\phi. \tag{A.14}$$

The electric potential V and the electric field $\boldsymbol{E}$ are found by solving the Laplace equation, $\nabla^2 V = 0$. For a system where the hyperboloids represent equipotential surfaces, $V = V(\nu)$, the Laplace equation is satisfied for [78]

$$V(\nu) = A + C \ln\tan\frac{\nu}{2}, \tag{A.15}$$

where the constants A and C are defined by boundary conditions. Given $V(\nu = \pi/2) = 0$ at the xz-plane and $V(\nu = \nu_0) = V_0$ at the ν_0-hyperboloid, yields $A = 0$ and

$$C = \frac{V_0}{\ln \tan(\nu_0/2)}. \tag{A.16}$$

Consequently, the electric field $\boldsymbol{E} = -\boldsymbol{\nabla} V$ becomes

$$\boldsymbol{E} = \frac{C\,\hat{\boldsymbol{\nu}}}{h_\nu \sin\nu}, \tag{A.17}$$

where $\hat{\boldsymbol{\nu}}$ is unit length in the direction of $\boldsymbol{\nu}$,

$$\hat{\boldsymbol{\nu}} = \frac{\boldsymbol{\nu}}{|\nu|} = \frac{\partial_\nu(\boldsymbol{x}+\boldsymbol{y}+\boldsymbol{z})}{h_\nu} = \frac{\boldsymbol{x}+\boldsymbol{y}-\boldsymbol{z}\tan^2\nu}{h_\nu \tan\nu}. \tag{A.18}$$

Equations (A.15), (A.17) are both illustrated in figure A2. The figure shows the differences in behavior between the electric potential and the electric field, the latter increases rapidly close to the tip of the hyperboloid.

Explicit transformation between Cartesian and prolate spheroid coordinates requires trigonometric and hyperbolic functions, which are costly when it comes to computations. There is, however, no need to calculate μ, ν, and ϕ explicitly, as both the potential (A.15) and the electric field (A.17) may be obtained by using (A.6), (A.7), and trigonometric relations such as

$$\begin{aligned} 2a\sin\nu &= 2a\sqrt{1-\cos^2\nu} \\ &= \sqrt{4a^2-(p-m)^2}. \end{aligned} \tag{A.19}$$

ORCID iDs

P-O Åstrand https://orcid.org/0000-0003-3384-7585
M Unge https://orcid.org/0000-0002-3149-4045

References

[1] Wedin P 2014 Electrical breakdown in dielectric liquids—a short overview *IEEE Electr. Insul. Mag.* **30** 20–5
[2] Lesaint O 2016 Prebreakdown phenomena in liquids: propagation 'modes' and basic physical properties *J. Phys. D. Appl. Phys.* **49** 144001
[3] Devins J C, Rzad S J and Schwabe R J 1981 Breakdown and prebreakdown phenomena in liquids *J. Appl. Phys.* **52** 4531–45
[4] Felici N J 1988 Blazing a fiery trail with the hounds *IEEE Trans. Electr. Insul.* **23** 497–503
[5] Gournay P and Lesaint O 1993 A study of the inception of positive streamers in cyclohexane and pentane *J. Phys. D. Appl. Phys.* **26** 1966–74
[6] Tobazèon R, Filippini J C and Marteau C 1994 On the measurement of the conductivity of highly insulating liquids *IEEE Trans. Dielectr. Electr. Insul.* **1** 1000–4
[7] Biller P 1996 A simple qualitative model for the different types of streamers in dielectric liquids *ICDL'96. 12th Int. Conf. Conduct. Break. Dielectr. Liq., IEEE* 189–92
[8] Massala G and Lesaint O 1998 Positive streamer propagation in large oil gaps: electrical properties of streamers *IEEE Trans. Dielectr. Electr. Insul.* **5** 371–80
[9] Lundgaard L, Linhjell D, Berg G and Sigmond S 1998 Propagation of positive and negative streamers in oil with and without pressboard interfaces *IEEE Trans. Dielectr. Electr. Insul.* **5** 388–95
[10] Kolb J F, Joshi R P, Xiao S and Schoenbach K H 2008 Streamers in water and other dielectric liquids *J. Phys. D. Appl. Phys.* **41** 234007
[11] Ingebrigtsen S, Smalø H S, Åstrand P-O and Lundgaard L E 2009 Effects of electron-attaching and electron-releasing additives on streamers in liquid cyclohexane *IEEE Trans. Dielectr. Electr. Insul.* **16** 1524–35
[12] Joshi R P, Kolb J F, Xiao S and Schoenbach K H 2009 Aspects of plasma in water: streamer physics and applications *Plasma Process. Polym.* **6** 763–77
[13] Smalø H S, Hestad O L, Ingebrigtsen S and Åstrand P-O 2011 Field dependence on the molecular ionization potential and excitation energies compared to conductivity models for insulation materials at high electric fields *J. Appl. Phys.* **109** 073306
[14] Joshi R P and Thagard S M 2013 Streamer-like electrical discharges in water: I. Fundamental mechanisms *Plasma Chem. Plasma Process.* **33** 1–15
[15] Lesaint O and Massala G 1998 Positive streamer propagation in large oil gaps: experimental characterization of propagation modes *IEEE Trans. Dielectr. Electr. Insul.* **5** 360–70
[16] Dumitrescu L, Lesaint O, Bonifaci N, Denat A and Notingher P 2001 Study of streamer inception in cyclohexane with a sensitive charge measurement technique under impulse voltage *J. Electrostat.* **53** 135–46
[17] Kattan R, Denat A and Lesaint O 1989 Generation, growth, and collapse of vapor bubbles in hydrocarbon liquids under a high divergent electric field *J. Appl. Phys.* **66** 4062–6
[18] Tobazeon R 1994 Prebreakdown phenomena in dielectric liquids *Proc. 1993 IEEE 11th Int. Conf. Conduct. Break. Dielectr. Liq. (ICDL '93)* vol 1 (Piscataway, NJ: IEEE) pp 172–83
[19] Lewis T J 1998 A new model for the primary process of electrical breakdown in liquids *IEEE Trans. Dielectr. Electr. Insul.* **5** 306–15
[20] Joshi R P, Qian J, Zhao G, Kolb J, Schoenbach K H, Schamiloglu E and Gaudet J 2004 Are microbubbles necessary for the breakdown of liquid water subjected to a submicrosecond pulse? *J. Appl. Phys.* **96** 5129–39
[21] Derenzo S E, Mast T S, Zaklad H and Muller R A 1974 Electron avalanche in liquid xenon *Phys. Rev.* A **9** 2582–91
[22] Haidara M and Denat A 1991 Electron multiplication in liquid cyclohexane and propane *IEEE Trans. Electr. Insul.* **26** 592–7
[23] Lesaint O and Gournay P 1994 On the gaseous nature of positive filamentary streamers in hydrocarbon liquids: I. Influence of the hydrostatic pressure on the propagation *J. Phys. D. Appl. Phys.* **27** 2111–6

[24] Halpern B and Gomer R 1969 Field ionization in liquids *J. Chem. Phys.* **51** 1048–56
[25] Denat A, Gosse J P and Gosse B 1988 Electrical conduction of purified cyclohexane in a divergent electric field *IEEE Trans. Electr. Insul.* **23** 545–54
[26] Atten P and Saker A 1993 Streamer propagation over a liquid-solid interface *10th Int. Conf. Conduct. Break. Dielectr. Liq.* **28** 441–5
[27] Bruggeman P J *et al* 2016 Plasma-liquid interactions: a review and roadmap *Plasma Sources Sci. Technol.* **25** 053002
[28] Niemeyer L, Pietronero L and Wiesmann H J 1984 Fractal dimension of dielectric breakdown *Phys. Rev. Lett.* **52** 1033–6
[29] Wiesmann H J and Zeller H R 1986 A fractal model of dielectric breakdown and prebreakdown in solid dielectrics *J. Appl. Phys.* **60** 1770–3
[30] Satpathy S 1986 Dielectric breakdown in three dimensions: results of numerical simulation *Phys. Rev.* B **33** 5093–5
[31] Biller P 1993 Fractal streamer models with physical time *Proc. 1993 IEEE 11th Int. Conf. Conduct. Break. Dielectr. Liq. (ICDL '93)* 199–203
[32] Kim M, Hebner R E and Hallock G A 2008 Modeling the growth of streamers during liquid breakdown *IEEE Trans. Dielectr. Electr. Insul.* **15** 547–53
[33] Kupershtokh A L and Medvedev D A 2006 Lattice Boltzmann equation method in electrohydrodynamic problems *J. Electrostat.* **64** 581–5
[34] Qian J *et al* 2005 Microbubble-based model analysis of liquid breakdown initiation by a submicrosecond pulse *J. Appl. Phys.* **97** 113304
[35] Qian J, Joshi R P, Schamiloglu E, Gaudet J, Woodworth J R and Lehr J 2006 Analysis of polarity effects in the electrical breakdown of liquids *J. Phys. D. Appl. Phys.* **39** 359–69
[36] Hwang J G, Zahn M and Pettersson L A A 2012 Mechanisms behind positive streamers and their distinct propagation modes in transformer oil *IEEE Trans. Dielectr. Electr. Insul.* **19** 162–74
[37] Jadidian J, Zahn M, Lavesson N, Widlund O and Borg K 2013 Stochastic and deterministic causes of streamer branching in liquid dielectrics *J. Appl. Phys.* **114** 063301
[38] Naidis G V 2015 Modelling of streamer propagation in hydrocarbon liquids in point-plane gaps *J. Phys. D. Appl. Phys.* **48** 195203
[39] Naidis G V 2016 Modelling the dynamics of plasma in gaseous channels during streamer propagation in hydrocarbon liquids *J. Phys. D. Appl. Phys.* **49** 235208
[40] Hestad O L, Grav T, Lundgaard L E, Ingebrigtsen S, Unge M and Hjortstam O 2014 Numerical simulation of positive streamer propagation in cyclohexane *2014 IEEE 18th Int. Conf. Dielectr. Liq.*
[41] Lesaint O and Jung M 2000 On the relationship between streamer branching and propagation in liquids: influence of pyrene in cyclohexane *J. Phys. D. Appl. Phys.* **33** 1360–8
[42] Pedersen A 1989 On the electrical breakdown of gaseous dielectrics—an engineering approach *IEEE Trans. Electr. Insul.* **24** 721–39
[43] UNSCEAR 2008 *Sources and Effects of Ionizing Radiation, Volume I: Sources* (*Sources and Effects of Ionizing Radiation, Volume I: Sources* Sources and Effects of Ionizing Radiation, Volume I: Sources) (New York: United Nations)
[44] Schmidt W F 1997 *Liquid State Electronics of Insulating Liquids* (Boca Raton, FL: CRC Press)
[45] Holroyd R 2003 Electrons in nonpolar liquids *Charged Particle and Photon Interactions with Matter* (Boca Raton, FL: CRC Press)
[46] Gee N and Freeman G R 1992 Free ion yields, electron thermalization distances, and ion mobilities in liquid cyclic hydrocarbons: cyclohexane and trans- and cis-decalin *J. Chem. Phys.* **96** 586–92
[47] Dodelet J-P and Freeman G R 1972 Mobilities and ranges of electrons in liquids: effect of molecular structure in C5 -C12 alkanes *Can. J. Chem.* **50** 2667–79
[48] Schmidt W F and Allen A O 1970 Mobility of electrons in dielectric liquids *J. Chem. Phys.* **52** 4788–94
[49] Schmidt W F 1984 Electronic conduction processes in dielectric liquids *IEEE Trans. Electr. Insul.* **EI-19** 389–418
[50] Holroyd R A and Schmidt W F 1989 Transport of electrons in nonpolar fluids *Annu. Rev. Phys. Chem.* **40** 439–68
[51] Winokur P S, Roush M L and Silverman J 1975 Ion mobility measurements in dielectric liquids *J. Chem. Phys.* **63** 3478–89
[52] Polak H and Jachym B 1977 Mobility of excess charge carriers in liquid and solid cyclohexane *J. Phys. C Solid State Phys.* **10** 3811–8
[53] Denat A, Gosse B and Gosse J P 1979 Ion injections in hydrocarbons *J. Electrostat.* **7** 205–25
[54] Alj A, Denat A, Gosse J P, Gosse B and Nakamura I 1985 Creation of charge carriers in nonpolar liquids *IEEE Trans. Electr. Insul.* **EI-20** 221–31
[55] Allen A O 1976 Drift mobilities and conduction band energies of excess electrons in dielectric liquids *Natl. Stand. Ref. Data Ser., Natl. Bur. Stand. Circ.* NSRDS-NBS-58
[56] Schmidt W F 1977 Electron mobility in nonpolar liquids: the effect of molecular structure, temperature, and electric field *Can. J. Chem.* **55** 2197–210
[57] Denat A 2011 Conduction and breakdown initiation in dielectric liquids *2011 IEEE Int. Conf. Dielectr. Liq.*
[58] Kim M and Hebner R 2007 Initiation from a point anode in a dielectric liquid *IEEE Trans. Dielectr. Electr. Insul.* **14** 762–3
[59] Gafvert U, Jaksts A, Tornkvist C and Walfridsson L 1992 Electrical field distribution in transformer oil *IEEE Trans. Electr. Insul.* **27** 647–60
[60] Heylen A E D 2000 The relationship between electron-molecule collision cross-sections, experimental Townsend primary and secondary ionization coefficients and constants, electric strength and molecular structure of gaseous hydrocarbons *Proc. R. Soc. A Math. Phys. Eng. Sci.* **456** 3005–40
[61] Atrazhev V M, Dmitriev E G and Iakubov I T 1991 The impact ionization and electrical breakdown strength for atomic and molecular liquids *IEEE Trans. Electr. Insul.* **26** 586–91
[62] Naidis G V 2015 On streamer inception in hydrocarbon liquids in point-plane gaps *IEEE Trans. Dielectr. Electr. Insul.* **22** 2428–32
[63] Lowke J J and D'Alessandro F 2003 Onset corona fields and electrical breakdown criteria *J. Phys. D. Appl. Phys.* **36** 2673–82
[64] Yamashita H, Yamazawa K and Wang Y S 1998 The effect of tip curvature on the prebreakdown streamer structure in cyclohexane *IEEE Trans. Dielectr. Electr. Insul.* **5** 396–401
[65] Lawson C L and Hanson R J 1995 Solving least squares problems *Classics in Applied Mathematics* (Philadelphia, PA : Society for Industrial and Applied Mathematics)
[66] Lesaint O and Tobazeon R 1988 Streamer generation and propagation in transformer oil under AC divergent field conditions *IEEE Trans. Electr. Insul.* **23** 941–54
[67] Davari N, Åstrand P-O, Unge M, Lundgaard L E and Linhjell D 2014 Field-dependent molecular ionization and excitation energies: implications for electrically insulating liquids *AIP Adv.* **4** 037117
[68] Davari N, Åstrand P-O, Ingebrigtsen S and Unge M 2013 Excitation energies and ionization potentials at high electric fields for molecules relevant for electrically insulating liquids *J. Appl. Phys.* **113** 143707
[69] Oliphant T E 2007 Python for scientific computing *Comput. Sci. Eng.* **9** 10–20

[70] van der Walt S, Colbert S C and Varoquaux G 2011 The NumPy array: a structure for efficient numerical computation *Comput. Sci. Eng.* **13** 22–30
[71] Hunter J D 2007 Matplotlib: a 2D graphics environment *Comput. Sci. Eng.* **9** 99–104
[72] Cleveland W S 1979 Robust locally weighted regression and smoothing scatterplots *J. Am. Stat. Assoc.* **74** 829–36
[73] Hibma T and Zeller H R 1986 Direct measurement of space-charge injection from a needle electrode into dielectrics *J. Appl. Phys.* **59** 1614–20
[74] Boggs S 2005 Very high field phenomena in dielectrics *IEEE Trans. Dielectr. Electr. Insul.* **12** 929–38
[75] Jadidian J, Zahn M, Lavesson N, Widlund O and Borg K 2014 Abrupt changes in streamer propagation velocity driven by electron velocity saturation and microscopic inhomogeneities *IEEE Trans. Plasma Sci.* **42** 1216–23
[76] Zener C 1934 A theory of the electrical breakdown of solid dielectrics *Proc. R. Soc. A Math. Phys. Eng. Sci.* **145** 523–9
[77] Metropolis N and Ulam S 1949 The Monte Carlo method *J. Am. Stat. Assoc.* **44** 335–41
[78] Moon P and Spencer D E 1971 *Field Theory Handbook* (Berlin: Springer)

II

Inge Madshaven, Øystein Leif Hestad,
Mikael Unge, Olof Hjortstam, Per-Olof Åstrand
Conductivity and capacitance of streamers in avalanche model for streamer propagation in dielectric liquids
Plasma Research Express **1**:035014 (2019)
DOI: 10/c933 | arXiv: 1902.03945

Plasma Research Express

PAPER

Conductivity and capacitance of streamers in avalanche model for streamer propagation in dielectric liquids

I Madshaven[1], OL Hestad[2], M Unge[3], O Hjortstam[3] and PO Åstrand[1,4]

[1] Department of Chemistry, NTNU—Norwegian University of Science and Technology, 7491 Trondheim, Norway
[2] SINTEF Energy Research, 7465 Trondheim, Norway
[3] ABB Corporate Research, 72178 Västerås, Sweden
[4] Author to whom any correspondence should be addressed.

E-mail: per-olof.aastrand@ntnu.no

OPEN ACCESS

RECEIVED
12 June 2019

REVISED
30 July 2019

ACCEPTED FOR PUBLICATION
2 September 2019

PUBLISHED
25 September 2019

Keywords: streamer, simulation model, dielectric liquid, conductivity, capacitive model

Abstract

Propagation of positive streamers in dielectric liquids, modeled by the electron avalanche mechanism, is simulated in a needle–plane gap. The streamer is modeled as an RC-circuit where the channel is a resistor and the extremities of the streamer have a capacitance towards the plane. The addition of the RC-model introduces a time constant to the propagation model. Increase in capacitance as a streamer branch propagates reduces its potential, while conduction through the streamer channel increases its potential, as a function of the time constant of the RC-system. Streamer branching also increases the capacitance and decreases the potential of the branches. If the electric field within the streamer channel exceeds a threshold, a breakdown occurs in the channel, and the potential of the streamer is equalized with the needle electrode. This is interpreted as a re-illumination. According to this model, a low conductive streamer branch can propagate some distance before its potential is reduced to below the propagation threshold, and then the RC time constant controls the streamer propagation speed. Channel breakdowns, or re-illuminations, are less frequent when the channels are conductive and more frequent for more branched streamers.

1. Introduction

When dielectric liquids are exposed to a sufficiently strong electric field, partial discharges occur and a gaseous channel called a streamer is formed. The many characteristics of streamers, such as shape, propagation speed, inception voltage, breakdown voltage, current, and charge are described by numerous experiments performed throughout the last half century for various liquids and different experimental setups [1–6]. A streamer bridging the gap between two electrodes can cause an electric discharge, and a better understanding of the mechanisms governing the inception and the propagation of streamers is essential for the production of e.g. better power transformers and the prevention of failure in such equipment [7].

Simulating a low temperature plasma in contact with a liquid is a challenge in itself [8]. For a propagating streamer, phase change and moving boundaries complicates the problem further and simplifications are therefore required. The finite element method has been used in models simulating streamer breakdown through charge generation and charge transport [9, 10], even incorporating phase change [11]. However, the first simulations of streamer breakdown in liquids applied Monte Carlo methods on a lattice [12], and have since been expanded, for instance by including conductivity [13]. Another model use the electric network model to calculate the electric field in front of the streamer, which is used to evaluate the possibility for streamer growth or branching [14].

For positive streamers in non-polar liquids, it is common to define four propagation modes based on their propagation speed, ranging from around 0.1 km s^{-1} for the 1st mode and exceeding 100 km s^{-1} for the 4th mode. 2nd mode streamers propagate at speeds of some km s^{-1} creating a branching filamentary structure that can lead to a breakdown if the applied voltage is sufficiently high [15].

Our previous work describes a model for propagation of 2nd mode positive streamers in dielectric liquids governed by electron avalanches [16, 17]. According to the model, electron avalanches can be important for streamer propagation, but the results also showed a relatively low propagation speed and a low degree of branching. The streamer channel was represented by a fixed electric field within the channel between the needle electrode and the extremities of the streamer. The model focuses on the phenomena occurring in the high electric field in front of a streamer, assuming these are the main contributors to the propagation. However, processes in the channel may be important for the electric field at the streamer extremities, which is why it is addressed in this study. Here, the channel is included by considering its conductivity as well as capacitance between the streamer and the plane.

2. Simulation model and theory

2.1. Electron avalanche model

We simulate streamer propagation in a liquid-filled needle–plane gap. The needle is represented by a hyperboloid and the streamer is represented by a number of hyperboloidal streamer heads, see figure 1. Each hyperboloid i has a potential V_i and an electric field $\boldsymbol{E}_i$. A potential V_0 is applied to the needle when the simulation begins. Since we here are interested in propagation rather than initiation of streamers, a square wave with infinite risetime is applied. The potential of each streamer head V_i is dependent on the potential and capacitance of the streamer (see section 2.3), and changes with time (see section 2.4). The method of calculation gives a drop in potential between the needle tip and the streamer tip, which is an important feature of the model. The Laplacian electric field $\boldsymbol{E}_i$ is dependent on the potential V_i and calculated using the hyperbole approximation [17]. The potential and electric field at a given position $\boldsymbol{r}$ is given by the superposition principle,

$$V(\boldsymbol{r}) = \sum_i k_i V_i(\boldsymbol{r}) \quad \text{and} \quad \boldsymbol{E}(\boldsymbol{r}) = \sum_i k_i \boldsymbol{E}_i(\boldsymbol{r}), \tag{1}$$

where the electrostatic shielding coefficients k_i are optimized such that $V(\boldsymbol{r}_i) = V_i(\boldsymbol{r}_i)$, i.e. the superposition of potentials gives the correct potential at the tip of each head. Each head with k_i lower than k_c (shielding threshold) is removed and heads closer than d_m (head merge threshold) are merged [17]. A number of anions, given by the anion number density n_{ion}, is placed at random positions in the liquid volume surrounding the streamer. Anions are considered as sources of seed electrons, which can turn into electron avalanches if the electric field is sufficiently high. The number of electrons $N_e = \exp(Q_e)$ in an avalanche increases each simulation time step Δt. The change in $Q_e = \ln N_e$, ΔQ_e, is given by

$$\Delta Q_e = E\ \mu_e\ \alpha_m \exp\left(-\frac{E_\alpha}{E}\right)\Delta t, \tag{2}$$

where μ_e is the electron mobility, and α_m and E_α are experimentally estimated parameters. An avalanche is considered 'critical' if Q_e exceeds a threshold Q_c (Townsend–meek criterion, $N_e = \exp Q_e > \exp Q_c$). Critical avalanches are removed, replaced by a new streamer head. The tip of the new streamer head is positioned where the avalanche became critical, and this way, the streamer grows [17].

The potential of the new head was set assuming a fixed electric field E_s in the streamer channel [17], but here the model is extended so that the potential is instead calculated by considering an RC-circuit.

2.2. RC-circuit analogy for streamers

A simple RC-circuit is composed of a resistor and a capacitor connected in series. When voltage is applied, the capacitor is charged and its potential increases as a function of time. The time constant τ of an RC-circuit is

$$\tau = RC, \tag{3}$$

where R is the resistance and C is the capacitance. Similarly, the streamer channel is a conductor with an associated resistance, and the gap between the streamer and the opposing electrode is associated with a capacitance, see figure 1. This is a reasonable assumption when modeling a dielectric liquid where the dielectric relaxation time is long compared to the duration of a streamer breakdown [6].

For a given streamer length ℓ, cross-section A, and conductance σ, the resistance is given by

$$R = \frac{\ell}{A\sigma}. \tag{4}$$

The resistance is proportional to the streamer length, calculated as the straight distance from the needle to the streamer head. Also A and σ may change during propagation. For instance, during a re-illumination, one or more of the streamer channels emit light [18]. This is likely the result of the buildup of a strong electric field within the channel, causing a a gas discharge within the channel, increasing σ and lowering R significantly [19]. It seems reasonable to assume that the resistance is reduced for some time after a re-illumination, however,

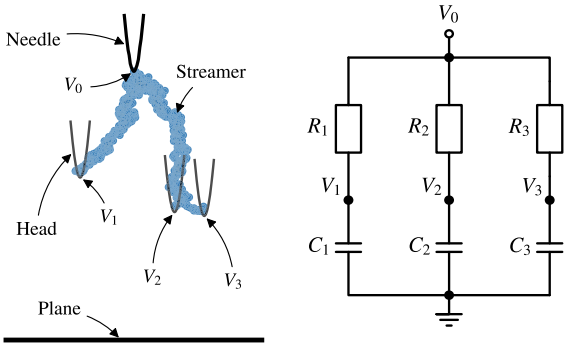

Figure 1. (left) Illustration of the needle electrode, a branched streamer, and three streamer heads above a planar electrode, and (right) the equivalent RC-circuit.

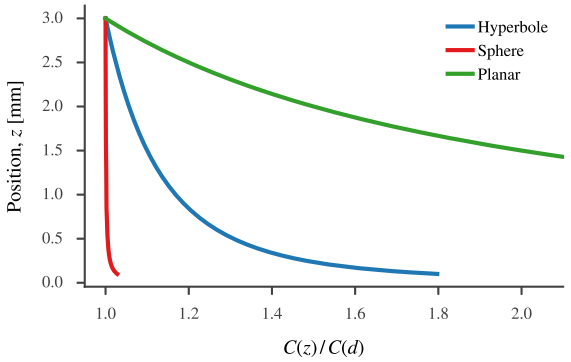

Figure 2. The three proposed models for capacitance as a function of the position in gap.

measurements shows just a brief spike in the current, typically lasting about 10 ns [18], which is consistent with the time scale for charge relaxation of ions in the channel [20].

The total charge of a streamer can be found by integrating the current and is in the range of nC to μC [6, 21, 22]. The 'capacitance' of the streamer can be approximated by considering the streamer to be a conducting half-sphere (slow and fine-branched modes) or a conducting cylinder (fast and single-branched modes), which also enables the calculation of the field in front of the streamer [3, 21, 23]. We associate each streamer head with the capacitance between itself and the planar electrode, as illustrated in figure 1. The capacitance then depends on the geometry of the gap between them, and an increase in streamer heads increases the total capacitance of the streamer. The capacitance for a hyperbole is applied for the avalanche model, while models for a sphere over a plane and a parallel plate capacitor are included here as limiting cases.

The capacitance of a hyperbole is approximated in appendix by integrating the charge on the planar electrode,

$$C_{\mathrm{H}}(z) \propto \left(\ln \frac{4z + 2r_{\mathrm{p}}}{r_{\mathrm{p}}}\right)^{-1}, \tag{5}$$

where r_{p} is the tip curvature of the hyperboloid and z is the distance to the plane. The capacitance of a parallel plane capacitor is

$$C_{\mathrm{P}}(z) \propto \frac{1}{z}, \tag{6}$$

where z is the distance between the planes, and the capacitance for a sphere above a plane is [24]

$$C_{\mathrm{S}}(z) \propto r_{\mathrm{p}}\left(1 + \frac{1}{2}\ln\left(1 + \frac{r_{\mathrm{p}}}{z}\right)\right), \tag{7}$$

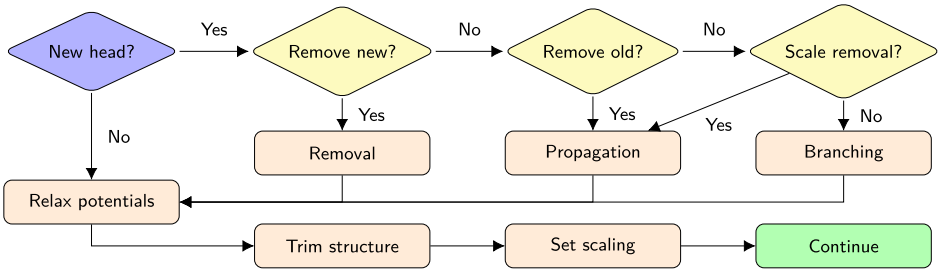

Figure 3. Algorithm for updating the streamer structure. 'Collision' and 'merging' checks decides whether the head should be removed immediately. The same checks are then performed to see if the addition of the head causes an existing head to be removed. Then, a 'scale removal' check is performed at equipotential. See text in section 2.4 for details on these checks. If the new head is not removed and a check finds a head to remove, the new head is a 'propagating' head and its potential is set by (10). Else, it is a 'branching head' and its potential is set by (12), which changes the potential of an existing streamer head as well. All potentials are then relaxed according to (13). Finally, the structure is trimmed by checking 'collision', 'merging' and 'scale', and the correct scale is set, as described in [17].

where r_p is the radius of the sphere. The difference in capacitance for the three models is substantial, see figure 2. A single sphere does not take a conducting channel into account, and this is the reason why its capacitance does not change significantly before z is about ten times r_p. Conversely, for the planar model, the capacitance grows rapidly as it doubles every time z is halved, but assuming parallel planes is considered an extreme case.

To test the impact of the variation in streamer channel conductivity and capacitance on the streamer propagation we will use a simplified model, where electrical breakdown within the channel is also included. Each streamer head is assigned a time constant τ, which is split into several contributions,

$$\tau = fgh\tau_0 \quad \text{with} \quad \tau_0 = \frac{Cd}{A\sigma}, \tag{8}$$

where d is the gap distance. The contributions

$$f = \frac{\ell}{d}, \quad g = \frac{C(z)}{C(d)}, \quad \text{and} \quad h = \Theta(E_{bd} - E_s), \tag{9}$$

represent change in resistance in the channel (f), capacitance between the streamer head and the plane (g), and the breakdown in the channel (h), respectively. The Heaviside step function Θ is zero when the electric field in the channel is larger than the breakdown threshold ($E_s > E_{bd}$) and one otherwise. When a breakdown in the channel occurs $\Theta = 0$, giving $\tau = 0$, and thus the potential at the streamer head is instantly relaxed to the potential of the needle. We therefore assume that breakdowns in the channel is the cause of re-illuminations. Since the heads are individually connected to the needle, a breakdown only affects one channel.

Having τ longer or shorter than the streamer propagation time implies relatively low or high conductivity, respectively. Since the contributions f, g, and h are on the order of magnitude 1 for most parts of the gap, the same is true for τ_0 (although $\tau_0 = R(0)\,C(d)$ does not have a physical interpretation). Throughout the simulations, an increase in τ_0 is considered to arise from a decrease in the channel conductivity σ, and vice-versa. The influence of channel expansion (increasing A), is included in the discussion in section 5, as well as evaluation of conductivity from τ_0.

2.3. Electrical potential of new streamer heads

The potential of a new head m is dependent on the closest streamer head n only. This is an approximation compared with using an electric network model for the streamer [14] and in contrast to our previous model using fixed electric field in the streamer channel [17]. Two different cases are implemented, depending on whether the new head can cause a branching event or not (see details in section 2.4 and figure 3). If the new head is not considered to be a new branch its potential is calculated assuming charge transfer from n to m,

$$V_m = V_n \frac{C_n}{C_m}. \tag{10}$$

Secondly, the potential for a branching head is calculated by sharing the charge between n and m, reducing the potential of n as well. Isolating the two heads from the rest of the system, the total charge is $Q = V_n C_n$, and this charge should be divided in such a way that the heads obtain the same potential, $V(\boldsymbol{r}_m) = V(\boldsymbol{r}_n)$, using (1) for both m and n. Introducing $M_{ij} = V_j(\boldsymbol{r}_i)/V_j(\boldsymbol{r}_j)$, (1) is simplified as

$$V_i(\boldsymbol{r}_i) = \sum_j M_{ij} k_j V_j(\boldsymbol{r}_j) \;\Rightarrow\; 1 = \sum_j M_{ij} k_j, \tag{11}$$

when all $V_i(\boldsymbol{r}_i)$ are equal. The coefficients k_j are obtained by NNLS-optimization [17], like the potential shielding coefficients. Finally, the potential for both m and n is calculated as

$$V_m(\boldsymbol{r}_m) = \frac{Q}{\sum k_i C_i}. \tag{12}$$

In the case where one k_i is close to unity and the other is close to zero, the result resembles (10), however, $\sum k_i \geqslant 1$, so the potential will drop when the capacitance of the new head is similar to or larger than its neighbor. The potential of a new head could also have been set to the potential at its position calculated before it is added, but that probably overestimates the reduction in potential, since the avalanche itself distorts the electric field and since transfer of charge from neighboring heads is faster than from the needle.

2.4. Updating the streamer

In [17], critical avalanches are replaced by new streamer heads and added to the streamer. Any head within another head has 'collided' with the streamer and is removed. If two heads are too close to each other they are 'merged', implying that the one closest to the plane is kept and the other one is removed. Also, the potential shielding coefficients are calculated and any head with a low coefficient is removed, 'scale removal'. Finally, the shielding coefficients are set.

The algorithm is now changed, see figure 3 (replacing the block labeled 'Streamer' in figure 5 in [17]). New heads are either removed, or classified as 'propagating' or 'branching', and their potential is set using (10) or (12). If a head can be added without causing another to be removed, it can cause a branching event, else it represents propagation of the streamer. The addition of one extra head is by itself not sufficient for streamer branching, often there are several heads within one propagating branch. Branching occurs through a process of adding new heads to opposing sides of a cluster of heads while removing the heads in the center (cf figure 28 in [17]). With this approach, branching follows as a consequence of propagation, contrary to models in which streamers propagate by adding branches [12, 14] or models which rely on inhomogeneities [10].

The difference in potential between each head V_i and the needle V_0 is first found and then reduced,

$$\Delta V_i = V_0 - V_i(\boldsymbol{r}_i) \;\rightarrow\; V_i(\boldsymbol{r}_i) = V_0 - \Delta V_i\, e^{-\Delta t/\tau_i}. \tag{13}$$

where the time constant of each head τ_i is calculated by (8). Finally, the streamer structure is trimmed (collision, merge and scale removal) and the potential scaling is optimized as described in [17]. Note trimming and rescaling is performed to remove heads lagging behind and to ensure correct potential at each streamer head, however, it does not preserve charge and capacitance. For this reason, we do not calculate the total charge or capacitance of the streamer.

3. Single channel streamer at constant speed

As a model system, a simplified numerical model is investigated by considering a streamer propagating as a single branch at constant speed. The parameters used are gap distance $d = 3$ mm, propagation speed $v_\mathrm{p} = 3$ km s^{-1}, tip radius $r_\mathrm{p} = 6$ μm, minimum propagation voltage $V_\mathrm{p} = 50$ kV, and breakdown in the channel at $E_\mathrm{bd} = 5$ kV mm^{-1}. The time constant τ is modeled by (8), (9) and the potential is calculated by (10).

The result of varying τ_0 for the different capacitance models g, is shown in figure 4. When applying the sphere model in (7), the change in potential is small and the time constant has little influence, as expected based on figure 2. The potential changes faster with the hyperbole model in (5) and breakdown in the channel occurs in the final part of the gap. Decreasing τ_0, i.e. increasing the conductivity, reduces the potential drop and delays the onset of breakdowns in the channel. This is similar for the plane model in (6), where rapid breakdowns at the start of the propagation are suppressed by decreasing τ_0. The propagation for the plane model is stopped when the potential drops below V_p, which occurs at about the same position for both low and high τ_0. Where the propagation stops depends on the capacitance model, the breakdown in channel threshold, the time constant, and the initial voltage V_0. A reduction of V_0 by 10 kV for the hyperbole model would have stopped these streamers as well, but the one with higher conduction would have propagated most of the gap, stopping close to the opposing electrode.

By assuming an initial capacitance $C = 0.1$ pF, the energy ($W = \frac{1}{2}CV^2 = \frac{1}{2}Q^2C^{-1}$) of each streamer head in figure 4 is some hundred μJ. From figure 2, the capacitance of the hyperbole model increases by about 20% during the first 2 mm, which amounts to some tens of μJ, and more than approximately 5 μJ mm^{-1} required for propagation [25]. Just before the first breakdown for the low-conductivity 'hyperbole streamer' in figure 4, there is a voltage difference of about 10 kV. Given a τ of about 10 μs this equals a continuous current of about 100 μA, while the first breakdown adds about a nC of charge. In comparison, the high-conductivity 'hyperbole streamer'

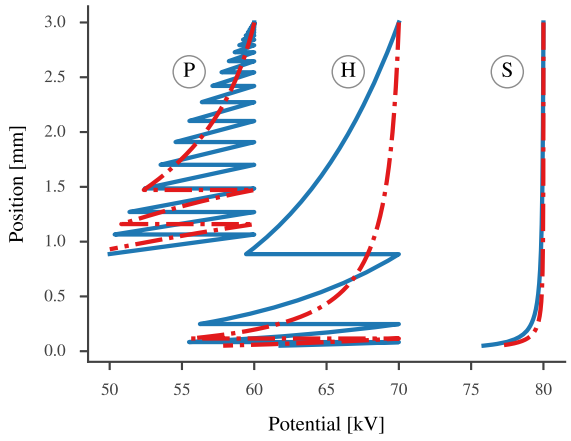

Figure 4. Potential of single head propagating at constant speed, starting at at different potentials for different capacitance models: (P) lane, (H)yperbole, and (S)phere, Time constants $\tau_0 = 0.1$ μs (dashed red) and $\tau_0 = 10$ μs (solid blue), and breakdown in channel at $E_{bd} = 5$ kV mm^{-1}.

has a current of more than a mA, sustaining the potential at the streamer head for the first part of the propagation. As such, the current and charge are comparable to experimental results [22].

4. Numerical simulation results

Positive streamers in cyclohexane are simulated in a needle-plane gap. Model parameters discussed in this work are given in table 1. The base parameters and their influence on the model were discussed in [17] and is therefore not repeated here. The values for α_m and E_α have been taken from [26] rather than [27], decreasing the propagation voltage from about 60 kV to about 40 kV [17], which is closer the experimentally estimated 33 kV [22]. Experimentally, the propagation voltage is determined from either the streamer shape, the measured current, or interpolation of the propagation length [22, 28]. For our simulations investigating propagation, however, the minimum requirement is simply a streamer length of 25% of the gap, since most simulated non-breakdown streamers stop within the first few hundred μm [17]. In the updated model, the field in the streamer E_s is not fixed but calculated by applying the RC-model described here. The influence of the conduction and breakdown in the streamer channel is investigated by changing values for τ_0 and E_{bd}. Interesting values for τ_0 are within some orders of magnitude of the propagation time for a streamer. The interpretation in terms of streamer radius and conductivity is discussed in the next section. For E_{bd} to affect streamers in a mm-sized gap, minimum some kVmm^{-1} are needed, however, the average electric field within the streamer E_s is dependent on both τ_0 and E_{bd}. In section 3, we indicate how conductivity and capacitance influence the potential of a streamer propagating at constant speed. In this section, however, only the hyperbole model for capacitance is used. Furthermore, the propagation speed depends on the potential in the simulation model [17], and allowing multiple heads increases the total capacitance of the streamer, which gives a drop in potential when an extra streamer head is added.

The simulations presented in figure 5 have equal voltage and equal initial anion placement (initial random number). The streamers are visualized in figure 5(a), showing some increase in thickness and decrease in branching when the conductivity increases, however, their propagation speeds in figure 5(b) clearly differ. The propagation speed is mainly influenced by the number of streamer heads and the potential of the streamer heads [17]. Figure 5(c) shows that when there is no breakdown in the channel, and the conductivity is low, i.e. τ_0 is high compared to the gap distance and propagation speed, the potential is reduced as the streamer propagates. For some short distances, the slow potential reduction is similar to the results in figure 4, however, when an extra head is added to the streamer (possible branching) there is a distinct reduction in the potential of some kV. Increased conductivity increases the speed and average potential of the streamers in figure 5(c). At $\tau_0 = 10^{-6}$ s, a single branch may gain potential during propagation while branching reduces the overall potential. This is reasonable since τ_0 is about a tenth of the time to cross the gap, see figure 5(b). By further increasing the conductivity (decreasing τ_0 to 10^{-8} s), the potential is kept close to that of the needle and the speed is increased, but τ_0 is now less than a hundredth of the time to cross, implying that it has little influence on the simulation.

For low channel conductivity, there is less 'scatter' in the streamer potential, which makes it easier to interpret the results when investigating the effect of breakdown in the streamer channel, see figure 5(d).

Table 1. Model parameter values.

Gap distance	d_g	3.0 mm
Needle curvature	r_n	6.0 μm
Streamer head curvature	r_s	6.0 μm
Scattering constant	E_α	1.9 GV m^{-1}
Max avalanche growth	α_m	130/μm
Meek constant	Q_c	23
Electron mobility	μ_e	45 mm^2 Vs^{-1}
Anion number density	n_{ion}	2×10^{12} m^{-3}
Head merge threshold	d_m	50 μm
Shielding threshold	k_c	0.10
Simulation time step	Δt	1.0 ps

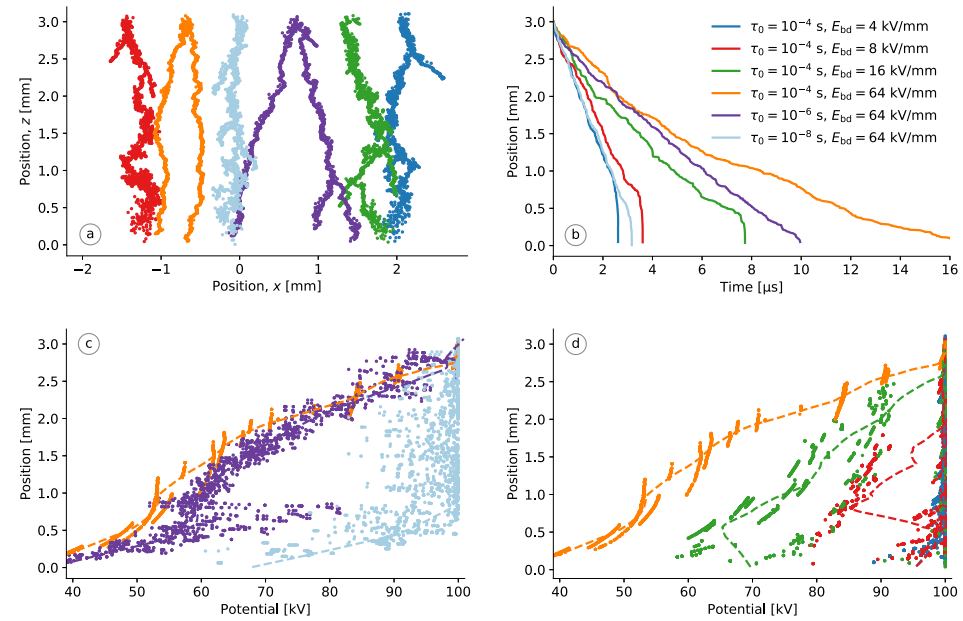

Figure 5. Simulations carried out at 100 kV using the same initial anion placement for a number of time constants τ_0 and breakdown thresholds E_{bd}. (a) 'Shadowgraphic plot' where the position of each streamer head is marked and (b) 'streak plot' showing the leading streamer head versus time. (c) and (d) show the potential of streamer heads versus position, and can be compared with figure 4. They show how decreasing τ_0 or E_{bd}, respectively, increases the average potential. Dots close to 100 kV in (d) indicate a recent channel breakdown (re-illumination). In (d), $E_{bd} = 4$ kV mm^{-1} is close to maximum and mostly hidden behind the others. The dashed lines are moving averages. All streamer heads involved in each simulation is shown in (a), only the leading head is shown in (b). In (c) and (d), data is sampled every 3 μm of the propagation. Each dot in (b), (c) and (d) is also shown in (a), but not vice-versa.

Breakdown in the channel can occur in the first part of the gap even when the threshold E_{bd} is high, since a potential difference of some kV gives an electric field of several kV mm^{-1} when the streamer length is some hundred μm. For $E_{bd} = 16$ kV mm^{-1} in figure 5(d), the average field inside the streamer is about 13 kV mm^{-1}. Rapid breakdowns gives E_s close to zero for $E_{bd} = 8$ kV mm^{-1}, except for about 0.5 mm in the middle of the gap. The average field in a streamer is on the order of kV mm^{-1} [20]. It is seen in figure 5(b) that the streamer slows down for the portion of the gap where the potential is decreased, and that streamers having similar average potential also use similar times to cross the gap.

Figure 5 gives a good qualitative indication of how τ_0 and E_{bd} affects the simulations. Different initial configuration of seed electrons show similar trends. Increasing concentration of seeds increases streamer propagation speed, but not branching [17]. However, changing the initial configuration changes the entire streamer breakdown and adds stochasticity to the model, while changing the needle voltage influences most results, such as the propagation speed, the jump distances, the number of branches, and the propagation length [17]. The effect of τ_0 and E_{bd} on the propagation speed is shown in figure 6 for a range of voltages, with several simulations performed at each voltage. The simulations with the lowest τ_0 are similar to those with the lowest E_{bd}. For these simulations, the potential of the streamer is equal to the potential of the needle, and the results are

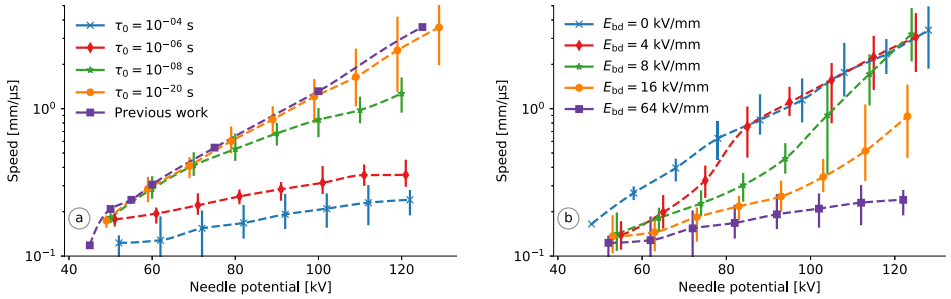

Figure 6. Propagation speed calculated for the mid 1.5 mm of the gap. (a) for different time constants τ_0 with $E_{bd} = 64$ kV mm^{-1}, and (b) for different breakdown thresholds E_{bd} with $\tau_0 = 10^{-4}$ s. Twenty simulations are performed for each voltage, the dashed lines are interpolated to the average values and the bars cover the minimum and maximum values. 'Previous work' is data from [17] (figure 15, $E_\alpha = 2$ GV m^{-1}). Simulations where $\tau_0 = 10^{-20}$ s or $E_{bd} = 0$ kV mm^{-1} are comparable to our previous work since τ is effectively zero for all of them. Each simulation is initiated with a random number to ensure that the configurations of seeds are uncorrelated.

similar to those presented in figure 15 in [17], as expected. Increasing τ_0 can reduce the propagation speed for a given voltage, and the time constant seems to dampen the increase in speed following increased voltage. Adding the possibility of a breakdown in the channel reverses this, since the net effect is a reduction in the average time constant, i.e. an increase in net conductivity. At low needle potential, there are fewer breakdowns in the channel and the speed is mainly controlled by the conductivity through τ_0, however, breakdowns become more frequent with increasing needle potential, which in turn increase the streamer potential and speed.

5. Discussion

As for our original model [17], this updated model still predicts a low propagation speed (see figure 6) and a low degree of branching (see figure 5(a)) compared with experimental results [22, 29]. Low propagation speed can be caused by low electron mobility, low electron/anion seed density, or too high shielding between streamer heads [17]. Increasing the time constant seems to increase the number of branches by regulating their speed and introducing breakdown in the channel reverses this effect. The hyperbole approximation of the electric field gives a strong electric field directed towards the planar electrode. Thus, electron avalanches in front of the head, giving forward propagation is favored over off-axis propagation and the chance of branching is reduced. A hyperbole can be a good approximation in the proximity of a streamer head, while possibly overestimating the potential in regions farther away. An overestimation of the potential from the streamer heads results in lower k_i values for the heads, which in turn gives lower electric fields, slower streamers, and a higher probability of a branch stopping, especially for branches lagging behind the leading head. Since we model an 'infinite' planar electrode, the capacitance does not change with the xy-position of an individual branch (unlike e.g. [14]). The coefficients k_i scale the streamer heads when the electric potential from the streamer is calculated, and changing a k_i can be interpreted as changing the capacitance of a streamer head. Two heads give a streamer a higher capacitance, but not twice the amount of a single head. However, the scaling is calculated from the potential and not the geometry, so this interpretation is an approximation, and for this reason we do not explicitly calculate the total capacitance or injected charge from the electrodes. The total injected current will reflect the behavior of individual heads discussed in section 3, having both a continuous component and impulses following breakdowns.

The conductivity of the channels can be approximated from the time constants. Consider that $d = 3$ mm, $C = 0.1$ pF, and $A = 100$ μm^2, results in that $\sigma = 3$ S m^{-1} is required for $\tau_0 = 1$ μs according to (8). Figure 6 thus shows that a conductivity of some S m^{-1} regulates the propagation speed, and that increased conductivity increases the speed. This is the order of magnitude as estimated for the streamer channel [2] and used by other models [14, 30], which is a very high conductivity compared with the liquid (about 10^{-13} S m^{-1} [6]). A streamer propagating at 1 km s^{-1} bridges a gap of 1 mm in 1 μs, which implies that τ has to be shorter than this to have a significant effect on the propagation, in line with the results in figure 6. However, how frequent and how large the loss in potential is as the streamer propagates, is also important in this context.

The streamer model permits a streamer branch to propagate with a low reduction in potential, enabling a branch to propagate a short distance even when the channel is non-conducting. However, propagation and branching events increases the capacitance, which reduces the potential at the streamer head, and can result in a breakdown in the channel, i.e. a re-illumination. A re-illumination increases the potential of the streamer head,

possibly causing other branches to be removed, and increases the chance of a new branching. A breakdown in the channel of one streamer head does not cause the nearby heads to increase in potential since each streamer head is individually 'connected' to the needle (see figure 1). Streamer experiments sometimes show re-illumination of single branches [18], but often more than one branch light up at the same time, which is a limitation in the present model. Such effects can be investigated by further development towards an electric network model for the streamer channels and streamer heads [14].

A streamer channel is not constant in size, but grows and collapses dynamically [31]. This implies that A in (4) changes with time, but so does σ, which depends on the density and mobility of the charge carriers. In turn, the creation, elimination, and mobility of the charge carriers is dependent on the pressure in the channel.Hence, it is not straightforward to evaluate how the conductivity of the channel is affected by the expansion. Conversely, external pressure reduces the diameter of the streamer channels [25], and reduce stopping lengths without affecting the propagation speed [32]. In a network model, each zigzag in each branch can be assigned specific parameters allowing greater control of the individual parts of the streamer, such as channel radius and conductivity. In the current implementation of the model, the channel length calculation and the constant conductivity (except for breakdowns), are aspects that can be improved in the future. Accounting for the actual length of the streamer channel is a minor correction, whereas branched streamer heads 'sharing' parts of a channel can influence the simulation to a larger degree.

From section 3 we find that a channel with high conductivity has less frequent re-illuminations, in line with experiments [19]. The results in figures 4 and 5 also indicate that even with a collapsed channel (where low/none conductivity is assumed) a streamer is able to propagate some distance. Whereas experiments indicate that, 1st mode streamers may propagate only a short distance after the channel disconnects from the needle [33], but the stopping of second mode streamers occur prior to the channel collapsing [25]. In our model, restricting the conductivity reduces potential in the extremities of the streamer as the streamer propagates, which regulates the propagation speed and increases branching (figure 6). The potential is reduced until either the streamer stops, the propagation potential loss is balanced by conduction, or a re-illumination occurs and temporary increases the conductivity. This seems to contrast experimental results where the propagation speed of 2nd mode streamers is just weakly dependent on the needle potential [32] and re-illuminations does not change the speed [19]. However, whether a channel is 'dark' or 'bright' can affect the propagation speed of higher modes [34].

6. Conclusion

We have presented an RC-model which includes conductivity and capacitance of the streamer. This model has been applied in combination with a streamer propagation model based on the avalanche mechanism [17]. The RC-model introduces a time constant that regulates the speed of streamer propagation, depending on the conductivity of the channel and the capacitance in front of of the streamer. The streamer can propagate even when the channels are non-conducting, but then with reduction in potential which reduces the speed and may cause stopping. However, re-illuminations, breakdowns in the channel, increase its conductivity and the speed of the streamer. It is also found that streamer branching, which increases the capacitance and reduces the potential at the streamer heads, can give rise to re-illuminations. Some limitations of our previous model [17], such as the low propagation speed and low degree of branching, are not significantly affected by the addition of the RC-model, and need to be investigated further.

Acknowledgments

The work has been supported by The Research Council of Norway (RCN), ABB and Statnett, under the RCN contract 228850. The authors would like to thank Dag Linhjell and Lars Lundgaard for interesting discussions and for sharing their knowledge on streamer experiments.

Appendix. Hyperbole capacitance

The electric field from a hyperbole is [17]

$$E = \frac{c}{a \sin\nu \sqrt{\sinh^2\mu + \sin^2\nu}}, \tag{A.1}$$

where c and a are constants given by the potential and the geometry, and μ and ν are prolate spheroid coordinates. In the xy-plane, $\sin\nu = 1$ giving $\sinh^2\mu + 1 = \cosh^2\mu$, and E becomes a function of the radius r,

$$E = \frac{c}{a\cosh\mu} = \frac{c}{\sqrt{r^2 + a^2}}, \tag{A.2}$$

by using relations from [17]. The charge Q of a system is given by the capacitance C and the potential V through $Q = CV$. The charge of the hyperbole is equal to the charge on the surface electrode, which is found by integration of the electric field using Gauss' law

$$Q = 2\pi\epsilon_0 \int_0^R E\, r\, \mathrm{d}r = 2\pi\epsilon_0 c(\sqrt{R^2 + a^2} - a), \tag{A.3}$$

where ϵ_0 is the vacuum permittivity. Implying that $Q \propto c$ for a plane of a finite radius $R \gg a$. From [35], $c \approx 2V/\ln(4a/r_\mathrm{p})$ and by using $a = z + \frac{1}{2}r_\mathrm{p}$, we find an expression for the capacitance of a hyperbole

$$C_\mathrm{H} = \frac{Q}{V} \propto \frac{c}{V} = 2\left(\ln\frac{4z + 2r_\mathrm{p}}{r_\mathrm{p}}\right)^{-1}, \tag{A.4}$$

which depends on the tip curvature r_p and the distance from the plane z.

ORCID iDs

I Madshaven https://orcid.org/0000-0002-2443-7448
OL Hestad https://orcid.org/0000-0001-7585-1326
PO Åstrand https://orcid.org/0000-0003-3384-7585

References

[1] Devins J C, Rzad S J and Schwabe R J 1981 Breakdown and prebreakdown phenomena in liquids *J. Appl. Phys.* **52** 4531–45
[2] Torshin Y V 1995 On the existence of leader discharges in mineral oil *IEEE Trans. Dielectr. Electr. Insul.* **2** 167–79
[3] Lundgaard L, Linhjell D, Berg G and Sigmond S 1998 Propagation of positive and negative streamers in oil with and without pressboard interfaces *IEEE Trans. Dielectr. Electr. Insul.* **5** 388–95
[4] Kolb J F, Joshi R P, Xiao S and Schoenbach K H 2008 Streamers in water and other dielectric liquids *J. Phys. D: Appl. Phys.* **41** 234007
[5] Joshi R P and Thagard S M 2013 Streamer-like electrical discharges in water: I. fundamental mechanisms *Plasma Chem Plasma Process* **33** 1–15
[6] Lesaint O 2016 Prebreakdown phenomena in liquids: propagation 'modes' and basic physical properties *J. Phys. D: Appl. Phys.* **49** 144001
[7] Wedin P 2014 Electrical breakdown in dielectric liquids—a short overview *IEEE Electr. Insul. Mag.* **30** 20–5
[8] Bruggeman P J *et al* 2016 Plasma-liquid interactions: a review and roadmap *Plasma Sources Sci. Technol.* **25** 053002
[9] Qian J *et al* 2005 Microbubble-based model analysis of liquid breakdown initiation by a submicrosecond pulse *J. Appl. Phys.* **97** 113304
[10] Jadidian J, Zahn M, Lavesson N, Widlund O and Borg K 2014 Abrupt changes in streamer propagation velocity driven by electron velocity saturation and microscopic inhomogeneities *IEEE Trans. Plasma. Sci.* **42** 1216–23
[11] Naidis G V 2016 Modelling the dynamics of plasma in gaseous channels during streamer propagation in hydrocarbon liquids *J. Phys. D: Appl. Phys.* **49** 235208
[12] Niemeyer L, Pietronero L and Wiesmann H J 1984 Fractal dimension of dielectric breakdown *Phys. Rev. Lett.* **52** 1033–6
[13] Kupershtokh A L and Karpov D I 2006 Simulation of the development of branching streamer structures in dielectric liquids with pulsed conductivity of channels *Tech. Phys. Lett.* **32** 406–9
[14] Fofana I and Beroual A 1998 Predischarge models in dielectric liquids *Jpn. J. Appl. Phys.* **37** 2540–7
[15] Lesaint O and Massala G 1998 Positive streamer propagation in large oil gaps: experimental characterization of propagation modes *IEEE Trans. Dielectr. Electr. Insul.* **5** 360–70
[16] Hestad O L, Grav T, Lundgaard L E, Ingebrigtsen S, Unge M and Hjortstam O 2014 Numerical simulation of positive streamer propagation in cyclohexane *In 2014 IEEE 18th Int Conf Dielectr Liq* 1–5
[17] Madshaven I, Åstrand P O, Hestad O L, Ingebrigtsen S, Unge M and Hjortstam O 2018 Simulation model for the propagation of second mode streamers in dielectric liquids using the Townsend-Meek criterion *J. Phys. Commun.* **2** 105007
[18] Linhjell D, Lundgaard L and Berg G 1994 Streamer propagation under impulse voltage in long point-plane oil gaps *IEEE Trans. Dielectr. Electr. Insul.* **1** 447–58
[19] Dung N V, Hoidalen H K, Linhjell D, Lundgaard L E and Unge M 2012 A study on positive streamer channels in Marcol Oil *In 2012 Annu. Rep. Conf. Electr. Insul. Dielectr. Phenom.* **7491** 365–70
[20] Saker A and Atten P 1996 Properties of streamers in transformer oil *IEEE Trans. Dielectr. Electr. Insul.* **3** 784–91
[21] Massala G and Lesaint O 1998 Positive streamer propagation in large oil gaps: electrical properties of streamers *IEEE Trans. Dielectr. Electr. Insul.* **5** 371–80
[22] Ingebrigtsen S, Smalø H S, Åstrand P O and Lundgaard L E 2009 Effects of electron-attaching and electron-releasing additives on streamers in liquid cyclohexane *IEEE Trans. Dielectr. Electr. Insul.* **16** 1524–35
[23] Top T, Massala G and Lesaint O 2002 Streamer propagation in mineral oil in semi-uniform geometry *IEEE Trans. Dielectr. Electr. Insul.* **9** 76–83
[24] Crowley J 2008 Simple expressions for force and capacitance for a conductive sphere near a conductive wall *Proc. Electrochem. Soc. Am. Annu. Meet. Electrost.* **Paper D1** 1–15 http://www.electrostatics.org/images/ESA_2008_D1.pdf
[25] Gournay P and Lesaint O 1994 On the gaseous nature of positive filamentary streamers in hydrocarbon liquids. II: propagation, growth and collapse of gaseous filaments in pentane *J. Phys. D: Appl. Phys.* **27** 2117–27
[26] Naidis G V 2015 On streamer inception in hydrocarbon liquids in point-plane gaps *IEEE Trans. Dielectr. Electr. Insul.* **22** 2428–32
[27] Haidara M and Denat A 1991 Electron multiplication in liquid cyclohexane and propane *IEEE Trans. Electr. Insul.* **26** 592–7

[28] Gournay P and Lesaint O 1993 A study of the inception of positive streamers in cyclohexane and pentane *J. Phys. D: Appl. Phys.* **26** 1966–74
[29] Ingebrigtsen S, Lundgaard L E and Åstrand P O 2007 Effects of additives on prebreakdown phenomena in liquid cyclohexane: II. Streamer propagation *J. Phys. D: Appl. Phys.* **40** 5624–34
[30] Aka-Ngnui T and Beroual A 2006 Determination of the streamers characteristics propagating in liquids using the electrical network computation *IEEE Trans. Dielectr. Electr. Insul.* **13** 572–9
[31] Kattan R, Denat A and Lesaint O 1989 Generation, growth, and collapse of vapor bubbles in hydrocarbon liquids under a high divergent electric field *J. Appl. Phys.* **66** 4062–6
[32] Lesaint O and Gournay P 1994 On the gaseous nature of positive filamentary streamers in hydrocarbon liquids. I: Influence of the hydrostatic pressure on the propagation *J. Phys. D: Appl. Phys.* **27** 2111–6
[33] Costeanu L and Lesaint O 2002 On mechanisms involved in the propagation of subsonic positive streamers in cyclohexane *Proc 2002 IEEE 14th Int. Conf. Dielectr. Liq. ICDL* **2002** 143–6
[34] Lu W and Liu Q 2016 Prebreakdown and breakdown mechanisms of an inhibited gas to liquid hydrocarbon transformer oil under positive lightning impulse voltage *IEEE Trans. Dielectr. Electr. Insul.* **23** 2450–61
[35] Coelho R and Debeau J 1971 Properties of the tip-plane configuration *J. Phys. D: Appl. Phys.* **4** 1266–80

III

Inge Madshaven, Øystein Leif Hestad,
Mikael Unge, Olof Hjortstam, Per-Olof Åstrand
Photoionization model for streamer propagation mode change in simulation model for streamers in dielectric liquids
Plasma Research Express **2**:015002 (2020)
DOI: 10/DG8M | ARXIV: 1909.12694

IOP Publishing Plasma Res. Express 2 (2020) 015002 https://doi.org/10.1088/2516-1067/ab6320

Plasma Research Express

PAPER

Photoionization model for streamer propagation mode change in simulation model for streamers in dielectric liquids

I Madshaven[1], OL Hestad[2], M Unge[3], O Hjortstam[3] and PO Åstrand[1,4]

[1] Department of Chemistry, NTNU—Norwegian University of Science and Technology, 7491 Trondheim, Norway
[2] SINTEF Energy Research, 7465 Trondheim, Norway
[3] ABB Corporate Research, 72178 Västerås, Sweden
[4] Author to whom any correspondence should be addressed.

E-mail: per-olof.aastrand@ntnu.no

Keywords: streamer, prebreakdown, dielectric liquid, photoionization, simulation model

OPEN ACCESS

RECEIVED
23 September 2019

REVISED
14 November 2019

ACCEPTED FOR PUBLICATION
17 December 2019

PUBLISHED
14 January 2020

Abstract

Radiation is important for the propagation of streamers in dielectric liquids. Photoionization is a possibility, but the effect is difficult to differentiate from other contributions. In this work, we model radiation from the streamer head, causing photoionization when absorbed in the liquid. We find that photoionization is local in space (μm-scale). The radiation absorption cross section is modeled considering that the ionization potential (IP) is dependent on the electric field. The result is a steep increase in the ionization rate when the electric field reduces the IP below the energy of the first electronically excited state, which is interpreted as a possible mechanism for changing from slow to fast streamers. By combining a simulation model for slow streamers based on the avalanche mechanism with a change to fast mode based on a photoionization threshold for the electric field, we demonstrate how the conductivity of the streamer channel can be important for switching between slow and fast streamer propagation modes.

1. Introduction

Dielectric liquids are widely used in high-voltage equipment, such as power transformers, because of their high electrical withstand strength and ability to act as a coolant [1]. If the electrical withstand strength of the liquid is exceeded, partial discharges followed by propagating discharges can occur and create prebreakdown channels called 'streamers'. Streamers are commonly classified by their polarity and propagation speed, ranging from below 0.1 kms^{-1} for the 1st mode to above 100 kms^{-1} for the 4th mode [2]. Streamers can be photographed by schlieren techniques, which captures the difference in permittivity between the gaseous streamer channel and the surrounding liquid [3], or by capturing light emitted by the streamer [4]. Continuous dim light has been observed from both the streamer channel and the streamer tip [5], as well as bright light from the streamer tip and re-illuminations of the streamer channel [5, 6]. The intensity of the emitted light and the occurrence of re-illuminations increases with higher streamer propagation modes. Photoionization by light absorbed in the liquid has been proposed as a possible feed-forward mechanism involved in the fast 3rd and 4th mode streamers [6, 7].

Streamer propagation is a multiscale, multiphysics phenomenon involving numerous mechanisms and processes [2]. Developing predictive models and simulations is challenging, but many attempts exist [8, 9]. Simulations have often focused on one aspect of the problem, such as the electric field [10, 11], production of free electrons ([12]), conductance of the streamer channels ([13]), inhomogeneities ([14]), or the plasma within the channels [15].

In this work we investigate a model for photoionization [16, 17] and combine it with a simulation model for propagation of streamers through an avalanche mechanism [18, 19]. The simplified cases studied in [16, 17], mimicking a streamer in a tube, can give only one streamer mode change. However, by not restricting the streamer to a 'tube' and including the dynamics of the streamer channel, we now demonstrate that the streamer

can change between slow and fast mode multiple times during a simulation. The present work is organized as follows: Theory on molecular energy states and radiation is given in the next section. The photoionization model is presented, evaluated and discussed in sections 3, 4 and 5, respectively. Section 6 describes the simulation model based on electron avalanches, with photoionization included, and the results of this model is presented in section 7. The model and the results are discussed in section 8, with the main conclusions summarized in section 9.

2. Molecular energy states and radiation

Molecules exist in quantum states with different energy $\mathcal{E}_n$. Excitation to a state of higher energy or relaxation to a state of lower energy can be achieved by absorbing or emitting a photon, respectively. The energy difference between molecular vibrational states is in the range meV to about 0.5 eV, while molecular electronic states have energies from some eV and up to around 20 eV. Change in vibrational states corresponds to infrared (IR) radiation (room temperature is about 25 meV), whereas visible (VIS) light (1.7–3.1 eV) and ultraviolet (UV) light (above 3.1 eV) normally correspond to electronic excitations. The transition probabilities to lower states gives the lifetime of an excited state, which varies from fs to several μs. In the case of fluorescence, an excited molecule relaxes through one or more states, before relaxing to the electronic ground state. The final relaxation is the most energetic and has the longest decay time, e.g. about 7.3 eV and 1 ns in liquid cyclohexane [20].

The ionization potential (IP) of a molecule is the energy required to excite an electron from the ground state $\mathcal{E}_0$ to an unbound state. Applying an external electric field $\boldsymbol{E}$ decreases the IP [21]

$$\mathcal{E}_{\mathrm{FDIP}}(E,\,\theta_{\mathrm{e}}) = \mathcal{E}_{\mathrm{IP}} - \beta\cos\theta_{\mathrm{e}}\sqrt{\frac{E}{\epsilon_{\mathrm{r}}E_{a_0}}}, \tag{1}$$

where $\mathcal{E}_{\mathrm{IP}}$ is the zero-field IP, $E_{a_0} = 5.14 \times 10^{11}\ \mathrm{Vm}^{-1}$, ϵ_r is the relative permittivity of the liquid, $\cos\theta_{\mathrm{e}} = \hat{\boldsymbol{k}}_{\mathrm{e}} \cdot \hat{\boldsymbol{E}}$, and $\boldsymbol{k}_{\mathrm{e}}$ is the momentum of emitted electron.The parameter $\beta = 54.4$ eV for the hydrogen atom, and similar values have been estimated for cyclohexane and several other molecules [21]. The energy of excited states is usually not significantly affected by the electric field in comparison to the field-dependence of the IP [21–23].

Spectral analysis of the light emitted from streamers show a broad band of photon energies up towards 3–4 eV [24, 25]. Distinct peaks in the emission spectrum reveal the presence of entities such as H_2, C_2, and CH_4, which are likely products of dissociation and recombination of hydrocarbon molecules from the base liquid [24, 26]. Stark broadening of the H_α-line can be investigated to find electron densities above $10^{24}\mathrm{m}^{-3}$, while the relation between the H_α and the H_β-line point to electron temperatures in the area of 10 kK [27]. Furthermore, rotational and vibrational temperatures of several kK can be estimated from spectral emission of C_2 Swan bands [28].

During a streamer breakdown, electrons (and other charged particles) are gaining energy and are accelerated in the electric field. Energy can be exchanged with other particles through collisions, possibly resulting in excitation, ionization or dissociation of molecules. Subsequently, relaxation or recombination can cause photon emission. The radiation B is absorbed by the medium, given by $\nabla B = -B\sigma\rho$ (Beer–Lambert law), where σ is the absorption cross section and ρ is the number density of the medium. Integration in spherical symmetry yields

$$\boldsymbol{B}(r) = \boldsymbol{B}_0\left(\frac{r_0}{r}\right)^2 \exp\left(-\int_{r_0}^{r} \rho\ \sigma\ \mathrm{d}\ell\right), \tag{2}$$

where $\boldsymbol{B}(r = r_0) = \boldsymbol{B}_0 = B_0\hat{\boldsymbol{r}}$. The ionization cross section of cyclohexane, for instance, increases from close to zero below the IP to about $5 \times 10^{-21}\ \mathrm{m}^2$ over the range of around 1 eV [29]. For single photons, cyclohexane begins to absorb around the first excitation energy and the absorption cross section increases steadily for higher photon energies [30]. A streamer could generate high-energy photons, which are rapidly absorbed by the liquid and therefore not measured by experiments [24].

From the radiation B, the photon number density n_γ is given by [31]

$$n_\gamma = B/\mathcal{E}_\gamma c, \tag{3}$$

where $\mathcal{E}_\gamma$ is the photon energy and c is the speed of light in vacuum. From the Beer–Lambert law and (3) it follows that $\nabla n_\gamma = -n_\gamma\sigma\rho$. Generally, σ is a superposition of all (absorption) cross sections, however, when excitations can be neglected and only ionization is considered, the ionization rate W (per volume) is given by the change in n_γ,

$$W = -\partial_t n_\gamma = n_\gamma\sigma\rho c, \tag{4}$$

where we have used the continuity equation $\partial_t n_\gamma + \nabla(c n_\gamma) = 0$. Within a given volume $\mathcal{V}$, the rate of ionizing events is $W\mathcal{V}$ and the number of molecules is $\rho\mathcal{V}$, which gives the ionization rate per molecule

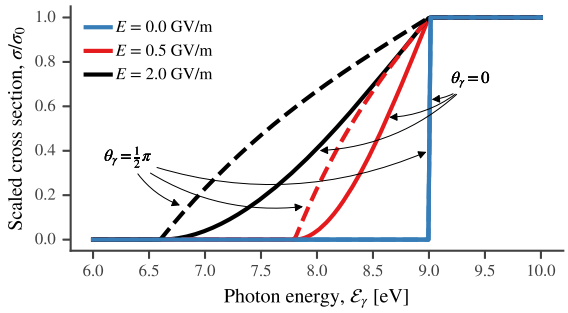

Figure 1. Photoionization cross section σ for different electric fields E and angles θ_γ as a function of photon energy $\mathcal{E}_\gamma$, calculated from (7) combined with (1).

$$w(r) = \frac{W\mathcal{V}}{\rho\mathcal{V}} = \int \frac{B(r,\,\mathcal{E}_\gamma)\,\sigma(r,\,\mathcal{E}_\gamma)}{\mathcal{E}_\gamma}\,\mathrm{d}\mathcal{E}_\gamma, \tag{5}$$

where we have explicitly stated the radiation and cross section as functions of the position r and the photon energy $\mathcal{E}_\gamma$. For instance, $w = 10^{-3}$ μs implies that 0.1% of the molecules would be ionized within a μs.

3. Defining the streamer radiation model

Streamers can emit light sporadically from the channel (re-illuminations) and continuously from the streamer head, with fast streamers emitting more light than slow streamers [6]. In this work, we investigate the possibility of light emitted from the gaseous streamer head causing ionization in the liquid, resulting in a change to a faster streamer mode.

The probability of emitting the electron in a given direction is dependent on the momentum of the absorbed photon, i.e. the differential cross section $\mathrm{d}\sigma$ is dependent on the differential solid angle $\mathrm{d}\Omega$,

$$\mathrm{d}\sigma \propto \sin^2\theta\,\mathrm{d}\Omega, \tag{6}$$

where $\cos\theta = \hat{\boldsymbol{k}}_\mathrm{e}\cdot\hat{\boldsymbol{k}}_\gamma$. When $\mathcal{E}_\gamma < \mathcal{E}_\mathrm{IP}$ we solve for $\mathcal{E}_\gamma = \mathcal{E}_\mathrm{FDIP}(E,\,\Theta)$ in (1) to find the maximum possible angle Θ of electron emission. Then we integrate (6) over all angles where $\theta < \Theta$ to arrive at an expression for the photoionization cross section

$$\begin{aligned}\sigma/\sigma_0 = 1 &- \tfrac{1}{4}(1+\cos^2\theta_\gamma)(3\cos\Theta - \cos^3\Theta)\\ &- \tfrac{1}{2}\sin^2\theta_\gamma\cos^3\Theta,\end{aligned} \tag{7}$$

where $\cos\theta_\gamma = \hat{\boldsymbol{k}}_\gamma\cdot\hat{\boldsymbol{E}}$. Since (6) just gives a proportionality relation, (7) has been scaled such that $\sigma(\Theta = \frac{1}{2}\pi,\,\theta_\gamma) = \sigma_0$. This is illustrated by figure 1, where $\sigma = 0$ when $\mathcal{E}_\gamma < \mathcal{E}_\mathrm{FDIP}$, $\sigma = \sigma_0$ when $\mathcal{E}_\gamma > \mathcal{E}_\mathrm{IP}$, and dependent on $\boldsymbol{E}$ and $\boldsymbol{k}_\gamma$ when $\mathcal{E}_\mathrm{FDIP} < \mathcal{E}_\gamma < \mathcal{E}_\mathrm{IP}$. For example, for $\mathcal{E}_\gamma = 7.5$ eV and $E = 2GV\ m^{-1}$, we find $\Theta = 0.3\pi$, implying that $\mathcal{E}_\mathrm{FDIP}(E,\,\theta_\mathrm{e} < 0.3\pi) < \mathcal{E}_\gamma$. According to (6), photons with $\theta_\gamma = \frac{1}{2}\pi$ (perpendicular to $\boldsymbol{E}$) have a higher chance of emitting an electron in this region ($\theta_\mathrm{e} < \Theta$) than photons with $\theta_\gamma = 0$. This is reflected in the different cross sections in figure 1.

We choose $z = (d + r_\mathrm{p})$ as the origin of radiation with a radiance $\boldsymbol{B}(r = r_\mathrm{p}) = \boldsymbol{B}_0$, see figure 2. Generally, B_0 is comprised of a distribution of photon energies, however, we choose to limit the model to only consider radiation from a single low-energy excited state ($\mathcal{E}_\gamma = \mathcal{E}_n - \mathcal{E}_0$), since low-energy states are likely the most abundant ones. Radiation can cause ionization if the photon energy exceeds the field-dependent IP, i.e. $\mathcal{E}_\gamma > \mathcal{E}_\mathrm{FDIP}$. Prolate spheroid coordinates are used to calculate the Laplacian electric field magnitude and direction [18], in order to calculate σ by (7). The radiance $\boldsymbol{B}$ in (2) and the ionization rate w in (5) can then be calculated, assuming low density ($\rho \approx 0$) within the streamer head and constant density in the liquid. The integration of σ is performed numerically in a straight line from $z = (d + r_\mathrm{p})$. Two-photon excitations (absorption to excited states) and scattering (absorption and re-emission) are assumed to have low influence and are ignored in this work.

4. Properties of the radiation model

To evaluate the radiation model, a hyperbolic streamer head with tip curvature $r_\mathrm{p} = 6$ μm is placed with a gap $d = 10$ mm towards a planar electrode (see figure 2). The model liquid is similar to cyclohexane, assuming radiation from the lowest excited state, i.e. $\mathcal{E}_\gamma = \mathcal{E}_1 - \mathcal{E}_0 = 7$ eV, $\mathcal{E}_\mathrm{IP} = 9$ eV, $\sigma_0 = 10^{-21}$ m^2 and

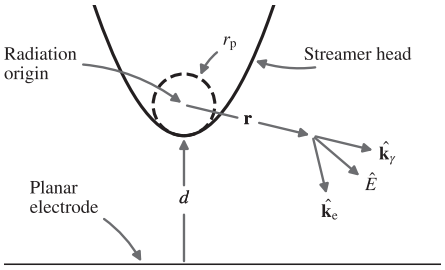

Figure 2. Sketch of a hyperbolic streamer head and relevant variables.

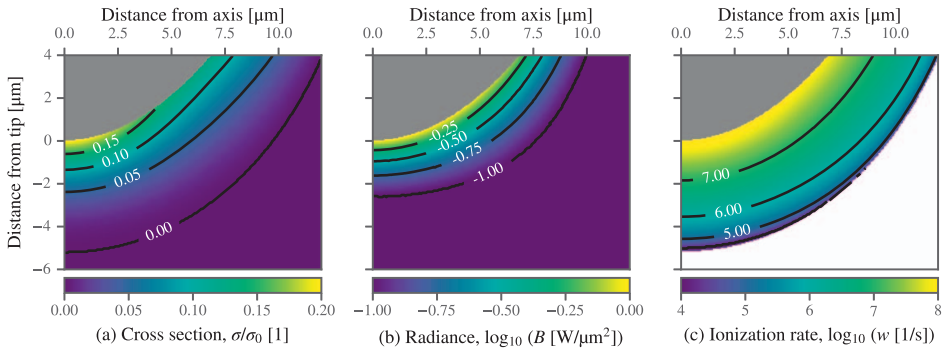

Figure 3. Streamer head (in grey) with $r_p = 6$ μm and $V_0 = 100$ kV, placed $d = 10$ mm from the planar electrode. The cross section (a), radiance (b), and photoionization rate (c) are calculated by (7), (2), and (5), respectively, applying the parameter values stated in the first paragraph of section 4. The y-axis is equal for all the plots.

$\rho = 5.6 \times 10^{27}/\mathrm{m}^3$ [16]. The initial power of the radiation is set to $B_0 = 1\mathrm{W}\ \mu\mathrm{m}^{-2}$, which is in the range of the power needed to evaporate the liquid [32]. Several other factors, such as Joule heating, can contribute to evaporate the liquid, and the contribution from radiation is unknown. Furthermore, the actual radiation power of a streamer is unknown and likely to fluctuate. However, since the results are linear in B_0, setting a value enables a discussion of whether the results are reasonable.

The area where ionization is possible increases with V_0 and covers a range of about 5 μm from the streamer head when $V_0 = 100$ kV, see figure 3(a). At the z-axis, $\sin\theta_\gamma = 0$, the cross section σ is yet the largest close to the streamer head, because of the strong electric field E. Figure 3(a) shows how σ declines as the distance from the streamer head increases. One could expect that σ would decline fast close to the streamer head as the distance from the z-axis increases, since E declines, however, an increase in $\sin\theta_\gamma$ when moving away off-axis counteracts the reduction in E, resulting in just a slight decrease in σ. Numeric integration of σ in figure 3(a) is applied to find B in (2), see figure 3(b). The rapid decay of the radiance is expected considering that $\rho\sigma_0 = 5.6/\mu$m (i.e. a penetration depth of $\delta = 1/\sigma\rho = 0.18$ μm) is included in the exponent in (2). The ionization rate per molecule w in (5) is presented in figure 3(c). A major finding is that photoionization is indeed a very local effect in dielectric liquids, mainly occurring within a few μm of the source, which is the streamer head in this case.

Increasing V_0 increases the ionization rate w close to the streamer head and increases the reach of the ionization zone in figure 4(a) up to about 100 kV. At higher potentials, the ionization rate at a distance of some μm decreases since much of the radiation is absorbed within the first μm. This is evident from the contour for $w = 10^6/\mathrm{s}$, for instance. We may hypothesize that photoionization cause streamer propagation once a degree of ionization p is obtained. The time t_w required to reach p is $t_w = p/w$, and this time varies with the distance from the streamer head Δr. Both the time and the distance are important, obtaining p fast very close to the streamer have to be weighed against having a longer t_w at a distance further from the streamer. As such, we define the photoionization speed of the streamer,

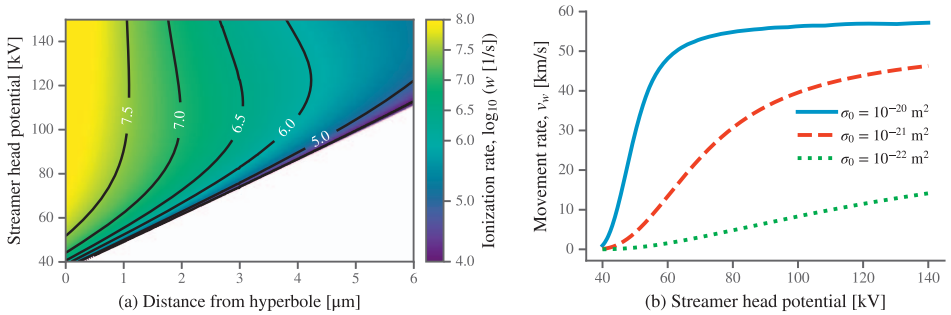

Figure 4. (a) Ionization rate w along z-axis for different V_0. 100 kV corresponds to figure 3(c). (b) Maximum movement rate v_w calculated by (8) assuming $p = 0.001$. The transition is sharpest for $\sigma_0 = 10^{-20}$ m^2 followed by 10^{-21} m^2, while 10^{-22} m^2 resembles a linear increase. The magnitude is linearly dependent on B_0 and inversely dependent on p.

$$v_w = \max\left\{\frac{\Delta r}{t_w}\right\} = \max\left\{\frac{\Delta r w}{p}\right\}. \tag{8}$$

The speed v_w is set to the maximum value of the product of Δr and w, where $w = w(\Delta r)$ is calculated numerically, for a range of Δr close to the streamer head. Since measured electron densities in streamers point to a degree of ionization in the range of 0.1% to 1% [27, 28], we assume that $p = 0.001$ is required for propagation. The photoionization speed v_w of the data in figure 4(a) is presented in figure 4(b), showing an increase in v_w as $\mathcal{E}_{\mathrm{FDIP}}$ is reduced below $\mathcal{E}_\gamma$. Changing to $p = 0.01$ would yield the same result if also B was increased tenfold since the magnitude of v_w is dependent on the radiated power ($v_w \propto w \propto B_0$). Neither the value of B_0 or p is known and we cannot assert that photoionization indeed leads to such a drastic speed increase v_w as shown in figure 4(b), however, the important part of the model is to show that photoionization can be affected by the electric field strength and that the effect is local. Physically, when the liquid no longer can absorb light to a bound excited state, the result is direct ionization, and it is reasonable that ionization contributes more to the propagation speed than emission of light or local heating. The transition from low to high speed (low to high ionization rate) in figure 4(b) for the largest cross section ($\sigma_0 = 10^{-20}$m^2) occurs over a short voltage range of about 20 kV.

5. Discussion of the radiation model

The modeled photoionization cross section increased from zero towards a maximum of 10^{-21} m^2, which resulted in rapid absorption within a few μm. The real absorption might be even more rapid, since the cross section of cyclohexane is about 5 times larger for ionizing radiation [29]. An increase in the cross section to $\sigma_0 = 5 \times 10^{-21}$ m^2 gives a shorter penetration depth $\delta = 1/\sigma\rho$, which results in even shorter range for the radiance and ionization than shown in figure 3. According to figure 4(b) this gives a steep increase in the movement rate v_w. The fluorescence of cyclohexane is consistent with radiation from the first excited state [20], but the absorption to this state is intrinsically low [30]. Radiation from fluorescence may thus transport energy away from the streamer head.

Excited molecules in the liquid have a high probability of non-radiative relaxation which heats the liquid. In strong electric fields, the IP is reduced and bound excited states become unbound, i.e. they appear above the ionization threshold [22], and instead of heating, absorption causes ionization. It is, however, difficult to assess how an electric field affects cross sections. By assuming an increase in the cross section when the field is increased (see figure 1), more radiation is absorbed, but the effect also becomes more local. The model therefore predicts a faster propagation when the radiation from the streamer head is absorbed directly in front of the streamer, in line with figure 4(b) where higher cross sections results in higher speeds.

The photoionization cross sections σ for linear alkanes and aromatics differ by more than a decade, from about 1×10^{-22} m^2 to 5×10^{-21} m^2 [33]. Given a number density $\rho = 5 \times 10^{27}$/ m^3, the penetration depth δ is between 2 μm and 0.04 μm, respectively. Ionizing radiation emitted when electrons recombine with cations is therefore rapidly absorbed, however, non-ionizing radiation having lower absorption cross section can propagate further. If we assume that fluorescent radiation from cyclohexane is absorbed with a cross section of 1/100 of the ionizing radiation, this radiation has a reach of several μm. In combination with a low-IP aromatic additive, having a larger cross section, the reach of the radiation is reduced, but radiation absorbed by the additive causes ionization whereas absorption to cyclohexane results in heat. For instance, pyrene ($\mathcal{E}_{\mathrm{IP}} = 7$ eV [23]) is ionized when absorbing fluorescent radiation from cyclohexane, and could facilitate streamer growth by

providing seed electrons for new avalanches. A similar result is found for gases where additives absorbing ionizing radiation can increase the streamer propagation speed for a single branch [34]. Furthermore, excited states of the additives can have lifetimes of tens to hundreds of ns [35], which increases the probability of two-photon ionization compared with a lifetimes up to about a ns in pure cyclohexane [20]. As such, low-IP additives can facilitate slow streamers by reducing the inception voltage, increase the propagation length, and reduce the breakdown voltage [36]. Facilitated growth can lead to more branching, which is possibly why such additives can increase the acceleration voltage [36]. Increased branching can stabilize the streamer through electrostatic shielding, however, photoionization in front of the streamer can be involved in a change to a fast mode [6, 7]. For instance, if onebranch escapes the shielding from the others, the electric field surrounding it would increase, reducing the IP and allowing more of the radiation to cause ionization.

Under normal conditions, electrical insulation in liquids is a steady-state process where the added energy by the applied electrostatic potential is released through radiation as either heat or light in the UV/VIS region. Similarly, during a streamer breakdown, the added energy can dissipate in the liquid, but also cause streamer propagation when the energy dissipation is concentrated. The availability of electronic excited states is therefore crucial, and because of the strong field-dependence of the IP, the number of available excited states decrease with increasing field [22]. Additives with lower excitation energies, sustaining to higher fields, may therefore be an approach to increase the acceleration voltage, as indicated experimentally [37, 38]. The available excited states and absorption probabilities are therefore important to consider. One additive that has been studied [36], pyrene, has excited states between 4 and 7 eV (in gas) [23]and can thus absorb and radiate energy which is generally not absorbed by cyclohexane. Pyrene and dimethylaniline (DMA) have a similar $\mathcal{E}_{\mathrm{IP}}$ and first excitation energy, and both additives increase the acceleration voltage in cyclohexane [36, 39]. However, whereas pyrene absorbs radiation at the lowest excitation energy which is a π to π^* transition, the lowest excited state of DMA is non-absorbing [40] and thus the second lowest excitation energy should be considered instead. This increases the excitation energy from 4 to 5 eV [40]. It is not uncommon that the lowest state is non-absorbing. For example in azobenzenes, also studied as an additive in streamer experiments [37], the lowest n to π^* transition is non-absorbing, whereas the second excitation, π to π^*, has a high absorbance and gives the molecules their color [41]. Excited states most likely play a role both in collision events with primary electrons (affecting impact ionization) and in absorption of light (affecting photoionization), but the different contributions are difficult to disentangle from other mechanisms. In the end, which effects that are significant under realistic conditions need to be established by cleverly designed experiments.

There is a relatively small number of electronic states available below the IP, but a large number of states above the IP, often considered as a continuum. This makes the cross section for ionization larger than the cross section for absorption to a bound excited state. Consequently, as the IP decreases with an increase in the electric field, the cross section at certain energies increases. A local electric field in excess of 0.5 GV m^{-1} is sufficient to remove all excited states of cyclohexane in gas phase [22]. In a liquid where $\epsilon_r = 2$, we find that a local field of 1.4 GV m^{-1} reduce the IP by 2 eV from (1), which is sufficient to reduce $\mathcal{E}_{\mathrm{FDIP}}$ below the first excited state in cyclohexane. When the electric field is above this threshold, cyclohexane cannot absorb radiation to a bound state and is ionized instead. For a hyperbolic streamer head with $r_{\mathrm{p}} = 6$ μm in a gap $d = 10$ mm, this threshold is reached at a potential of 37 kV, assuming that the local field is the same as the macroscopic field, and the transition in speed occurs above this in figure 4(b). The threshold is close to the acceleration voltage in a tube [42], but much lower than the acceleration voltage in a non-constricted large gap [36]. However, the actual tip radius of the streamer and the degree of branching are important when calculating the tip field, as well as space charge generated in the liquid. Furthermore, the local field can differ from the macroscopic field. For instance, the field is increased by a factor of 1.3 in a spherical cavity in a non-polar liquid [21]. The model mainly demonstrates how rapid ionizing radiation (high cross section) is absorbed in the liquid.

6. Avalanche model with photoionization

In earlier work we have developed a model for simulating the propagation of positive streamers in non-polar liquids through an electron avalanche mechanism [18, 19]. Here we incorporate the photoionization mechanism into the streamer model. A short overview of the model is given below.

Simulation parameters are similar with those used in our previous works [18, 19], i.e. a needle-plane gap with cyclohexane as a model liquid. The needle is represented by a hyperbole (see figure 2) with tip curvature $r_{\mathrm{n}} = 6.0$ μm, placed $d = 10$ mm above a grounded plane. The potential V_0 applied to the needle gives rise to an electric field $\boldsymbol{E}$ in the gap. The Laplacian electric field is calculated analytically in prolate spheroid coordinates. Electrons detach from anions in the liquid (assumed ion density $n_{\mathrm{ion}} = 2 \times 10^{12}$ m^{-3}) and grow into electron avalanches if the field is sufficiently strong. The number of electrons N_{e} in an avalanche is given by

$$\ln N_e = \sum_i E_i \, \mu_e \, \alpha_m \, e^{-E_\alpha/E_i} \Delta t, \tag{9}$$

where $\alpha_m = 130\ /\mu$m and $E_\alpha = 1.9$GV, m^{-1} for cyclohexane [43], $\mu_e = 45$ mm^{2}Vs^{-1} is the electron mobility, i denotes a simulation iteration, and $\Delta t = 1$ ps is the time step. If an avalanche obtains a number of electrons $N_e > 10^{10}$, it is considered 'critical'. The streamer grows by placing a new streamer head wherever an avalanche becomes critical. Each streamer head, an extremity of the streamer, is represented by a hyperbole with tip curvature $r_s = 6.0\ \mu$m. After the inception of the streamer, the electric potential V and the electric field $\boldsymbol{E}$ for a given position $\boldsymbol{r}$ is calculated by a superposition of the needle and all the streamer heads,

$$V(\boldsymbol{r}) = \sum_i k_i V_i(\boldsymbol{r}), \quad \boldsymbol{E}(\boldsymbol{r}) = \sum_i k_i \boldsymbol{E}_i(\boldsymbol{r}), \tag{10}$$

where i denotes a streamer head. The coefficients k_i correct for electrostatic shielding between the heads. Whenever a new head is added, the streamer structure is optimized, possibly removing one or more existing heads. Streamer heads within 50 μm of another head closer to the plane, and heads with $k_i < 0.1$, are removed [18].

Each streamer head is associated with a resistance in the channel towards the needle and a capacitance in the gap towards the planar electrode [19]. The resistance R and capacitance C is given by

$$R \propto \ell, \ \text{and} \ C \propto \left(\ln \frac{4z + 2r_s}{r_s} \right)^{-1}, \tag{11}$$

where ℓ is the distance from the needle to the streamer head and z is the position of the streamer head in the gap. New streamer heads are given a potential which magnitude depends on their position as well as the configuration of the streamer. The potential V_i of each streamer head is relaxed towards the potential of the needle electrode V_0 each simulation time step. This is achieved by reducing the difference in potential,

$$\Delta V_i = V_0 - V_i \ \rightarrow \ V_i = V_0 - \Delta V_i e^{-\Delta t/\tau_i}, \tag{12}$$

where the time constant is given by $\tau = \tau_0 RC$ and $\tau_0 = 1\ \mu$s. If the electric field within the streamer channel $E_s = \Delta V_i / \ell_i$ exceeds a threshold E_{bd}, a breakdown in the channel occurs, equalizing the potential of the streamer head and the needle. A channel breakdown affects the potential of a single streamer head since each streamer head is 'individually' connected to the needle [19].

Calculating the photoionization cross section in (7) is a computational expensive operation, contrary to our avalanche simulation model which is intended to be relatively simple and computationally efficient. The photoionization model indicates an increase in speed (see figure 4) when $\mathcal{E}_{FDIP} < \mathcal{E}_n$ over a short distance into the liquid. To model photoionization in an efficient way, we add a 'photoionization speed' v_w to each streamer head exceeding a threshold $E_w = 3.1$GV m^{-1}. This is implemented by moving such streamer heads a distance $\boldsymbol{s}_w = v_w \Delta t \ \hat{\boldsymbol{z}}$. Equation (8) predicts a speed v_w given a set of parameter values (see figure 4(b)), where some, such as radiation power and degree of ionization, are unknown. The chosen power of 1W μm^{-2} exceeds 100 W in total when distributed over a streamer head with a radius of some μm. Since a streamer requires about 5 mJ/m for propagation [32], the expected speed exceeds 20km s^{-1}, which is in line with figure 4(b). We choose $v_w = 20$km s^{-1} for the simulations, which is the order of magnitude given by figure 4(b), but slow compared to some 4th mode streamers exceeding 100km s^{-1}. However, this is sufficient to investigate transitions between slow and fast mode since it is more than an order of magnitude above the speed predicted by the simulations without a photoionization contribution [18].

7. Results from avalanche model with photoionization

For evaluating the model we investigate the influence of the applied voltage V_0 (square wave), the threshold for breakdown in the channel E_{bd}, while excluding or including photoionization. Figure 5 illustrates the behavior of two different single head streamers. Streamer 1 starts in a fast mode, but after propagating some mm the electric field at the streamer head has dropped below the threshold for fast propagation E_w and the streamer changes to a slower mode of propagation. Streamer 2 starts in a slow mode, but having no potential drop within the streamer channel, the electric field at the streamer head increases during propagation and the streamer changes to a fast mode for the final few mm of the gap.

Both streamer 1 and 2 in figure 5 are simplified cases with a single head and a constant E_s, however, the simulations in figure 6(a) show a similar behavior, but at higher voltages. In the simulations with low E_{bd}, resulting in a low E_s, the streamers switch to fast mode for the final portion of the gap, and the portion increases with increasing voltage. According to figure 5, all of the streamers in figure 6(a) starts above the threshold of $E_w = 3.1$GV m^{-1}, however, as the streamer propagates and more streamer heads are added, electrostatic shielding between the heads quickly reduces the electric field below this threshold. Increasing E_{bd} gives an on average higher E_s and figure 6(a) illustrates how this can make streamers change between fast and slow propagation.

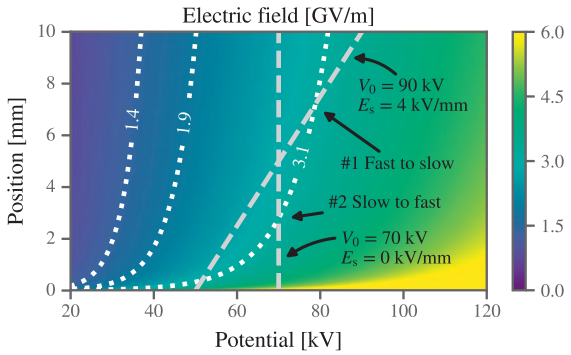

Figure 5. Electric field strength at the tip of an electric hyperboloid with a tip curvature of 6.0 μm for a given position and potential. The dotted white lines show the electric field thresholds for IP reduction by 2 eV (1.4 GV m^{-1}) and 3 eV (E_w = 3.1GV m^{-1}), as well as E_α = 1.9GV m^{-1}. The dashed gray lines represent streamers. (1) indicate how an electric field of E_s = 4kV mm^{-1} can change the propagation mode from fast to slow in the beginning of the gap. (2) indicate how a highly conducting streamer can change from slow to fast towards the end of the gap.

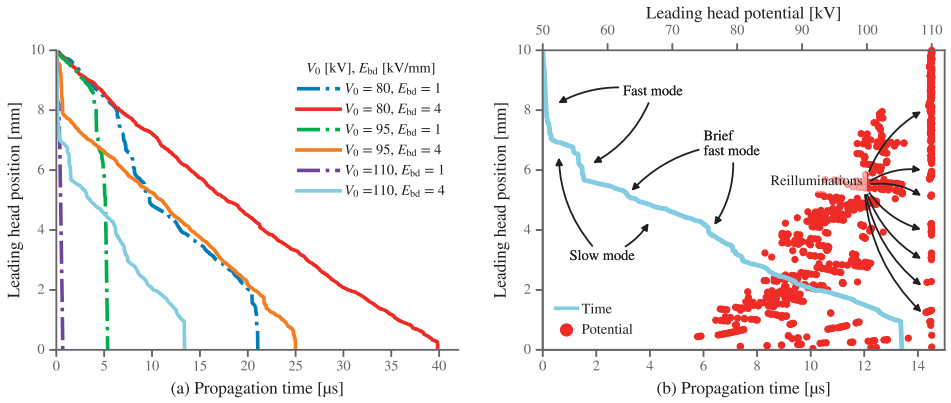

Figure 6. (a) Streak plots showing the position of the leading streamer head as a function of time. The transition from slow to fast or from fast to slow is dependent on the needle potential and the channel breakdown threshold. (b) Propagation time and leading head potential, each as a function of leading head position in the gap, for V_0 = 110 kV and E_{bd} = 4kV mm^{-1} in (a). The above data is generated by sampling the position and potential of the leading streamer head (closest to the opposing electrode) for every 10 μm of propagation of each simulation.

Figure 6(b) details a streamer beginning in fast mode and changing to slow propagation mode. Propagation reduces the potential at the streamer head. When the electric field at the tip is sufficiently reduced, the streamer changes to a slow mode. Re-illuminations, breakdowns within the streamer channel, sporadically increases the potential and can push the streamer over in a fast mode, however, often this 'fast mode' is brief and difficult to notice.

By considering a wider range of voltages in figure 7, the transition from slow to fast mode occurs at about 100 kV for a highly conducting streamer. Increasing E_{bd} decreases the average (in time) electric field at the streamer heads and thus delays the onset of the fast mode to about 120 kV. An acceleration voltage of 120 kV is consistent with longer gaps [36, 39], while for shorter gaps (5 mm) about 60 kV has been found [42]. As mentioned in our previous work, the propagation voltage predicted by the simulations is somewhat high compared with experiments, whereas the propagation speed is low for second mode streamers [18]. The present work does not aim to improve on these limitations for slow streamers, but rather demonstrate how changes between slow and fast propagation can occur in different parts of the gap. The propagation speed for slow-mode streamers is about ten times of that predicted by figure 7, but the difference can be removed by assuming a higher electron mobility or a higher seed density [18].

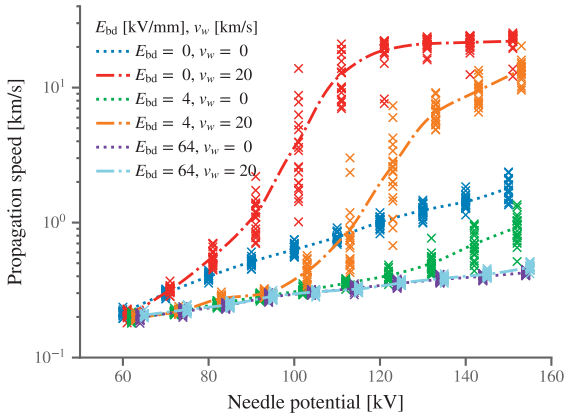

Figure 7. Average propagation speed for the middle of the gap (z between 2.5 mm and 7.5 mm). The onset of the fast mode is delayed when the field within the streamer channel is increased. Each marker is a simulation (20 for each voltage, 1200 in total) and the lines are interpolated to the average. $v_w = 0\text{km s}^{-1}$ implies no added speed from photoionization.

8. Discussion

The role of photoionization during discharge in liquids is difficult to assess. For breakdown in gases, ionizing radiation can penetrate far into the medium, providing seed electrons for avalanches. While similar reasoning have been suggested for liquids, we argue that, given the higher density of the liquid and the large cross section for ionizing radiation, the penetration depth is short and photoionization occurs locally. Which radiation energies that are ionizing and where they can cause direct ionization are dependent on the electric field, given the field-dependence of the IP as well as the ionization cross-section. Non-ionizing, low-energy radiation have longer range and can provide seed electrons through a two-step ionization process. However, ionization of impurities or additives are far more likely, especially when the radiation from the base liquid can ionize them directly or they have long-lived excited states.

Assuming that increasing the applied potential increases the amount of radiation, it also increases generation of seed electrons for avalanches. Seeds likely facilitates both propagation speed and branching, while electrostatic shielding between branches can regulate the propagation speed. One hypothesis is that the change to a fast mode occurs when one fast branch escapes the electrostatic shielding from the others. If the radiation from such a branch can penetrate deep into the liquid, energy is transported away from the streamer head, while new seeds and subsequent avalanches can result in electrostatic shielding. Both of these mechanisms can reduce the speed. However, we have presented a model where a strong electric field makes photoionization more localized, suppressing energy transport and branching. This can explain how a streamer changes to a fast propagation mode when the electric field is sufficiently strong.

The model is limited in the sense that we do not know the actual value for the radiated power (or its energy distribution) or the degree of ionization it takes for a streamer to propagate. To assess the model we chose a value for the radiated power, and showed that this would be sufficient to ionize the liquid at a reasonable rate. Whether obtaining this radiated power is feasible remains unknown.

9. Conclusion

Emission and absorption of light is important for streamer propagation. Radiation can transport energy away from the streamer as heat or create free electrons through ionization, however, ionizing radiation is rapidly absorbed and thus unlikely to create seed electrons at some distance from the streamer head. Furthermore, since increasing the electric field reduces the ionization potential, it also increases the ionization cross section, making photoionization a local process. The model based on the electron avalanche mechanism in combination with modeling photoionization close to the steamer tip is found to capture the feature of acceleration of the streamer tip above a critical voltage. The photoionization model is missing a proper estimation of the spectral intensity of the radiation as well as the resulting speed, and this need to be investigated in the future. Radiation and photoionization is often mentioned in streamer literature, however, the potential short reach of the ionizing radiation is an important aspect to consider in understanding streamers in dielectric liquids.

Acknowledgments

This work has been supported by The Research Council of Norway (RCN), ABB and Statnett, under the RCN contract 228850.

ORCID iDs

I Madshaven https://orcid.org/0000-0002-2443-7448
OL Hestad https://orcid.org/0000-0001-7585-1326
PO Åstrand https://orcid.org/0000-0003-3384-7585

References

[1] Wedin P 2014 Electrical breakdown in dielectric liquids—a short overview *IEEE Electr Insul Mag* **30** 20–5
[2] Lesaint O 2016 Prebreakdown phenomena in liquids: propagation 'modes' and basic physical properties *J Phys. D: Appl. Phys.* **49** 144001
[3] Farazmand B 1961 Study of electric breakdown of liquid dielectrics using Schlieren optical techniques *Br. J. Appl. Phys.* **12** 251–4
[4] Sakamoto S and Yamada H 1980 Optical study of conduction and breakdown in dielectric liquids *IEEE Trans. Electr. Insul.* **EI-15** 171–81
[5] Dung N V, Høidalen H K, Linhjell D, Lundgaard L E and Unge M 2013 Effects of reduced pressure and additives on streamers in white oil in long point-plane gap *J Phys. D: Appl. Phys.* **46** 255501
[6] Linhjell D, Lundgaard L and Berg G 1994 Streamer propagation under impulse voltage in long point-plane oil gaps *IEEE Trans. Dielectr. Electr. Insul.* **1** 447–58
[7] Lundgaard L, Linhjell D, Berg G and Sigmond S 1998 Propagation of positive and negative streamers in oil with and without pressboard interfaces *IEEE Trans. Dielectr. Electr. Insul.* **5** 388–95
[8] Biller P 1996 A simple qualitative model for the different types of streamers in dielectric liquids *ICDL'96 12th Int. Conf. Conduct Break Dielectr Liq.* 189–92 IEEE.
[9] Beroual A 2016 Pre-breakdown mechanisms in dielectric liquids and predicting models *2016 IEEE Electr. Insul. Conf.* 117–28
[10] Niemeyer L, Pietronero L and Wiesmann H J 1984 Fractal dimension of dielectric breakdown *Phys. Rev. Lett.* **52** 1033–6
[11] Fofana I and Beroual A 1998 Predischarge models in dielectric liquids *Jpn. J. Appl. Phys.* **37** 2540–7
[12] Kim M, Hebner R and Hallock G 2008 Modeling the growth of streamers during liquid breakdown *IEEE Trans. Dielectr. Electr. Insul.* **15** 547–53
[13] Kupershtokh A L and Karpov D I 2006 Simulation of the development of branching streamer structures in dielectric liquids with pulsed conductivity of channels *Tech. Phys. Lett.* **32** 406–9
[14] Jadidian J, Zahn M, Lavesson N, Widlund O and Borg K 2014 Abrupt changes in streamer propagation velocity driven by electron velocity saturation and microscopic inhomogeneities *IEEE Trans. Plasma Sci.* **42** 1216–23
[15] Naidis G V 2016 Modelling the dynamics of plasma in gaseous channels during streamer propagation in hydrocarbon liquids *J Phys. D: Appl. Phys.* **49** 235208
[16] Madshaven I, Smalø H S, Unge M and Hestad O L 2016 Photoionization model for the transition to fast mode streamers in dielectric liquids *In 2016 IEEE Conf. Electr. Insul. Dielectr Phenom.* 400–3
[17] Madshaven I, Åstrand P O, Hestad O L, Unge M and Hjortstam O 2017 Modeling the transition to fast mode streamers in dielectric liquids *In 2017 IEEE 19th Int. Conf. Dielectr Liq.* 1–4
[18] Madshaven I, Åstrand P O, Hestad O L, Ingebrigtsen S, Unge M and Hjortstam O 2018 Simulation model for the propagation of second mode streamers in dielectric liquids using the Townsend-Meek criterion *J Phys. Commun.* **2** 105007
[19] Madshaven I, Hestad O L, Unge M, Hjortstam O and Åstrand P O 2019 Conductivity and capacitance of streamers in avalanche model for streamer propagation in dielectric liquids *Plasma Res. Express* **1** 035014
[20] Wickramaaratchi M A, Preses J M, Holroyd R A and Weston R E 1985 The lifetime of the fluorescent excited state in solid, liquid, and vapor phase cyclohexane *J Chem. Phys.* **82** 4745–52
[21] Smalø H S, Hestad O L, Ingebrigtsen S and Åstrand P O 2011 Field dependence on the molecular ionization potential and excitation energies compared to conductivity models for insulation materials at high electric fields *J Appl. Phys.* **109** 073306
[22] Davari N, Åstrand P O, Ingebrigtsen S and Unge M 2013 Excitation energies and ionization potentials at high electric fields for molecules relevant for electrically insulating liquids *J Appl. Phys.* **113** 143707
[23] Davari N, Åstrand P O and Unge M 2015 Density-functional calculations of field-dependent ionization potentials and excitation energies of aromatic molecules *Chem. Phys.* **447** 22–9
[24] Wong P and Forster E 1982 The dynamics of electrical breakdown in liquid hydrocarbons *IEEE Trans. Electr. Insul.* **EI-17** 203–20
[25] Bonifaci N and Denat A 1991 Spectral analysis of light emitted by prebreakdown phenomena in non-polar liquids and gases *IEEE Trans. Electr. Insul.* **26** 610–4
[26] Beroual A 1993 Electronic and gaseous processes in the prebreakdown phenomena of dielectric liquids *J Appl. Phys.* **73** 4528–33
[27] Bårmann P, Kröll S and Sunesson A 1996 Spectroscopic measurements of streamer filaments in electric breakdown in a dielectric liquid *J Phys. D: Appl. Phys.* **29** 1188–96
[28] Ingebrigtsen S, Bonifaci N, Denat A and Lesaint O 2008 Spectral analysis of the light emitted from streamers in chlorinated alkane and alkene liquids *J Phys. D: Appl. Phys.* **41** 235204
[29] Cool T A, Wang J, Nakajima K, Taatjes C A and Mcllroy A 2005 Photoionization cross sections for reaction intermediates in hydrocarbon combustion *Int. J. Mass. Spectrom.* **247** 18–27
[30] Jung J and Gress H 2003 Single-photon absorption of liquid cyclohexane, 2,2,4 trimethylpentane and tetramethylsilane in the vacuum ultraviolet *Chem. Phys. Lett.* **377** 495–500
[31] Carroll B W and Ostlie D A 2007 *An Introduction to Modern Astrophysics* 2nd edn. (San Francisco: Pearson Education)
[32] Gournay P and Lesaint O 1994 On the gaseous nature of positive filamentary streamers in hydrocarbon liquids. II: propagation, growth and collapse of gaseous filaments in pentane *J Phys. D: Appl. Phys.* **27** 2117–27

[33] Eschner M S and Zimmermann R 2011 Determination of photoionization cross-sections of different organic molecules using gas chromatography coupled to single-photon ionization (SPI) time-of-flight mass spectrometry (TOF-MS) with an electron-beam-pumped rare gas excimer light source (EBEL) *Appl. Spectrosc.* **65** 806–16
[34] Naidis G V 2018 Effects of photoionization characteristics on parameters of positive streamers *Plasma Res. Express* **1** 017001
[35] Brownrigg J T and Kenny J E 2009 Fluorescence intensities and lifetimes of aromatic hydrocarbons in cyclohexane solution: evidence of contact charge-transfer interactions with oxygen *J Phys. Chem.* A **113** 1049–59
[36] Lesaint O and Jung M 2000 On the relationship between streamer branching and propagation in liquids: influence of pyrene in cyclohexane *J Phys. D: Appl. Phys.* **33** 1360–8
[37] Unge M, Singha S, Dung N V, Linhjell D, Ingebrigtsen S and Lundgaard L E 2013 Enhancements in the lightning impulse breakdown characteristics of natural ester dielectric liquids *Appl. Phys. Lett.* **102** 172905
[38] Liang S, Wang F, Huang Z, Chen W, Wang Y and Li J 2019 Significantly improved electrical breakdown strength of natural ester liquid dielectrics by doping ultraviolet absorbing molecules *IEEE Access* **7** 73448–54
[39] Linhjell D, Ingebrigtsen S, Lundgaard L and Unge M 2011 Streamers in long point-plane gaps in cyclohexane with and without additives under step voltage *In 2011 IEEE Int Conf Dielectr Liq* 1–5
[40] Galván I F, Martín M E, Muñoz-Losa A and Aguilar M A 2009 Solvatochromic shifts on absorption and fluorescence bands of N,N-dimethylaniline *J Chem. Theory Comput.* **5** 341–9
[41] Åstrand P O, Ramanujam P S, Hvilsted S, Bak K L and Sauer S P A 2000 *Ab initio* calculation of the electronic spectrum of azobenzene dyes and its impact on the design of optical data storage materials *J. Am. Chem. Soc.* **122** 3482–7
[42] Linhjell D, Ingebrigtsen S, Lundgaard L and Unge M 2013 Positive breakdown streamers and acceleration in a small point-plane liquid gap and their variation with liquid properties *In Proc. Nord Insul. Symp.* 191–6
[43] Naidis G V 2015 On streamer inception in hydrocarbon liquids in point-plane gaps *IEEE Trans. Dielectr Electr. Insul.* **22** 2428–32

IV

Inge Madshaven, Øystein Leif Hestad, Per-Olof Åstrand
Cerman: Software for simulating streamer propagation in dielectric liquids based on the Townsend–Meek criterion
Submitted | arXiv: 2007.02999

Cerman: Software for simulating streamer propagation in dielectric liquids based on the Townsend–Meek criterion

I. Madshaven[a], O. L. Hestad[b], P.-O. Åstrand[a,*]

[a] *Department of Chemistry, NTNU – Norwegian University of Science and Technology, 7491 Trondheim, Norway*
[b] *SINTEF Energy Research, 7465 Trondheim, Norway*

Abstract

We present a software to simulate the propagation of positive streamers in dielectric liquids. Such liquids are commonly used for electric insulation of high-power equipment. We simulate electrical breakdown in a needle–plane geometry, where the needle and the extremities of the streamer are modeled by hyperboloids, which are used to calculate the electric field in the liquid. If the field is sufficiently high, electrons released from anions in the liquid can turn into electron avalanches, and the streamer propagates if an avalanche meets the Townsend–Meek criterion. The software is written entirely in Python and released under an MIT license. We also present a set of model simulations demonstrating the capability and versatility of the software.

Keywords:
Streamer breakdown
Dielectric liquid
Simulation model
Python
Computational physics

1. Introduction

1.1. Streamers in liquids

Dielectric liquids, specifically transformer oils, are used as electric insulation in high-power equipment such as power transformers [1]. Equipment failure is always a possibility, and in a world with ever-growing need for energy, there is a continuous effort to make equipment better, cheaper, more compact, and more environmentally friendly. To prevent equipment failure due to electrical

*Corresponding author: `per-olof.aastrand@ntnu.no`

discharges, new insulating liquids as well as additives are tested, experiments are carried out to better understand the physical nature of the phenomena, and simulations are performed to test the validity of predictive models [2, 3].

Since electrical discharge events are rare at operating conditions, model experiments are designed to induce discharge in the liquid. In one such model experiment, a needle electrode is placed opposing a planar electrode, where the needle–plane gap is insulated by a liquid [2]. If high voltage is applied, resulting in a sufficiently strong electric field close to the needle, the liquid will lose its insulating properties and begin to conduct electricity, and subsequent (partial) discharges from the needle into the liquid can occur. The charge transported into the liquid can increase the electric field and lead to partial discharges in new regions in a self-induced manner. Shadowgraphic images (an imaging technique exploiting differences in permittivity) reveal that a gaseous channel, a "streamer", is formed and how it branches as it propagates through the liquid [4]. If a streamer bridges the gap between two electrodes, an electric discharge can follow, possibly destroying the affected equipment.

Streamers are commonly classified by their polarity and speed of propagation from the slow 1st mode to the fast 4th mode, ranging from below 0.1 km/s to well above 100 km/s [2]. Streamers with negative polarity typically have a lower inception voltage than streamers with positive polarity (positive streamers), however, positive streamers typically lead to breakdowns at lower voltage than negative streamers, and as such, research is mainly concerned with positive streamers. The streamer phenomenon involves processes covering several length and time scales. Speed and branching is studied in gaps of different sizes (mm–m), while many of the interesting processes, such as field ionization, high-field conduction, electro-hydrodynamic movement, bubble nucleation, cavitation, electron avalanches, photoionization, occur on a µm-scale [2, 3]. A streamer usually stops or leads to a breakdown on a µs-scale (km/s = mm/µs), whereas processes such as recombination of electrons and anions can occur within picoseconds. Consequently, experimentation as well as simulation is challenging.

1.2. Modeling and simulations

While sophisticated equipment is required for experiments, simulations often investigate the effect of given processes through relatively simple models. The fractal nature of the streamer structure can be simulated by considering a lattice where each point is either part of an electrode, the liquid, or the streamer [5]. Here, the streamer expands to new lattice points when some criterion, such as electric field strength, is obtained. Through kinetic Monte Carlo methods, the stochastic nature and the physical time can also be studied in such simulations [6]. By considering the streamer as an electrical network of resistors and capacitors, the charge and conduction can be studied, without necessarily confining the points of the network to a grid [7]. Models where the streamer consists of a set of discrete points are simplistic but also efficient. Conversely, with a higher demand for computational power, computational fluid dynamic (CFD) methods can be applied to solve the equations for generation and transport of charged particles (the flow of natural particles is often ignored) during a streamer discharge [8, 9],

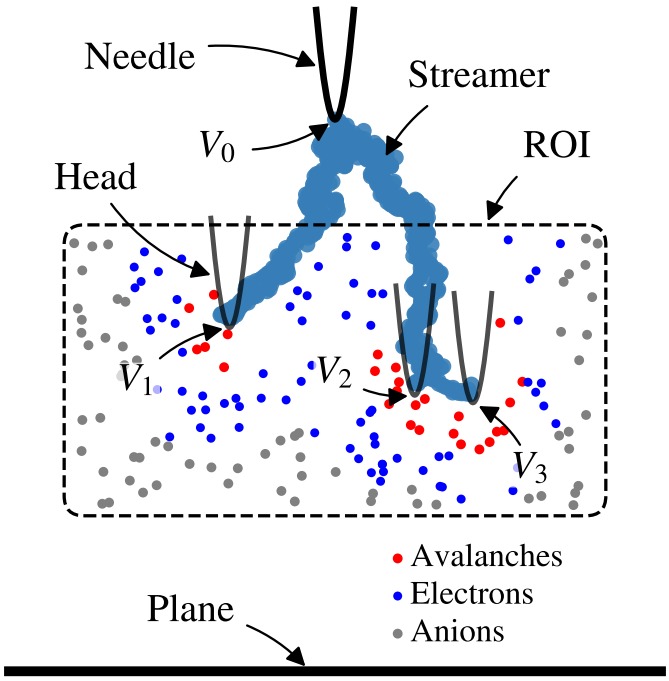

Figure 1: Illustration of the main components in the simulation model. The needle electrode and the streamer heads are hyperboloids, each with a potential V_i. A region of interest (ROI) is used to limit the computational effort to a region surrounding the active part of streamer. The ROI controls the position of the "seeds", which are classified as anions, electrons, or avalanches, depending on the electric field strength at their position. The "shadowgraphic" image of the streamer is created by plotting all former positions of streamer heads.

while the stochasticity and branching of streamers can be introduced by adding impurities [10]. Such CFD-calculations often ignore the phase change from liquid to gas as well and are confined to a small region because of the computational complexity. However, for simplified, single-channel streamers, both the phase change and the processes in the channel can be simulated [11, 12]. Code used for simulation of streamers in liquids is rarely published, in fact, we found just a single example [13].

1.3. Avalanche model

We have previously described our streamer model for positive streamers where the propagation is based on an electron avalanche mechanism [14]. The model has been extended to account for conductance in the streamer channel and capacitance between the streamer and the planar electrode [15], as well as photoionization in front of the streamer [16], the latter as a mechanism for the transition from slow to fast propagation.

Streamer propagation is simulated in a setup resembling model experiments, a needle–plane gap filled with a model liquid, see figure 1 for details. The needle and streamer give rise to an electric field, affecting charged particles in the liquid. A number of anions, "seeds" for electron avalanches, is modeled within a volume surrounding the streamer, a "region of interest" (ROI). Electrons released from the anions can create electron avalanches, and the streamer propagates when an avalanche meets the Townsend–Meek criterion, i.e. exceeds a critical number of electrons [14]. The needle and the streamer heads (the extremities of the streamer) are modeled as hyperboloids, which simplifies calculating the electrical field since the Laplacian is analytic in prolate spheroid coordinates [17]. The electric field and potential is calculated by considering electrostatic shielding [14], as well as the conductance in the channel and the capacitance towards the planar electrode [15]. The streamer undergoes a transition into a fast propagation mode when radiation from the streamer head can ionize molecules directly in front of the streamer [16]. More details on the model is given in section 3.

The main output of the simulations include the propagation speed, the streamer shape (branching), and propagation distance. In addition, properties such as the initiation time, the potential of individual streamer heads, electric breakdown within the streamer channel, and avalanche growth, can also be investigated. Simulations show how various parameters affect the results, where the gap size, applied voltage, and type of liquid are important parameters for a simulation. Furthermore, other parameters such as the size of a streamer head, the conductivity of the streamer channel, properties of additives, and avalanche growth parameters can be varied to validate whether the underlying physical models are reasonable.

1.4. Scope

The present work describes the use, functionality and implementation of *Cerman* [18], a software to do simulations with our model [14, 15, 16], with the purpose to make the software publicly available. Section 2 demonstrates how to set up, simulate, and evaluate results of a relevant problem. Further details on the model and its implementation are given in section 3, whereas section 4 outlines the current functionality and some prospects for the future. A summary is then given in section 5. Furthermore, details on the algorithm is included in Appendix A, simulation parameters in Appendix B, and simulation example input files in Appendix C.

2. Simulation – using the software

2.1. Software overview

The software name *Cerman* is an abbreviation of *ceraunomancy*, which means to control lightning or to use lightning to gain information. The implementation is done in Python, an open-source, interpreted, high-level, dynamic programming language [19], and the software is available on GitHub [18] under an MIT license. The software is script-based, and controlled through the command `cerman`,

Listing 1: Example of JSON-input file, `cmsim.json`, defining a simulation series with several values for the needle voltage V_0 and the threshold for breakdown in the streamer channel E_{bd}, both with and without photoionization enabled. Furthermore, each permutation is to be carried out 10 times with different initial seed positions. Note, by setting `alphakind` to `A1991`, α is calculated by (5). See Appendix B for a description of the parameters.

```
{
    "gap_size": 0.010,
    "needle_radius": 6e-06,
    "needle_voltage": "linspace(60e3, 150e3, 10)",
    "liquid_name": "cyclohexane",
    "alphakind": "A1991",
    "liquid_Ealpha": 0.65e09,
    "liquid_IP": 9,
    "streamer_head_radius": 3e-06,
    "streamer_U_grad": 0e+06,
    "streamer_d_merge": 12.5e-6,
    "streamer_scale_tvl": 0.1,
    "streamer_photo_enabled": [false, true],
    "streamer_photo_efield": 3.1e9,
    "streamer_photo_speed": 20e3,
    "rc_tau0": 1e-6,
    "rc_breakdown": [0e6, 4e6, 8e6, 16e6, 64e6],
    "random_seed": 1,
    "simulation_runs": 10,
    "save_specs_enabled": {
        "stat": true,
        "gp5": true
    }
}
```

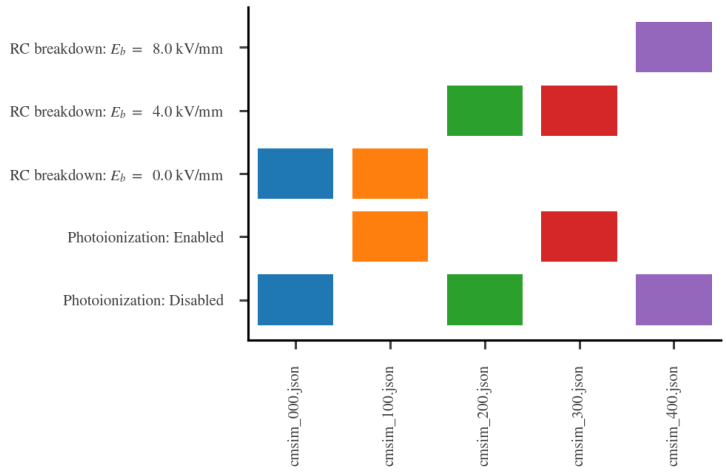

Figure 2: Visualization of the difference in parameter values between a selection of input files.

which is used for creation of input files, running simulations, and evaluating the results. When a simulation is started, the simulation parameters are loaded from an input file, and the classes for the various functions are initiated. See Appendix B for a summary of simulation parameters. The simulation itself is essentially a loop where seeds in the liquid are moved and the streamer structure is updated until the streamer stops or leads to a breakdown. The algorithm is detailed in Appendix A.

2.2. Getting started

Download Cerman from GitHub [18] and install it by running

```
pip install .
```

from the downloaded folder. This installs the python package and the script `cerman`. Python 3.6 or above is required, as well as the packages `numpy` [20], `scipy` [21], `matplotlib`, `simplejson`, and `statsmodels`. The dependencies are automatically installed by `pip`. The software has been developed in OSX and has been tested on Linux as well.

2.3. Create simulation input

Each simulation requires a JSON-formatted input file where the parameters are given. Such files can be created from a master input file, specifying the parameters for a simulation series. A master input file can be created from a regular input file by changing a parameter value into a list of values. More than one parameter can contain lists, and all possible combinations of values is found to create the input files for the simulation series. To demonstrate, we use `cmsim.json` in listing 1, which specifies a simulation series exploring the influence of various parameters. The ten values for the applied voltage are

specified through a `linspace`-command, while the values for the threshold for breakdown in the channel and photoionization (fast mode) enabled are given in list form. Furthermore, `simulation_runs` specifies the number of similar simulations, only differing by `random_seed`. If `random_seed` is `null`, then each input file is created with a random number as `random_seed`, and when a number is specified, a range of number is generated, in this case, the numbers 1 through 10. Note that `random_seed` refers to the seed number for initializing the random number generator, not to the seeds within the ROI. However, a given `random_seed` does corresponds to a given initial positions of the seed anions. Defining fixed a `random_seed` for each simulation series makes it easier to see how a change in a given value affects the simulation, but for analyzing a larger assemble of simulations, it is usually preferable that the simulations are uncorrelated, i.e. have random initial anion placement.

Individual input files are created by running the `cerman` with the argument `ci` (create input) and specifying which file to expand with `-f`:

```
cerman ci -f <filename>
```

This command creates a a number of new files by permutation of all lists in the given input file. The permutation of 10 random seeds, 10 applied voltages, 5 breakdown thresholds, and 2 modes for photoionization in listing 1 results in 1000 files. By default, the random seed is expanded first, followed by the needle voltage, which is is useful to consider when designing a simulation series. Choosing an appropriate number of values for these two parameters makes it easier to search for simulation files with given properties. When expanding the example in listing 1, the least significant digit `??X` indicates random seed number, the second digit `?X?` indicates the needle voltage, while the most significant digit `X??` indicates the threshold for breakdown in the streamer channel and whether photoionization is enabled or not.

The action `pp` (plot parameters) creates a matrix representation of the parameter variation in set of input files, and is used like

```
cerman pp -g <pattern>
```

The argument `-g` specifies the pattern to search (or "glob") for, e.g. `cmsim_?00.json`. The files are plotted at the x-axis and the varied parameters on the y-axis, see figure 2 for an example output. The name of the output file is based on the first file in the pattern.

After ensuring that the input parameter values are as desired, simulations are run using

```
cerman sims -g <pattern> -m <no>
```

which creates a queue of all files matching the pattern, and simulates a given number in parallel. For instance, `cerman sims -g "cmsim_?5?.json" -m 15`, simulates all input files with the same voltage, creating a queue where up to 15 separate subprocesses each run one simulation. These python processes are single threaded, and works best if `numpy` is limited to a single thread as well. Each simulation dumps the input parameters and progress information to a log

file. For each simulation we then have a parameter file, a log file, and one or more save files. The files are named by extending the name of the master file, e.g.

```
cmsim.json                # master file
cmsim_290.json            # input parameters
cmsim_290.log             # log file
cmsim_290_gp5.pkl         # save file
cmsim_290_stat.pkl        # save file
```

2.4. Evaluate results

The results are evaluated by parsing the data stored from one or more simulations. The input file, listing 1, defines two "save specifications" as `true`, i.e. enabled, each defining various simulation data to be dumped to disk at given intervals or occasions. The `save_spec` called `stat` saves iteration number, CPU time, simulation time, leading head z position, number of critical avalanches, and the position of each new streamer head, for every iteration. This enables evaluation of the shape of the streamer and its propagation speed. The `save_spec` called `gp5` saves most of the data available, including the position of all the seeds (anions/electrons/avalanches), for every 5 percent of streamer propagation, i.e. a total of 20 times for a breakdown streamer. The data is saved using `pickle` and can be loaded to analyze a given iteration, a whole simulation, or by combining data from several simulation.

Evaluate iterations. Iteration data can be used to analyze the details of a simulation. This is particularly useful when evaluating the validity of the simulation parameters. Use for instance

```
cerman pi seedheads -r <start stop> -g <pattern>
```

where `pi` means "plot iteration" and `seedheads` is a scatter plot of avalanches and the streamer head configuration. The option `-r` controls the range of iterations to plot. Figure 28 in [14] shows a number of such plots.

Evaluate simulations. Use `ps` for simulation plots. These are mainly plotted with the z-position in the gap on the y-axis. Plotting the x- or y-position of streamer heads on the x-axis, using `shadow`, gives a "shadowgraphic" plot of the streamer:

```
cerman ps shadow -g <pattern> -o <options>
```

Similarly, plotting the propagation time on the x-axis is done in a `streak` plot. Options can be added to control the limits/extents of the plot, the figure size, the behavior of the legend, redefining the axis labels, starting each plot with an offset, saving the plotted data to a JSON-file, and much more. Use `help` to show available commands and options, for instance:

```
cerman help               # for the main script
cerman ps help            # for plot simulation
cerman ps shadow -o help  # for shadow plot
```

Single simulation data may be of interest, but it is often better to compare several simulations in the same plot to visualize how the input parameters affect the results. The `gp5` save requires a lot of disk space, but can be very useful in analyzing the data. For plotting the potential of each head, use

```
cerman ps headsestr -g <pattern> -o <options>
```

The current (active) heads of the streamer is selected, their potential is scaled (electrostatic shielding, using a nnls-approach, cf. [14]), and then, the electric field at their position is calculated. However, the options can be used to specify the method for scaling and which positions to calculate the field for, e.g. at the position of each appended (new) streamer head. The electric field strength and electric potential are presented as scatter plots against the z-position of each given position, as well as dashed line indicating the average value, see figure 4.

Evaluate a series of simulations. The difference in the simulated parameters can be visualized using `pp` and globbing for the `pkl`-files or `log`-files. An existing `log`-file indicates that a simulation was initiated. The command

```
cerman psr -g <pattern>
```

parses log files and plots the reasons why the simulations were terminated. An example of such a plot is shown in figure 5. This is a good way to verify that simulations have completed successfully.

When all simulations are completed and verified, parse all the save files and build a combined database of the results:

```
cerman ca -g <pattern> -o mode=reload
```

The option `reload` forces files to be parsed, even if they already are in the database. When parsing the save files, a number of properties are extracted or calculated. Results such as propagation length (ls), average propagation speed (psa), inception time (ita), average jump distance (jda), simulation time (st), and computational time (ct) are saved in the database. The results are plotted by using

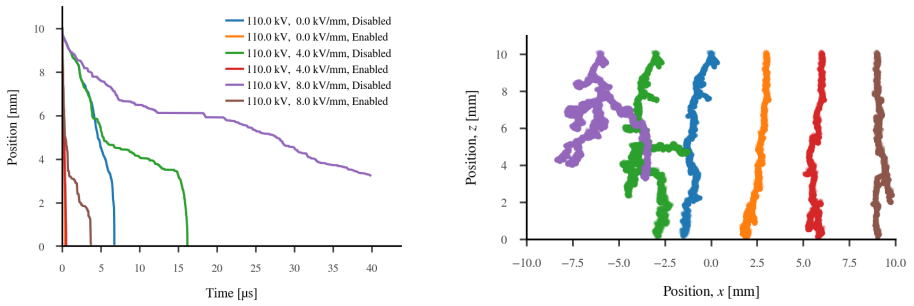

Figure 3: (left) Streak plots where "options" have been used to limit the x-axis and to show V, E_{bd}, and photoionization on the legend. (right) Shadow plots where each streamer is plotted with an offset and the legend is hidden. The legend is the same for both plots.

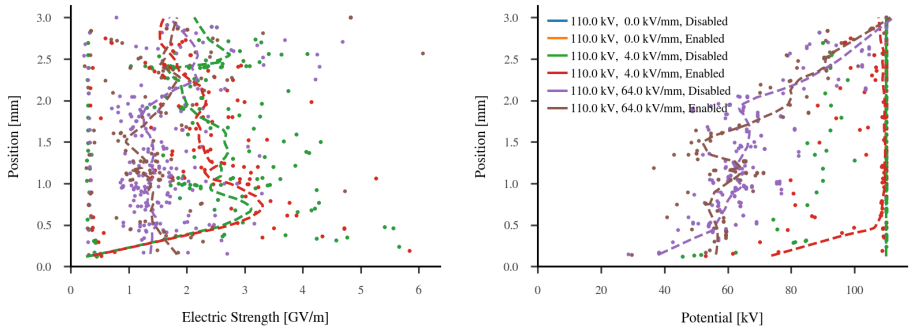

Figure 4: The electric strength (left) and the electric potential (right) at the tip of each new streamer head. The streamer heads are sampled for every 5 % of propagation. The "options" are used to control which streamer heads to use for the calculation and which positions to calculate for.

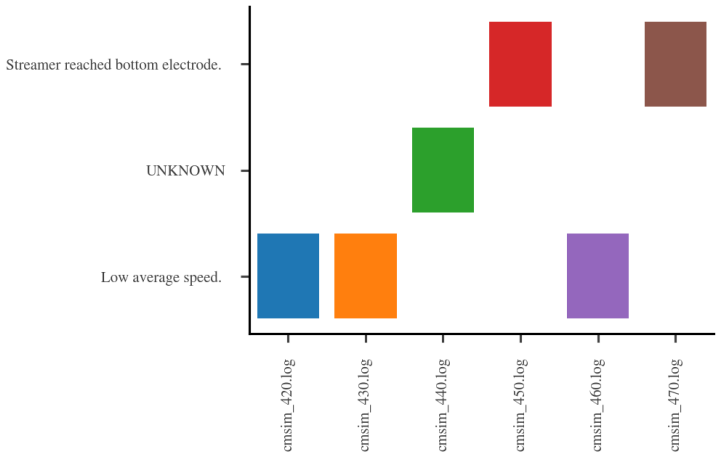

Figure 5: Example, parsing the log files to visualize how simulations have terminated. "Unknown" implies that the simulation is not complete (ongoing or aborted).

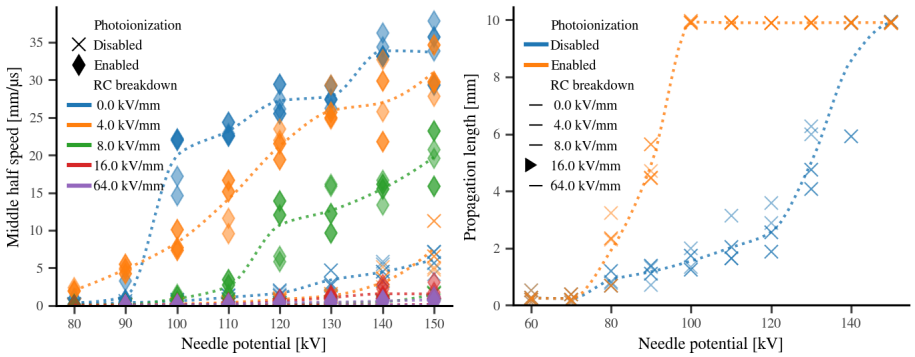

Figure 6: Example, combination plots: (left) propagation speed using both markers and colors, and (right) propagation length for only a given value of one parameter with the other parameter colored.

```
cerman pr <parameter> -f <file> -o <options>
```

The parameter gives the x-axis of the plot, for instance `v` (needle voltage). The results to plot is given through the option, e.g. `-o ykeys=ls_psa`. The software inspects the database of parsed save files for varied parameters and automatically create plots of all possible permutations using colors and markers. Figure 6 shows a selection of such plots, where needle voltage is on the x-axis and the other parameters have been added automatically.

As illustrated, the software has been designed to facilitate simulating and analyzing a large simulations series in a semi-automatic fashion. The individual simulations have their parameters defined in dedicated files, while the behavior of the `cerman`-script is defined by command line arguments.

3. Model implementation

This section describes the implementation of our model [14, 15, 16] in more detail. An overview of the model is already given in section 1.3, and figure 1 is useful for understanding the principal setup, a needle–plane gap where electron avalanches grow from single electron seeds.

The electric field. The needle electrode and the streamer heads are modeled as hyperboloids. The Laplacian electric potential V_i and electric field $\boldsymbol{E}_i$ from a streamer head i is calculated analytically in prolate spheroid coordinates [14]. For a position $\boldsymbol{r}$, the electric potential $V(\boldsymbol{r})$ and field $\boldsymbol{E}(\boldsymbol{r})$ is given by the superposition principle,

$$V(\boldsymbol{r}) = \sum_i k_i V_i(\boldsymbol{r}) \quad \text{and} \quad \boldsymbol{E}(\boldsymbol{r}) = \sum_i k_i \boldsymbol{E}_i(\boldsymbol{r})\,, \tag{1}$$

where the coefficients k_i are introduced to account for electrostatic shielding. An optimization is performed such that the unshielded potential at the tip of any

streamer head j equals the sum of all the shielded potentials at that position, $V_j(\boldsymbol{r_j}) = \sum k_i V_i(\boldsymbol{r_j})$ [14].

Region of interest (ROI). The ROI is a cylindrical volume used to control the position of seeds, see figure 1. Note, the *seeds* in this respect include all anions, electrons, and even all avalanches. The number of seeds in a simulation is given by the specified density of seeds and the volume of the ROI. Initially, the seeds are placed at random positions within the ROI. When a seed falls behind the ROI, collides with the streamer, or creates a critical avalanche, it is removed and replaced by a new seed. The new seed is placed with a z-position one ROI-height closer to the plane, at a random xy-position (at a radius less than the ROI radius). The ROI volume is defined by a distance from the z-axis, and a given length above and below the leading streamer head, which is the part of the streamer closest to the planar electrode. When a new streamer head is created closer to the plane, the streamer propagates, and the ROI moves as well.

Anions, electrons, and electron avalanches. The electric field E is calculated for each seed and the seeds are classified as avalanches ($E \geq E_\mathrm{c}$), electrons ($E \geq E_\mathrm{d}$), or anions ($E < E_\mathrm{d}$), where the avalanche threshold E_c and detachment threshold E_d are given as input parameters. Seeds move in the electric field with a speed dependent on their mobility μ, which gives the distance the seed moves, $\Delta \boldsymbol{s} = \boldsymbol{E}\mu\Delta t$, for a time step Δt. The number of electrons N_e in an electron avalanche, starting from a single electron, can be calculated by [14]

$$N_\mathrm{e} = \exp \sum_i \Delta s_i \alpha_i = \exp \sum_i E_i \, \mu_\mathrm{e} \, \alpha_\mathrm{m} \, e^{-E_\alpha / E_i} \Delta t_i \,, \tag{2}$$

where α is the avalanche growth, μ_e is the electron mobility, Δt is the time step, and i is an iteration, whereas the avalanche growth parameters α_m and E_α have been obtained from experiments [14]. In practice, however, we only calculate and store the exponent in (2), $Q_\mathrm{e} = \ln N_\mathrm{e}$,

$$Q_\mathrm{e} = \sum_i \Delta Q_i = \sum_i \Delta s_i \alpha_i \,, \tag{3}$$

for each electron avalanche. When a low-IP additive is present, α is modified by adding a factor [14]

$$\alpha_{i,\mathrm{add}} = \alpha_i (1 - x_\mathrm{add} + x_\mathrm{add} e^{k_\alpha (I_\mathrm{b} - I_\mathrm{a})}) \tag{4}$$

which is dependent on the mole fraction of the additive x_add, and the difference in IP between the base liquid I_b and the additive I_a modified by a factor k_α as prescribed by [22]. This is the default setting for the software. Another model for α given in [23] is also implemented:

$$\alpha_{i,\mathrm{mod}} = \frac{3eE_\alpha^2}{I_\mathrm{b} E_i} e^{-\frac{E_\alpha}{E_i}} \,. \tag{5}$$

This method is applied in listing 1.

Expanding the streamer structure. According to the Townsend–Meek criterion [24], streamer breakdown occurs when an avalanche exceeds a critical

number of electrons $N_\mathrm{c} = \exp(Q_\mathrm{c})$. When an avalanche obtains $Q_\mathrm{e} > Q_\mathrm{c}$, we place a new streamer head at its position [14]. The initial potential of a new streamer head is calculated by considering the capacitance and potential of the closest existing streamer heads [15]. If adding the new head implies removing another head (see the paragraph below), the potential changes slightly, mimicking transfer of charge. However, if both the new and the present head stays, they share the "charge", which gives a moderate reduction in the potential of both heads.

Optimizing the streamer structure. There are three criteria for removing heads. A streamer head i is removed if

$$\nu_j(\boldsymbol{r}_i) < \nu_j(\boldsymbol{r}_j) \quad \text{or} \quad k_i < k_\mathrm{c} \quad \text{or} \quad \big((|\boldsymbol{r}_i - \boldsymbol{r}_j| < d_\mathrm{m}) \text{ and } (z_i > z_j)\big)\,, \tag{6}$$

are satisfied for any other streamer head j [14]. The first condition checks whether the tip of one hyperbole ($\boldsymbol{r}_i$) is inside another hyperbole, a collision (the ν-coordinate describes a hyperboloid, specifically the asymptotic angle). The second condition removes heads whose potential are to a high degree shielded by other heads (if the coefficient k_i in (1) lower than a threshold k_c). The third condition checks whether two streamer heads are closer than d_m and should be merged to a single head, where the one at the highest z-coordinate is removed.

Conduction and breakdown in the streamer channel. Conduction in the streamer channel increases the potential of each streamer head i each iteration,

$$\Delta V_i = V_0 - V_i \quad \rightarrow \quad V_i = V_0 - \Delta V_i\, e^{-\Delta t/\tau_i}\,. \tag{7}$$

The time constant $\tau_i = RC\tau_0$ (for a given head i) is calculated from the resistance R in the channel and the capacitance C towards the plane [15]

$$R \propto \ell\,, \quad \text{and} \quad C \propto \left(\ln \frac{4z + 2r_\mathrm{s}}{r_\mathrm{s}}\right)^{-1}\,, \tag{8}$$

where ℓ is the channel length (distance to the needle), r_s is the tip curvature radius of the streamer head, and z is the z-position of the streamer head. As such, each streamer head is treated as an individual RC-circuit, e.g. the three streamer heads in figure 1 would each have an individual resistance (channel) as well as an individual capacitance towards the planar electrode. If the conduction is low, the potential difference ΔV_i increases as the streamer propagates, and the electric field within the streamer channel $E_\mathrm{s} = \Delta V_i/\ell_i$ may increase as well. If E_s exceeds a threshold E_b, a breakdown occurs, equalizing the potential of the streamer head and the needle, which is achieved by setting $\tau_i = 0$ in (7) for the given iteration.

Photoionization. Photoionization is a possible mechanism for fast streamer propagation [25]. We have proposed a mechanism in which the propagation speed of a streamer increases if the liquid cannot absorb radiation energy to excited states, as a result of a strong electric field reducing the ionization potential [16]. Since the full model, considering fluorescent radiation from the streamer head, and a field-dependent photoionization absorption cross section, is

computationally expensive, a simpler model is used in the simulations. Instead we calculate the field strength E_w required to reduce the ionization potential below the energy of the fluorescent radiation. In each iteration, if the electric field E at the tip of a streamer head i exceeds the parameter E_w, the head is moved a distance $\Delta \boldsymbol{s}_i$ towards the planar electrode,

$$\Delta \boldsymbol{s}_i = -v_w \, \Delta t \, \Theta(E(\boldsymbol{r}_i) - E_w) \; \hat{\boldsymbol{z}} \, , \tag{9}$$

where v_w is the photoionization speed, and Θ is the Heaviside step function. For more details on the entire model, see our previous work [14, 15, 16].

4. Current functionality and future prospects

The main function of the model and the software is to simulate streamers in a point–plane gap, using the Townsend–Meek criterion for propagation. The propagation criterion is met when electron avalanches obtain a given size. This model and the algorithm are fixed, but there are several parameters which can be adjusted. Changing experiment features such as needle tip radius, gap size, voltage, liquid properties, or the parameters of the algorithms, is straightforward. Proposals to extend the software to encompass new functionality is given in this section.

In [14] we explored the fundamental features off the model, i.e. a streamer consisting of charged hyperbolic streamer heads, and streamer growth by electron avalanches initiating from anions. The model predicts several aspects of streamer propagation, and shows how they are linked towards the values of given input parameters. The predicted propagation speed and the degree of branching were both lower than expected. We found how the speed was dependent mainly on the number of electron avalanches and their growth, while the branching was mainly related to how the streamer heads were configured and managed, which is mainly controlled by the parameters k_c and d_m in (6).

When new streamer heads were added, their potential was set assuming a constant electric field within the channel, resulting in a moderate voltage drop between the needle electrode and the streamer head [14]. To better represent the dynamics of the streamer channel, an RC-model was developed [15]. In the RC-model, the potential of new streamer heads is dependent of the potential of the closest existing streamer heads. If the conductance of the streamer channel is high, then the potential of the streamer head is kept close to that of the needle, giving results comparable to those without the RC-model. Conversely, having low conduction regulates the speed of the streamer, increasing the likelihood that more branches are able to propagate. Furthermore, the RC-model also allows for simulation of a breakdown within the streamer channel itself, which is likely what occurs during a re-illumination. This breakdown occurs when the electric field within the channel exceeds a given threshold.

The importance of photoionization during a streamer breakdown is unknown. We explored different aspects of photoionization in [16], and implemented a model for change to a fast propagating mode. Molecules excited by energetic

processes, such as electron avalanches, can relax to a lower energy state by emitting radiation. We argued that fluorescent radiation can be important, and modeled how this radiation can cause ionization in high-field areas, since the high-field reduces the ionization potential.

In the current implementation, a square wave voltage is applied to the needle at the beginning of the simulation. It is easy to change the behavior to a voltage ramp, from zero to max over a given time. This can be the basis for a study on streamer inception where other parameters such as needle size and the electron properties of the liquid are investigated as well. Simulating a dynamic voltage, such as a lightning impulse, requires some more work, but is also achievable.

We have focused on cyclohexane since many of its properties are well known, but other non-polar insulating liquids can be studied by changing relevant parameters. The seed density n_{ion} is based on the low-field conductivity σ and electron mobility μ_{e} of the liquid, and the propagation speed scales linearly with both seed density n_{ion} and electron mobility μ_{e}. The electron avalanche growth parameters are also liquid-dependent, and E_α in particular has a big impact on the results [14]. Streamer parameters, such as conductivity of the streamer channel and streamer head radius, need to be reevaluated as well for other liquids. The properties of the streamer channel are also important to simulate the effects of external pressure, which mainly affects processes in the gaseous phase [26].

The effect of additives with a low ionization potential (IP) are modeled as causing an increase in electron avalanche growth [22, 14]. Other additives can easily be used as long as the IP of both the base liquid and the additive are known. Low-IP additives are known to facilitate the propagation of slow streamers and to increase the acceleration voltage, possibly as a result of increased branching [27], however the mechanisms involved are not known. It is possible that low-IP additives are sources of electrons that can initiate avalanches, produced for instance through photoionization or fluctuations in the electric field. Such mechanisms can be added to the model and simulated, but will require some work. Furthermore, the mechanisms of added electron scavengers can also be interesting for further investigation, and particularly if negative streamers are to be simulated [22].

Our primary concern have been with positive streamers, since these are more likely to lead to a complete breakdown than negative streamers. The model relies on electrons detaching from anions, moving towards regions where the field is higher, and then forming electron avalanches. The polarity of our model can easily be reversed, however, the electrons would then drift away and be unable to form avalanches. As such, a model for creation of new electrons is needed to simulate negative streamers with the software. Charge injection from the needle and the streamer can be one such mechanism [28]. Another option is to model electron generation (charge separation) in the high-field region surrounding the needle and the streamer. Such mechanisms are interesting for simulating positive streamers as well.

The hyperbole approximation simplifies the calculation of the electric field, both from the needle electrode and from the streamer heads. Other experimental geometries, such as plane–needle–plane, or even more realistic real-life geometries

can be implemented. The challenge is to set the correct shielding or scaling of the streamer heads according to the influence of the geometry. Simpler geometric restrictions are easier to implement, for instance by manipulating the ROI. The streamer can be restricted to a tube by setting a low value for the maximum radius of the ROI. Another method is setting the "merge threshold" very high, such that the streamer is restricted to a single channel with a single head, which can be representative for a streamer in a tube [29].

There are many mechanisms that can be added to investigate different methods of streamer propagation, for instance effects of Joule heating or electro-hydrodynamic cavitation [30]. There are also several parts of the existing model that can be improved. Better calculation and balancing of charges and energy would greatly improve the model. For instance an electric network model where the streamer is consisting of several interconnected parts, in contrast to the current implementation where all the streamer heads are individually "connected" to the needle. Such an approach can give a better understanding of the charge flow in the different parts and branches of the streamer, as well as a better representation of the electric field. Development towards a model for a space-charge limited field [31] can further improve the electric field representation, however, possibly at a high computational cost.

5. Summary

We present a software for simulating the propagation of positive streamers in a needle–plane gap insulated by a dielectric liquid. The model is based on the Townsend–Meek criterion in which an electron avalanche have to obtain a given size for the streamer to propagate. The software was developed and used for simulating our models for electron avalanche growth [14], conductance and capacitance in the streamer channels [15], as well as photoionization in front of the streamer [16]. From the examples on how to set up, run, and evaluate simulations, others can recreate our previous results or create their own set of simulations. Furthermore, the overview of the implementation and algorithm serves as a good starting point for others to change or extend the functionality of the software.

Acknowledgment

This work has been supported by The Research Council of Norway (RCN), ABB and Statnett, under the RCN contract 228850.

Appendix A. The algorithm

This section describes the algorithm used to implement the model in more detail, essentially each part of figure 7, while referencing relevant parts from section 3.

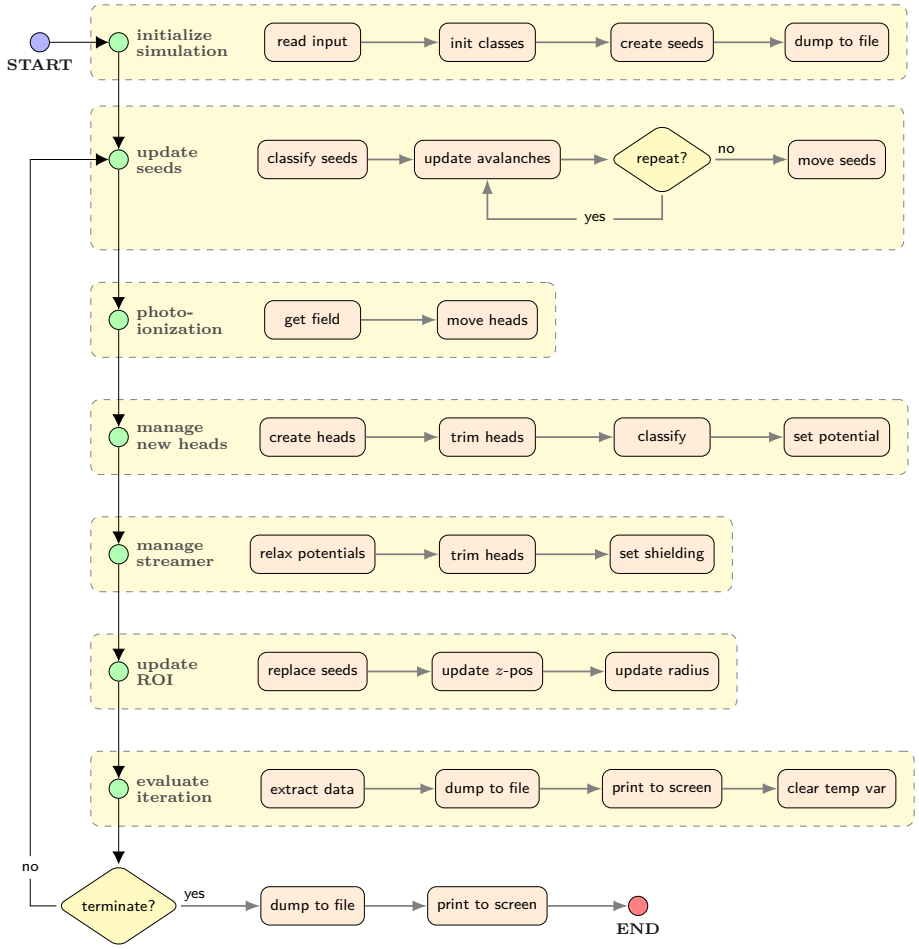

Figure 7: The simulation algorithm consists of initialization, a loop where the seeds and the streamer structure is updated, and then a finalization. It the loop, first the seeds (anions, electrons avalanches) are affected by the electric field, then the streamer structure is modified and this changes the electric field, finally the region of interest (ROI) is updated and the data from the iteration is evaluated. The loop concludes when one (of several) criterion is met, typically low propagation speed or reaching the opposing electrode. Details on each step is found in Appendix A.

Initialize simulation. The simulation input parameters are read and used to initialize classes for code profiling, simulation logging, calculation of avalanche growth, the needle, the streamer, the region of interest (ROI), the seeds (anions, electron, avalanches), how to save data, and how to evaluate simulation data. The initiation of the log file includes dumping the input parameters to the file. Given the ROI volume and the seed density, a number of seeds is created and placed within the ROI at random positions. Then, the save files are initialized by dumping the initial data, mainly information concerning the needle and the seeds.

Update seeds. The electric field E is calculated for each seed (applying (1)) and the seeds are classified as avalanches, electrons, and anions. All the avalanches move in the electric field and grow in size (see (2)). The procedure is repeated until an avalanche collides with a streamer head, an avalanche meets the Townsend–Meek criterion, or a total of N_{MSN} repetitions has been performed. The "time" spent in this inner loop sets the time step for the current iteration of the main simulation loop. Finally, all the electrons and anions are moved. The inner loop over just the avalanches save significant computational time since the calculation of the electric field is the most expensive part of the computation and the avalanches is usually a small fraction of all the seeds.

Photoionization. The electric field at the tip of each streamer head is calculated and compared with the threshold for photoionization. Each streamer head where $E > E_w$ is "moved" a distance $v_w \Delta t$ towards $z = 0$. Moving implies creating a new head, setting the potential by "transferring charge", and removing the old head.

Manage new heads. For each critical avalanche a new head is created. If the simulation time step is set sufficiently low, there is usually zero or just one new head. The new head is discarded if it satisfies any of the criteria in (6), however, if adding it will cause another to be removed (later), the new head is classified as "merging". If none of the criteria in (6) is met by adding the new head, i.e. all heads are kept, then it is a "branching" head, since adding it is potentially the start of a new branch. The potential of "merging" is set by "charge transfer" from the closest head, while "branching" heads have their potential set by "sharing charge" with the closest head, where the latter method also modifies the potential of the existing head [15].

Manage streamer. The potential of each streamer head is relaxed towards the potential of the needle by applying (7). This step increases the potential of the streamer head to the potential of the needle when a breakdown in the channel occurs. As mentioned above, the calculation of the electric field for the seeds is computationally expensive, and it actually scales with both the number of seeds and the number of streamer heads. It is therefore preferable to keep the number of heads to a minimum. Superfluous heads are trimmed according to the criteria in (6). Then, the electrostatic shielding is set for the trimmed structure.

Update ROI. Seeds that have moved behind the ROI, collided with the streamer, or lead to a critical avalanche are removed and replaced by a new seed. When a seed is replaced, the new seed is placed a distance, equal to the height of the ROI, closer to the plane, at a random xy-position within the ROI radius.

If the streamer has moved closer to the plane, the ROI moves as well, and seeds behind the new position are replaced. If a streamer head is close to the edge of the ROI, the ROI expands towards the maximum radius. New seeds are created at random position within the expanded region.

Evaluate iteration. Iteration data is extracted from the various classes to be saved for later use. The data is used to evaluate whether any stop condition is fulfilled, and stored to dedicated classes. Which data to store and how often to sample the data is controlled by the user input. The saved data is dumped to a file at regular intervals to keep memory requirements of the program low. Information to monitor the progress is printed to the screen, at regular intervals. Finally, a number of temporary variables, relevant only to the iteration is cleared, and the program is prepared for a new iteration.

Terminate? If none of the conditions for stopping a simulation are met, the next iteration is performed. These conditions includes low streamer speed, streamer head close to the plane (breakdown), simulation time exceeded, computation time exceeded, and more. When a criterion is met, any unsaved data is dumped to disk, and a final logging to file and screen is performed, before the program terminates.

Appendix B. Parameters

The parameters for a simulation is supplied by the user in a JSON-formatted file (see listing 1). A list of all important parameters are shown in table 1. The potential, position and size of the needle are important parameters in an experiment and included in the first section, followed by parameters controlling the creation and movement of seeds (anions, electrons, and avalanches). The third section contains parameters related to the threshold for electron detachment, electron avalanche growth, and critical avalanche size. The parameters for the streamer can be split in two groups. The first group controls creation of the streamer heads and how the streamer heads are treated in relation to each other, whereas the second groups is related to the RC-model, controlling the potential of the streamer heads and the electric field in the streamer channel. There is also the option to choose whether the electric field from the streamer, acting on the seeds, is calculated using 32- or 64-bit precision. The latter requires about twice the time to compute. The parameters in the last section are mainly related to the simulation algorithm itself. The time step and the number of steps per loop are essential for a good results. The random seed, used to initialize the random number engine, controls the initial placement of seed anions. Choosing the same random number enables the study of, for instance, changing voltage with the same initial seed configuration. Conversely, not setting the random number makes the simulations uncorrelated, which is better for statistics. The size of the ROI decides how many seeds that are included in a simulation. For instance, an ROI of $10\,\mathrm{mm}^3$ in combination with a seed density of $2 \times 10^{12}\,/\mathrm{m}^3$ results in 20 000 seeds generated, a size which is easily treated by most computers. Finally, several parameters can be used to control how long a simulations will run, or to stop a simulation if the streamer stops or reaches the other electrode. There are

Table 1: Main parameters for simulation program. The *experimental conditions* specifies an overvoltage applied to medium size needle–plane gap. The values of the physical parameters in *seeds and avalanches* and *streamer structure* are justified in our previous work [14, 15, 16]. Parameter values related to the *simulation algorithm*, or the model in general, have also been discussed in previous work. See further description in Appendix B.

Property	`Keyword`	Symbol	Default
Experimental conditions			
Distance from needle to plane	`gap_size`	d_g	10 mm
Voltage applied to needle	`needle_voltage`	V_n	100 kV
Needle tip radius	`needle_radius`	r_n	6.0 µm
Seeds and avalanches			
Seed number density	`seeds_cn`	n_seeds	$2 \times 10^{12}\,/\mathrm{m}^3$
Anion mobility	`liquid_mu_ion`	μ_ion	$0.30\,\mathrm{mm}^2/\mathrm{Vs}$
Electron mobility	`liquid_mu_e`	μ_e	$45\,\mathrm{mm}^2/\mathrm{Vs}$
Liquid low-field conductivity	`liquid_sigma`	σ_ion	0.20 pS/m
Electron detachment threshold	`liquid_Ed_ion`	E_d	1.0 MV/m
Growth calculation method	`alphakind`	–	`I2009`
Critical avalanche threshold	`Q_crit`	Q_c	23
Electron multiplication threshold	`liquid_Ec_ava`	E_c	0.2 GV/m
Electron scattering constant	`liquid_Ealpha`	E_α	1.9 GV/m
Max avalanche growth	`liquid_alphamax`	α_m	$130\,\mu\mathrm{m}^{-1}$
Additive IP diff. factor	`liquid_k1`	k_α	$2.8\,\mathrm{eV}^{-1}$
Base liquid IP	`liquid_IP`	I_b	10.2 eV
Additive IP	`additive_IP`	I_a	7.1 eV
Additive mole fraction	`additive_cn`	x_add	0.00
Streamer structure			
Streamer head tip radius	`streamer_head_radius`	r_s	6.0 µm
Minimum field in streamer channel	`streamer_U_grad`	E_s	2.0 kV/mm
Streamer head merge distance	`streamer_d_merge`	d_m	25 µm
Electrostatic shielding threshold	`streamer_scale_tvl`	k_c	0.20
Photoionization threshold field	`streamer_photo_efield`	E_w	3.1 GV/m
Photoionization added speed	`streamer_photo_speed`	v_w	20 km/s
Data type for field calculation	`efield_dtype`	–	`float32`
RC-model time constant	`rc_tau0`	τ_0	1 µs
RC resistance model	`rc_resistance`	–	`linear`
RC capacitance model	`rc_capacitance`	–	`hyperbole`
RC breakdown field	`rc_breakdown`	E_bd	6 kV/mm
Simulation algorithm			
Time step of avalanche movement	`time_step`	Δt	1.0 ps
Max avalanche steps per iteration	`micro_step_no`	N_MSN	100
Seed for random number generator	`random_seed`	–	`None`
Number of similar simulations	`simulation_runs`	–	10
ROI – behind leading head	`roi_dz_above`	z^+_ROI	1.0 mm
ROI – in front of leading head	`roi_dz_below`	z^-_ROI	1.0 mm
ROI – radius from center	`roi_r_max`	r_ROI	3.0 mm
Stop – low streamer speed	`stop_speed_avg`	v_min	100 m/s
Stop – streamer close to plane	`stop_z_min`	z_min	50 µm
Stop – avalanche time	`stop_time_since_avalanche`	$t^\mathrm{ava}_\mathrm{max}$	100 ns
Sequential start number	`seq_start_no`	–	0
Enable profiling of code	`profiler_enabled`	–	False
Interval – dump save data to file	`file_dump_interv`	–	500
Interval – display data on screen	`display_interv`	–	500
Level of logging to file	`log_level_file`	–	20
Level of logging to console	`log_level_console`	–	20

also parameters controlling how often information is logged, and how detailed the logging should be.

Appendix C. Example files

This appendix contains a number of examples of possible simulations. The files in listings 2 to 5 are all included in the folder `examples` on GitHub [18].

Listing 2: The example file `small_gap.json` specifies a small gap and a range of voltages along with many parameter values equal to the defaults (cf. table 1). Although all values used in a simulation is stored in the log, it is nice to be explicit in the input as well. By specifying 10 `simulation_runs` and 10 voltages, a total of 100 simulations is created from this file. Each simulation initiated with the seeds at uncorrelated positions since `random_seed` is `none`.

Listing 3: The example file `small_gap_mod.json` builds on listing 2, but a number of parameters are modified, notably the seed density and the electron avalanche parameters, as well as several parameters for the streamer. All data is stored every 5th percent of propagation by `gp5` and every 100th nanosecond by `ta07`. Storing the properties of tens of thousands of seeds enables plotting of the development of seeds, but also requires a lot of disk space. Specifying `streamer` saves all the streamer heads every 0.1 percent of propagation and is used to evaluate the development of the streamer. Since `random_seed` is 1 and `simulation_runs` is 10, a range of `random_seed` from 1 through 10 is generated, giving the same 10 initial seed positions for each voltage.

Listing 4: The example file `rc.json` specifies the low and high conductivity within the streamer channel, and a range of threshold fields for electric breakdown in the streamer channel. The `linspace`-command is a convenient method for creating a list of values. By combining 2 values for the conductivity and 5 values for breakdown with 10 values for the voltage, a total of 100 simulations are created from this file.

Listing 5: The example file `pi.json` specifies electrical breakdown in the streamer channel, with and without photoionization enabled, The keyword `user_comment` does not affect the simulations, but can be convenient to set. 600 input files are created when expanding this file (100 voltages, with and without photoionization, for three different breakdown thresholds).

Listing 2: The example file `small_gap.json` specifies simulations similar to the baseline studies in section 3.1 in [14].

```
{   "gap_size": 0.003,
    "needle_radius": 6e-06,
    "needle_voltage": [30e3, 40e3, 50e3, 60e3, 70e3,
                       80e3, 90e3, 100e3, 110e3, 120e3],
    "liquid_name": "cyclohexane",
    "liquid_alphamax": 200e06,
    "liquid_Ealpha": 3.0e09,
    "seeds_cn": 2e12,
    "Q_crit": 23,
    "streamer_head_radius": 6e-06,
    "streamer_U_grad": 2e+06,
    "streamer_d_merge": 50e-6,
    "streamer_scale_tvl": 0.2,
    "streamer_photo_enabled": false,
    "random_seed": null,
    "simulation_runs": 10,
    "stop_sim_time": 100e-06,
    "stop_time_since_avalanche": 1e-07,
    "stop_speed_avg": 100}
```

Listing 3: The example file `small_gap_mod.json` specifies simulations similar to the attempts to facilitate branching in section 3.5 in [14].

```
{   "gap_size": 0.003,
    "needle_radius": 6e-06,
    "needle_voltage": "linspace(30e3, 120e3, 10)",
    "liquid_name": "cyclohexane",
    "liquid_alphamax": 130e06,
    "liquid_Ealpha": 1.9e09,
    "seeds_cn": 8e12,
    "streamer_head_radius": 3e-06,
    "streamer_U_grad": 8e+06,
    "streamer_d_merge": 12.5e-6,
    "streamer_scale_tvl": 0.1,
    "streamer_photo_enabled": false,
    "random_seed": 1,
    "simulation_runs": 10,
    "save_specs_enabled": {
        "stat": true,
        "streamer": true,
        "gp5": true,
        "ta07": true}}
```

Listing 4: The example file `rc.json` specifies simulations similar to those performed in section 4 in [15].

```
{   "gap_size": 0.003,
    "needle_radius": 6e-06,
    "needle_voltage": "linspace(30e3, 120e3, 10)",
    "liquid_name": "cyclohexane",
    "liquid_alphamax": 130e06,
    "liquid_Ealpha": 1.9e09,
    "streamer_head_radius": 6e-06,
    "streamer_U_grad": 0,
    "streamer_d_merge": 50e-06,
    "streamer_scale_tvl": 0.1,
    "rc_tau0": [1e-8, 1e-4],
    "rc_resistance": "linear",
    "rc_capacitance": "hyperbole",
    "rc_breakdown": [0, 4e6, 8e6, 16e6, 64e6],
    "random_seed": null,
    "save_specs_enabled": {
        "streamer": true,
        "stat": false}}
```

Listing 5: The example file `pi.json` specifies simulations similar to those performed in section 7 in [16].

```
{   "user_comment": "Photoionization and breakdown",
    "gap_size": 0.010,
    "needle_radius": 6e-06,
    "needle_voltage": "linspace(60e3, 150e3, 100)",
    "liquid_alphamax": 130e06,
    "liquid_Ealpha": 1.9e09,
    "seeds_cn": 2e+12,
    "streamer_U_grad": 0,
    "streamer_d_merge": 50e-06,
    "streamer_scale_tvl": 0.1,
    "streamer_photo_enabled": [false, true],
    "streamer_photo_efield": 3.1e9,
    "streamer_photo_speed": 20e3,
    "rc_tau0": 1e-6,
    "rc_breakdown": [0e6, 4e6, 64e6],
    "simulation_runs": 1,
    "random_seed": null,
    "file_dump_interv": 500,
    "display_interv": 500,
    "save_specs_enabled": {
        "streamer": true,
        "stat": false}}
```

References

[1] P. Wedin (2014) Electrical breakdown in dielectric liquids - a short overview. *IEEE Electr Insul Mag* **30**:20–25. doi:10/cxmk

[2] O. Lesaint (2016) Prebreakdown phenomena in liquids: propagation 'modes' and basic physical properties. *J Phys D: Appl Phys* **49**:144001. doi:10/cxmf

[3] A. Sun, C. Huo, J. Zhuang (2016) Formation mechanism of streamer discharges in liquids: a review. *High Volt* **1**:74–80. doi:10/dbt2

[4] B. Farazmand (1961) Study of electric breakdown of liquid dielectrics using schlieren optical techniques. *Br J Appl Phys* **12**:251–254. doi:10/bhcrhp

[5] L. Niemeyer, L. Pietronero, H. J. Wiesmann (1984) Fractal dimension of dielectric breakdown. *Phys Rev Lett* **52**:1033–1036. doi:10/d35qr4

[6] P. Biller (1993) Fractal streamer models with physical time. In *Proc 1993 IEEE 11th Int Conf Conduct Break Dielectr Liq (ICDL '93)*, 199–203. doi:10/dctxz7

[7] I. Fofana, A. Beroual (1998) Predischarge models in dielectric liquids. *Jpn J Appl Phys* **37**:2540–2547. doi:10/bm4sd5

[8] J. Qian, R. P. Joshi, E. Schamiloglu, J. Gaudet, J. R. Woodworth, J. Lehr (2006) Analysis of polarity effects in the electrical breakdown of liquids. *J Phys D: Appl Phys* **39**:359–369. doi:10/c75hff

[9] I. Simonović, N. A. Garland, D. Bošnjaković, Z. L. Petrović, R. D. White, S. Dujko (2019) Electron transport and negative streamers in liquid xenon. *Plasma Sources Sci Technol* **28**:015006. doi:10/dcjj

[10] J. Jadidian, M. Zahn, N. Lavesson, O. Widlund, K. Borg (2014) Abrupt changes in streamer propagation velocity driven by electron velocity saturation and microscopic inhomogeneities. *IEEE Trans Plasma Sci* **42**:1216–1223. doi:10/f55gj5

[11] G. V. Naidis (2015) Modelling of streamer propagation in hydrocarbon liquids in point-plane gaps. *J Phys D: Appl Phys* **48**:195203. doi:10/cxmj

[12] G. V. Naidis (2016) Modelling the dynamics of plasma in gaseous channels during streamer propagation in hydrocarbon liquids. *J Phys D: Appl Phys* **49**:235208. doi:10/cxmg

[13] H. Fowler, J. Devaney, J. Hagedorn (2003) Growth model for filamentary streamers in an ambient field. *IEEE Trans Dielectr Electr Insul* **10**:73–79. doi:10/ffwcfd

[14] I. Madshaven, P.-O. Åstrand, O. L. Hestad, S. Ingebrigtsen, M. Unge, O. Hjortstam (2018) Simulation model for the propagation of second mode streamers in dielectric liquids using the Townsend-Meek criterion. *J Phys Commun* **2**:105007. doi:10/cxjf

[15] I. Madshaven, O. L. Hestad, M. Unge, O. Hjortstam, P.-O. Åstrand (2019) Conductivity and capacitance of streamers in avalanche model for streamer propagation in dielectric liquids. *Plasma Res Express* **1**:035014. doi:10/c933

[16] I. Madshaven, O. Hestad, M. Unge, O. Hjortstam, P. Åstrand (2020) Photoionization model for streamer propagation mode change in simulation model for streamers in dielectric liquids. *Plasma Res Express* **2**:015002. doi:10/dg8m

[17] R. Coelho, J. Debeau (1971) Properties of the tip-plane configuration. *J Phys D: Appl Phys* **4**:1266–1280. doi:10/fg43t7

[18] I. Madshaven. Cerman - A software for simulation of streamers in liquids. `https://github.com/madshaven/cerman`

[19] Python Software Foundation. Python Language Reference. `https://www.python.org`

[20] T. E. Oliphant (2007) Python for scientific computing. *Comput Sci Eng* **9**:10–20. doi:10.1109/MCSE.2007.58

[21] P. Virtanen, R. Gommers, T. E. Oliphant, M. Haberland, T. Reddy, et al. (2020) SciPy 1.0: fundamental algorithms for scientific computing in Python. *Nat Methods* **17**:261–272. doi:10/ggj45f

[22] S. Ingebrigtsen, H. S. Smalø, P.-O. Åstrand, L. E. Lundgaard (2009) Effects of electron-attaching and electron-releasing additives on streamers in liquid cyclohexane. *IEEE Trans Dielectr Electr Insul* **16**:1524–1535. doi:10/fptpt5

[23] V. M. Atrazhev, E. G. Dmitriev, I. T. Iakubov (1991) The impact ionization and electrical breakdown strength for atomic and molecular liquids. *IEEE Trans Electr Insul* **26**:586–591. doi:10/d2mg8n

[24] A. Pedersen (1989) On the electrical breakdown of gaseous dielectrics - an engineering approach. *IEEE Trans Electr Insul* **24**:721–739. doi:10/d2kthj

[25] D. Linhjell, L. Lundgaard, G. Berg (1994) Streamer propagation under impulse voltage in long point-plane oil gaps. *IEEE Trans Dielectr Electr Insul* **1**:447–458. doi:10/chdqcz

[26] D. Linhjell, L. E. Lundgaard, M. Unge (2019) Pressure Dependent Propagation of Positive Streamers in a long Point-Plane Gap in Transformer Oil. In *2019 IEEE 20th Int Conf Dielectr Liq*, vol. 2019-June, 1–3. doi:10/dvbz

[27] O. Lesaint, M. Jung (2000) On the relationship between streamer branching and propagation in liquids: influence of pyrene in cyclohexane. *J Phys D: Appl Phys* **33**:1360–1368. doi:10/c4xf84

[28] H. S. Smalø, O. L. Hestad, S. Ingebrigtsen, P.-O. Åstrand (2011) Field dependence on the molecular ionization potential and excitation energies compared to conductivity models for insulation materials at high electric fields. *J Appl Phys* **109**:073306. doi:10/dmkszm

[29] G. Massala, O. Lesaint (1998) Positive streamer propagation in large oil gaps: electrical properties of streamers. *IEEE Trans Dielectr Electr Insul* **5**:371–380. doi:10/cfk7km

[30] O. Lesaint, L. Costeanu (2018) Positive streamer inception in cyclohexane: Experimental characterization and cavitation mechanisms. *IEEE Trans Dielectr Electr Insul* **25**:1949–1957. doi:10/gfhkt8

[31] S. Boggs (2005) Very high field phenomena in dielectrics. *IEEE Trans Dielectr Electr Insul* **12**:929–938. doi:10/dmrb95